

**ISTANBUL TECHNICAL UNIVERSITY ★ GRADUATE SCHOOL OF SCIENCE**  
**ENGINEERING AND TECHNOLOGY**

**OPTIMAL STRUCTURAL CONTROL USING  
WAVELET-BASED LQR ALGORITHM**

**M.Sc. THESIS**

**MAHDI ABDOLLAHIRAD**

**Department of Civil Engineering**

**Earthquake Engineering Programme**

**January 2014**



**ISTANBUL TECHNICAL UNIVERSITY ★ GRADUATE SCHOOL OF SCIENCE**  
**ENGINEERING AND TECHNOLOGY**

**OPTIMAL STRUCTURAL CONTROL USING  
WAVELET-BASED LQR ALGORITHM**

**M.Sc. THESIS**

**MAHDI ABDOLLAHIRAD  
(501111222)**

**Department of Civil Engineering**

**Earthquake Engineering Programme**

**Thesis Advisor: Prof. Dr. Ünal Aldemir**

**January 2014**



**İSTANBUL TEKNİK ÜNİVERSİTESİ ★ FEN BİLİMLERİ ENSTİTÜSÜ**

**WAVELET YAKLAŞIMINI İÇEREN LQR TEKNİĞİ İLE YAPILARIN  
OPTİMAL KONTROLÜ**

**YÜKSEK LİSANS TEZİ**

**MAHDI ABDOLLAHIRAD  
(501111222)**

**İnşaat Mühendisliği Anabilim Dalı**

**Deprem Mühendisliği Programı**

**Tez Danışmanı: Prof. Dr. Ünal Aldemir**

**Ocak 2014**



**Mahdi Abdollahirad**, a **M.Sc.** student of ITU **Institute of Earthquake Engineering and Disaster Management** student ID 501111222, successfully defended the **thesis** entitled “**OPTIMAL STRUCTURAL CONTROL USING WAVELET-BASED LQR ALGORITHM**” which he prepared after fulfilling the requirements specified in the associated legislations, before the jury whose signatures are below.

**Thesis Advisor :**      **Prof. Dr. Ünal Aldemir**      .....

İstanbul Technical University

**Jury Members :**      **Prof. Dr. Kadir Güler**      .....

**Prof. Dr. Şevket Özden**      .....

**Date of Submission : 16 December 2013**

**Date of Defense : 21 January 2014**





*To my father and mother,*



## **FOREWORD**

Current trends in construction industry demands taller and lighter structures, which are also more flexible and having quite low damping value. This increases failure possibilities and also problems from serviceability point of view. Now-a-days several techniques are available to minimize the vibration of the structure. For the last thirty years or so, the reduction of structural response caused by dynamic effects has become a subject of intensive research. Many structural control concepts have been evolved for this purpose, and quite a few of them have been implemented in practice.

I express my deepest gratitude to my thesis advisor **Prof.Dr.Ünal Aldemir**, whose encouragement, guidance and support from the initial to the final level enabled me to develop an understanding of the subject.

Finally, I take this opportunity to extend my deep appreciation to my **family**, for all that they meant to me during the crucial times of the completion of my project.

January 2014

Mahdi Abdollahirad  
(Civil Engineering)



## TABLE OF CONTENTS

	<u>Page</u>
<b>FOREWORD</b> .....	<b>ix</b>
<b>TABLE OF CONTENTS</b> .....	<b>xi</b>
<b>ABBREVIATIONS</b> .....	<b>xiii</b>
<b>LIST OF TABLES</b> .....	<b>xv</b>
<b>LIST OF FIGURES</b> .....	<b>xvii</b>
<b>SUMMARY</b> .....	<b>xxi</b>
<b>ÖZET</b> .....	<b>xxiii</b>
<b>1. INTRODUCTION</b> .....	<b>1</b>
1.1 Introduction .....	1
<b>2. LITERATURE REVIEW</b> .....	<b>5</b>
2.1 Introduction .....	5
2.2 Classification Of Control Methods .....	16
2.2.1 Passive control .....	16
2.2.2 Active control .....	16
2.2.3 Hybrid control .....	18
2.2.4 Semi-active control .....	18
2.3 Type Of Control Devices .....	20
2.3.1 Metallic yeild dampers .....	20
2.3.2 Friction dampers .....	20
2.3.3 Viscoelastic dampers .....	21
2.3.4 Viscous fluid dampers .....	22
2.3.5 Tuned liquid dampers .....	23
2.3.6 Tuned mass dampers .....	23
2.4 The Equation Of Motion Of TMD .....	23
2.4.1 Consept of tuned mass damper using two mass system .....	23
2.4.2 Tuned mass damper theory for SDOF systems .....	26
2.4.2.1 Undamped structure,undamped TMD .....	26
2.4.2.2 Undamped structure,damped TMD .....	28
2.5 The Equation Of Motion Of ATMD .....	30
2.6 Optimal Linear Control (LQR) .....	31
2.7 Wavelet Method .....	33
2.7.1 History of wavelets .....	33
2.7.2 Advantages of wavelet transform to fourier transform .....	33
2.7.3 Continus wavelet transform .....	34
2.7.4 Discrete wavelet transform .....	36
2.7.4.1 One stage filtering .....	36
2.7.4.2 Multiple-level decomposition .....	38
<b>3. PROPOSED METHOD</b> .....	<b>41</b>
3.1 Introduction .....	41

3.2 Decomposition Of Signal .....	41
<b>4. NUMERICAL EXAMPLE.....</b>	<b>47</b>
3.1 Introduction .....	47
3.2 Results .....	47
<b>5. CONCLUSIONS AND RECOMMENDATIONS.....</b>	<b>73</b>
<b>6. FUTURE STUDIES .....</b>	<b>75</b>
<b>REFERENCES.....</b>	<b>67</b>
<b>CURRICULUM VITAE.....</b>	<b>81</b>

## ABBREVIATIONS

<b>ADAS</b>	: Adding Damping And Stiffness
<b>ASCL</b>	: Active Standoff Constrained Layer
<b>ATMD</b>	: Active Tuned Mass Damper
<b>CLD</b>	: Constrained Layer Damping
<b>CWT</b>	: Continues Wavelet Transform
<b>DOF</b>	: Degree of Freedom
<b>DTMD</b>	: Doubly Tuned Mass Damper
<b>DWT</b>	: Discrete Wavelet Transform
<b>FLC</b>	: Fuzzy Logic Controller
<b>IMSC</b>	: Independent Model Space Control
<b>LQG</b>	: Linear Quadratic Gaussian
<b>LQR</b>	: Linear Quadratic Regulation
<b>MDOF</b>	: Multi Degree Of Freedom
<b>MRA</b>	: Multi Resolution Analysis
<b>MTMD</b>	: Multiple Tuned Mass Damper
<b>NTMD</b>	: Nonlinear Tuned Mass Damper
<b>PF-MTMD</b>	: Passive Friction Multiple Tuned Mass Damper
<b>PMCLD</b>	: Piezo Magnetic Constrained Layer Damping
<b>PSD</b>	: Power Spectral Density
<b>PTMD</b>	: Passive Tuned Mass Damper
<b>RMM</b>	: Reverberation Matrix Method
<b>SAF-MTMD</b>	: Semi Active Friction Multiple Tuned Mass Damper
<b>SAPTMD</b>	: Semi Active Pendulum Tuned Mass Damper
<b>SATMD</b>	: Semi Active Tuned Mass Damper
<b>SAVS-TMD</b>	: Semi Active Variable Stiffness Tuned Mass Damper
<b>SDOF</b>	: Single Degree Of Freedom
<b>SSI</b>	: Soil Structure Interaction
<b>TLCD</b>	: Tuned Liquid Column Damper
<b>TLD</b>	: Tuned Liquid Damper
<b>TMD</b>	: Tuned Mass Damper





## LIST OF TABLES

	<u>Page</u>
<b>Table 4.1</b> : Comparison of effectiveness of two controller systems used in this study for Whittier Narrows earthquake ground motion.....	58
<b>Table 4.2</b> : Comparison of acceleration and velocity effectiveness of two controller systems used in this study for Whittier Narrows earthquake ground motion.....	59
<b>Table 4.3</b> : Comparison of effectiveness of two controller systems used in this study for Chi-Chi, Taiwan earthquake ground motion. ....	69
<b>Table 4.4</b> : Comparison of effectiveness of two controller systems used in this study for Yountville earthquake ground motion.....	70
<b>Table 4.5</b> : Comparison of acceleration and velocity effectiveness of two controller systems used in this study for Chi-Chi, Taiwan-1999 earthquake ground motion.....	71
<b>Table 4.6</b> : Comparison of acceleration and velocity effectiveness of two controller systems used in this study for Yountville. 2000 earthquake ground motion.....	71



## LIST OF FIGURES

	<u>Page</u>
<b>Figure 2.1</b> : Active control feed-back structure .....	18
<b>Figure 2.2</b> : X-shaped ADAS device .....	20
<b>Figure 2.3</b> : Pall friction damper.....	21
<b>Figure 2.4</b> : Viscoelastic damper.....	22
<b>Figure 2.5</b> : Taylor device fluid damper. ....	22
<b>Figure 2.6</b> : SDOD-TMD system.....	24
<b>Figure 2.7</b> : Undamped SDOF system coupled undamped TMD system.....	26
<b>Figure 2.8</b> : Undamped SDOF system coupled damped TMD system .....	29
<b>Figure 2.9</b> : Fourier transform.....	34
<b>Figure 2.10</b> : Continues wavelet transform.....	35
<b>Figure 2.11</b> : Wavelet filtering process.....	37
<b>Figure 2.12</b> : Wavelet down sampling process .....	37
<b>Figure 2.13</b> : Wavelet schematic diagram with real signals inserted into it .....	38
<b>Figure 2.14</b> : Wavelet decomposition tree .....	38
<b>Figure 2.15</b> : Wavelet decomposition can be continued indefinitely.....	39
<b>Figure 3.1</b> : Flowchart of proposed method .....	46
<b>Figure 4.1</b> : Whittier Narrows earthquake acceleration time history.....	48
<b>Figure 4.2</b> : Whittier Narrows earthquake velocity time history .....	49
<b>Figure 4.3</b> : Whittier Narrows earthquake displacement time history .....	49
<b>Figure 4.4</b> : Chi-Chi, Taiwan earthquake acceleration time history .....	50
<b>Figure 4.5</b> : Chi-Chi, Taiwan earthquake velocity time history .....	50
<b>Figure 4.6</b> : Chi-Chi, Taiwan earthquake displacement time history .....	51
<b>Figure 4.7</b> : Yountville earthquake acceleration time history.....	51
<b>Figure 4.8</b> : Yountville earthquake velocity time history .....	52
<b>Figure 4.9</b> : Yountville earthquake displacement time history .....	52
<b>Figure 4.10</b> : 10 stories building which has the lumped masse at top storey.....	53
<b>Figure 4.11</b> : Results for Whittier Narrows earthquake, compared uncontrolled response with proposed (WAVELET-LQR) controlled response for 10 <sup>th</sup> floor.....	54
<b>Figure 4.12</b> : Results for Whittier Narrows earthquake, controlled displacement response using LQR and proposed WAVELET-LQR algorithms for 10 <sup>th</sup> floor.....	54
<b>Figure 4.13</b> : Results for Whittier Narrows earthquake, control force compared in two method (LQR , WAVELET-LQR). .....	55
<b>Figure 4.14</b> : Results for Whittier Narrows earthquake, energy demand compared in two method (LQR , WAVELET-LQR). .....	55
<b>Figure 4.15</b> : Results for Whittier Narrows earthquake, compared uncontrolled response with proposed (WAVELET-LQR) controlled response for 1 <sup>th</sup> floor.....	56
<b>Figure 4.16</b> : Results for Whittier Narrows earthquake, controlled displacement response using LQR and proposed WAVELET-LQR algorithms for 1 <sup>th</sup> floor.....	56
<b>Figure 4.17</b> : Results for Whittier Narrows earthquake, compared uncontrolled response with proposed (WAVELET-LQR) controlled response for 5 <sup>th</sup> floor.....	57

<b>Figure 4.18</b> : Results for Whittier Narrows earthquake, controlled displacement response using LQR and proposed WAVELET-LQR algorithms for 5 <sup>th</sup> floor.....	57
<b>Figure 4.19</b> : Results for Whittier Narrows earthquake, displacement in each story compared in two method (LQR , WAVELET-LQR) .....	58
<b>Figure 4.20</b> : Results for Chi-Chi, Taiwan earthquake, compared uncontrolled response with proposed (WAVELET-LQR) controlled response for 10 <sup>th</sup> floor .....	60
<b>Figure 4.21</b> : Results for Chi-Chi, Taiwan earthquake, controlled displacement response using LQR and proposed WAVELET-LQR algorithms for 10 <sup>th</sup> floor .....	60
<b>Figure 4.22</b> : Results for Chi-Chi, Taiwan earthquake, control force compared in two methods (LQR, WAVELET-LQR).....	61
<b>Figure 4.23</b> : Results for Chi-Chi, Taiwan-03 (CHY080.1999) earthquake, energy demand compared in two methods (LQR, WAVELET-LQR). .....	61
<b>Figure 4.24</b> : Results for Chi-Chi, Taiwan earthquake compared uncontrolled response with proposed (WAVELET-LQR) controlled response for 1 <sup>th</sup> floor.....	62
<b>Figure 4.25</b> : Results for Chi-Chi, Taiwan earthquake controlled displacement response using LQR and proposed WAVELET-LQR algorithms for 1 <sup>th</sup> floor.....	62
<b>Figure 4.26</b> : Results for Chi-Chi, Taiwan earthquake compared uncontrolled response with proposed (WAVELET-LQR) controlled response for 5 <sup>th</sup> floor.....	63
<b>Figure 4.27</b> : Results for Chi-Chi, Taiwan earthquake controlled displacement response using LQR and proposed WAVELET-LQR algorithms for 5 <sup>th</sup> floor.....	63
<b>Figure 4.28</b> : Results for Yountville earthquake, compared uncontrolled response with proposed (WAVELET-LQR) controlled response for 10 <sup>th</sup> floor .	64
<b>Figure 4.29</b> : Results for Yountville earthquake, controlled displacement response using LQR and proposed WAVELET-LQR algorithms for 10 <sup>th</sup> floor.	65
<b>Figure 4.30</b> : Results for Yountville earthquake, control force compared in two method (LQR , WAVELET-LQR) .....	65
<b>Figure 4.31</b> : Results for Yountville earthquake, energy demand compared in two method (LQR , WAVELET-LQR). .....	66
<b>Figure 4.32</b> : Results for Yountville earthquake, compared uncontrolled response with proposed (WAVELET-LQR) controlled response for 1 <sup>th</sup> floor ...	66
<b>Figure 4.33</b> : Results for Yountville earthquake, controlled displacement response using LQR and proposed WAVELET-LQR algorithms for 1 <sup>th</sup> floor...	67
<b>Figure 4.34</b> : Results for Yountville earthquake, compared uncontrolled response with proposed (WAVELET-LQR) controlled response for 5 <sup>th</sup> floor ...	67
<b>Figure 4.35</b> : Results for Yountville earthquake, controlled displacement response using LQR and proposed WAVELET-LQR algorithms for 5 <sup>th</sup> floor...	68
<b>Figure 4.36</b> : Results for Chi-Chi, Taiwan-03 (CHY080.1999) earthquake, displacement for each story compared in two methods (LQR, WAVELET-LQR).....	69
<b>Figure 4.37</b> : Results for Yountville (Napa Fire Station #3, 2000) earthquake, displacement for each story compared in two method (LQR , WAVELET-LQR).....	70





# **OPTIMAL STRUCTURAL CONTROL USING WAVELET-BASED LQR ALGORITHM**

## **SUMMARY**

Current trends in construction industry demands taller and lighter structures, which are also more flexible and having quite low damping value. This increases failure possibilities and also problems from serviceability point of view. Now-a-days several techniques are available to minimize the vibration of the structure. In this study to control the response of buildings, a modified linear quadratic regulator (LQR) algorithm based on wavelet analysis has been proposed. The formulation of the proposed wavelet-LQR algorithm uses the information derived from the discrete wavelet transform (DWT) analysis of the motivation in real time. The real time DWT controller is applied to obtain the local energy distribution over frequency bands for each time interval. This information is used to adaptively design the controller by updating the weighting matrices. The optimal LQR control problem is solved for each time interval with updated weighting matrices, through the Riccati equation, leading to time-varying gain matrices. The positive aspect of current work is that, the gain matrices are achieved adaptively in real time. The method is tested on a 10-story structure subject to several historical pulse-like near-fault ground motions. The results indicate that the proposed method is more effective at reducing the displacement response of the structure in real time than conventional LQR controllers.





## WAVELET YAKLAŞIMINI İÇEREN LQR TEKNİĞİ İLE YAPILARIN OPTİMAL KONTROLU ÖZET

Yıkıcı depremler, kasırgalar ve tsunamiler gibi kuvvetli dinamik etkiler altındaki yapıların nasıl korunacağı fikri hep araştırma konusu olmuştur. Gelişmiş ülkelerde dahi ileri teknolojik malzeme ve teknikler kullanıldığı halde kuvvetli bir deprem veya kasırgada yapıların kesinlikle hasar görmeyeceği veya yıkılmayacağı garanti edilememektedir. Bu gibi dinamik kuvvetleri önceden tespit etmek mümkün olmadığından yapıların dizaynı belirli kriterleri sağlayan tasarım yüklerine göre yapılmaktadır. Dolayısıyla yapı tasarım yükünden farklı bir yüke maruz kaldığında ciddi hasarlar görebilmektedir. Geleneksel yaklaşımda yapıya iletilen sismik enerjinin tüketilmesi esas olarak plastik mafsalların oluşumu ile gerçekleşmektedir. Bu da yapının hasar görmesini kabul etme anlamına gelmektedir. Sismik enerjiyi yapısal hasara razı olarak tüketme yerine ek sönüm sistemleri ile tüketme alternatif bir yaklaşım olarak görülmektedir. İstatistikler göstermektedir ki maddi hasarın ve can kayıplarının önemli bir kısmı yapısal olmayan elemanların yüksek ivmeler altında hareket etmesi sonucunda oluşmaktadır. Dolayısıyla artık taşıyıcı sistemin çökmemesi yeterli görülmemekte buna ek olarak yapısal olmayan elemanların ve değerli hassas cihazlarında korunması istenmektedir. Bir başka önemli nokta ise malzeme teknolojisindeki gelişmeler neticesinde malzeme mukavemeti artarken rijitliğin aynı oranda artmamasıdır. Özellikle esneme kapasitesi fazla olan yüksek katlı çelik yapılarda büyük deplasmanların pratik açıdan kontrol edilmesi ek kontrol sistemlerinin kullanılmasını gerektirmektedir.

Son yıllarda yapıları ve yapısal olmayan elemanları dinamik dış etkilere karşı daha iyi korumak için mevcut klasik tasarıma ek olarak onu tamamlayıcı yeni yaklaşımlar üzerinde çalışılmaktadır. Bu yaklaşımlar, yapıya gelen etkileri o anda ölçüp karşı kuvvetler uygulayacak veya etkiyi kendi içinde sönümleyecek malzemeler ve sistemler üzerine yoğunlaşmıştır.

Dinamik etkilere karşı tasarıma yönelik yeni yaklaşımlar esas olarak aktif, pasif ve yarı aktif olmak üzere üç ana başlık altında toplanabilir. Aktif kontrol sistemlerinde kontrol kuvvetlerini üretebilmek için harici bir güç kaynağına ihtiyaç vardır. Zemine ve yapıya yerleştirilen sensörler aracılığıyla elde edilen bilgiler kontrol bilgisayarına iletilerek daha önceden belirlenmiş bir algoritmaya göre kontrol kuvvetleri hesaplanır. Bu kuvvetler kuvvet üreten mekanizmalar (actuator) aracılığıyla yapıya uygulanır. Pasif kontrol sistemleri ise harici bir güç kaynaklarına ihtiyaç duymazlar ve sismik enerjiyi kendi içlerinde sönümlerler. Değişken dinamik etkilere adaptasyon kabiliyeti olmayan bu sistemler çalışma prensipleri ve malzeme özellikleri itibari ile farklılıklar gösterir. Yapıya eklenecek sönümün optimum miktarı ve bu sönümün yapı yüksekliği boyunca optimum dağılımı ayrı bir inceleme konusudur.

Yarı aktif kontrol sistemleri sönüm ve rijitlikleri deprem esnasında kontrol edilebilen sistemlerdir. Aktif kontrolde büyük enerji ihtiyacı olmakla birlikte, yarı aktif

sistemlerde gereken enerji çok küçük bataryalarla bile sağlanabilmektedir. Yarı aktif sistemlerin büyük bir kısmı elektrik veya manyetik alana hassas özel sıvılar içermektedir. Önceden belirli kontrol algoritmalarına bağlı olarak elektrik veya manyetik alan şiddeti değiştirilerek yarı aktif sistemlerin mekanik özellikleri kontrol edilebilmektedir. Karma sistemler; aktif, yarı aktif ve pasif kontrol sistemlerinin bir arada kullanılması durumudur. örneğin, çelik bir yapı visko-elastik sönümleyiciler ile donatılmış ve buna ek olarak aynı zamanda en üst katta aktif kütleli sönümleyici yerleştirilmiş olabilir. Benzer şekilde, bazı yapılara tabanda sismik izolatörler yerleştirilmiş ve izolatör seviyelerinde büyük genlikli hareketlere karşı bu bölgelerde yarı aktif veya pasif olarak çalışan sönümleyiciler eklenmiş olabilir. Karma sistemler yüksek enerji ihtiyacı olmadan çalışabilmektedir.

Yapı tasarım tarihi üç döneme bölünebilir. Sadece statik yüklere göre tasarım yapılan dönem klasik dönem olarak adlandırılır. İkinci dönem modern dönem olarak isimlendirilir. Bu dönem, yapıdaki dinamik etkilerin de göz önüne alınarak tasarımların yapıldığı dönemdir. Statik yükler yapı ömrü boyunca çok fazla değişmezler. Fakat dinamik yükler gerek büyüklükleri gerekse yönleri açısından değişkendirler. Dış yüklerdeki bu değişimi kompanse etmek için yeni konseptler ortaya çıkmıştır. çüncü dönem olarak ortaya çıkan postmodern dönem bu bakış açısı ile doğmuştur. Yapıya gelebilecek yükleri önceden tahmin etmek çok zordur. Bilgisayar, elektro -hidrolik sistemler ve sensör teknolojilerindeki ilerlemeler sonucunda artık, yapıya gelen dinamik kuvvetler ölçülerek önceden belirlenen bir algoritmaya göre kontrol bilgisayarında gerekli kontrol kuvvetleri hesaplanabilmekte ve bu kuvvetler yapıya yerleştirilen aktif kuvvet mekanizmaları ile uygulanabilmektedir. Postmodern dönemde hedeflenen yapı deprem ve rüzgar gibi dinamik çevre etkilerine karşı öngörülen güvenlik, dayanım ve konforu sağlayacak şekilde kendini adapte edebilen bir yapıdır.

Dünyada yapı alanında yürütülen faaliyetler incelendiğinde, yapıların daha yüksek ve daha hafif yapılması yönünde ilerleme olduğu görülmektedir. Bu özelliklerinden dolayı söz konusu yapılar daha esnek ve sönüm oranları da daha azdır. Bunun sonucunda yapıların yaşam konforunda azalma olmaktadır. Günümüzde yapıların titreşimini minimuma indirmek için çeşitli teknikler mevcuttur. Bu araştırmada yapıların titreşim kontrolü için kullanılan LQR (doğrusal kuadratik düzenleyici) algoritmalarında wavelet tekniği ile yapılacak iyileştirme incelenmiştir.

Deprem gibi rastgele yükler karakter itibarıyla dinamik ve değişken frekans özelliğine sahiptir. Bundan dolayı sistemin doğal frekansı ve depremin baskın frekanslarının birbirlerine çok yakın olduğu durumlarda rezonans benzeri durumlara oluşur. Klasik LQR kontrolunda ağırlık matrisleri önceden belirlenir ve yapı dış kuvvetlerin etkisinde kontrol edilirken sabit kalırlar. Bu sebepten dolayı rezonansın yapıya etkisini göz önüne almak için LQR kontrol yönteminde iyileştirme amaçlı değişiklik yapmak gerekmektedir. Eğer R ağırlık matrisinin elemanları depremin tüm kontrol aralığında Q ağırlık matrisinin elemanlarından çok daha fazla olursa yapının tepkisi azalır. Fakat buna karşılık kontrol kuvvetleri ve dolayısıyla da maliyet artar.

Bu sorunu çözmek için, ağırlık matrisini yapının her andaki ihtiyacına göre değiştirmek uygun bir çözüm olabilir. Rezonansın olduğu frekanslarda yapının tepkisini azaltmak için ağırlık matrislerini belirtilen frekans bantlarında revize etmek

gerekir. Eđer R ađırlık matrisi rezonansın ortaya ıktıđı alt aralıklarda azaltılırsa kontrol enerjisinin gereksiz artışı nlenebilir. Bunun iin deprem sinyalinin ayırıştırmak gerekir ki; deprem frekansları her zaman aralıđında belirlensin.

Sinyalleri ayırıştırmak iin eřitli yollar mevcuttur. Fourier analizi sinyalleri zaman alanından frekans alanına dnüştüren klasik bir yöntemdir. Fourier analizi tekniđinin en nemli kusurlarından biri frekans alanına dnüştüirmede zaman alanındaki bilgiler silinmektedir. Sonu olarak, Fourier dnüşümündeki bir sinyale bakınca belirli bir olayın ne zaman olduđunu belirtmek zordur. Eđer sinyal zellikleri dnüşüm süresince fazla deđişmedi ise, başka bir deđişle sinyal sabit (stationary) kalırsa hiçbir sorun yaşanmaz. Ama deprem sabit olmayan zelliklere sahiptir ve bundan dolayı Fourier dnüşümüyle belirtilen zellikleri gözlemek mümkün deđildir.

Belirtilen sorunu özmek iin bu alıřmada daha nce geliřtirilen Wavelet yöntemi kullanılmıřtır. Wevelet yönteminin her andaki zaman-frekans dnüşüm zelliđinden yararlanarak LQR algoritmasını iyileřtirmek mümkündür. İlk andan itibaren son kontrol anına kadar, her frekans bandında deprem nedeniyle oluřan enerji sonucunda Wavelet in her andaki ayrıık kontrol deđeri güncellenir. Bu bilgiler her frekans bandındaki ađırlık matrislerini güncellemek iin kullanılır. Bu nedenle kazanç matrisleri zamanla deđiřtiđi iin karřı gelen Riccati matris denklemleri de deđişmektedir.

Klasik LQR kontrol yönteminde Q ve R ađırlık matrisleri sabit iken, bu alıřmada incelenen yöntemde kazanç matrislerinin nceden belirlenen ađırlık matrislerinden elde edilmesi yerine her andaki tepkiye bađlı olarak wavelet yaklařımı ile güncellenen ađırlık matrislerinden elde edilen kazanç matrisleri kullanılmaktadır.

Önerilen yöntemin etkinliđini gösterebilmek iin, deprem etkisinde ve en üst katında aktif sönümleyici olan ve fay hattına yakın 10 katlı bir binanın dinamik davranışı arařtırılmıř ve önerilen yöntemin LQR yaklařımını iyileřtirmek iin kullanılabileceđi gösterilmiřtir.



# **1. INTRODUCTION**

## **1.1 Introduction**

For seismic design of building structures, the traditional method, *i.e.*, strengthening the stiffness, strength, and ductility of the structures, has been in common use for a long time. Therefore, the dimensions of structural members and the consumption of material are expected to be increased, which leads to higher cost of the buildings as well as larger seismic responses due to larger stiffness of the structures. Thus, the efficiency of the traditional method is constrained. To overcome these disadvantages associated with the traditional method, many vibration-control measures, called structural control, have been studied and remarkable advances in this respect have been made over recent years. Structural control is a diverse field of study. Structural Control is the one of the areas of current research aims to reduce structural vibrations during loading such as earthquakes and strong winds.

For the last thirty years or so, the reduction of structural response caused by dynamic effects has become a subject of intensive research. Many structural control concepts have been evolved for this purpose, and quite a few of them have been implemented in practice. There are a number of motivating factors for conducting this research. They include: (i) reduction of undesirable vibrational levels of flexible structures due to unexpected large environmental loads; (ii) retrofitting existing structures against environmental hazards; (iii) protecting seismic equipments and important secondary systems; and finally, (iv) providing new concepts of design of structures against environmental loading. Broadly speaking, structural control methods can be classified as passive and active control methods. The passive control method is activated by the structural motion. No external force or energy is applied to effect the control.

On the other hand, active control method is effected by externally activated device, to change the response. The activation of external force is based on the measurement of external disturbance and/or structural response. Sensors are employed for the

measurement purposes, and with the help of computers, the digital signal activates (converted to analog signal) the required external force. A combination of these two methods of structural control has been used to evolve hybrid control methods, for realizing stringent control requirements. In recent years, a class of active control systems, for which the external energy requirements are orders of magnitude smaller than a typical active control system, have been evolved. They are known as semi-active control systems, in which the control action is produced by the movement of the structure but is regulated by an external source of energy.

Comprehensive studies have been done to determine the optimal force for the active vibration control systems. The most common methods are LQR, LQG, clipped control, bang-bang control, H<sub>2</sub>, H<sub>∞</sub> control, sliding mode control, pole assignment, independent model space control (IMSC), and so on (Datta, 1996, p.18-20; Yang, 1988). However, algorithms based on classical control algorithms such as linear quadratic regulator (LQR) suffer from some inherent shortcomings for structural applications, which have been acknowledged by researchers and improvement on the classical algorithms has been proposed (Adeli and Kim, 2004; Wu et al, 1998; Wu et al, 1994). One of the major shortcomings of the LQR algorithm for application to forced vibration control of structures is its inability to explicitly account for the excitation. While this is not of much concern for free the vibration scenarios or for stabilizing structural systems to de-stabilizing forces, the earthquake or wind excited structures are subjected forced vibration and for the control, the effect of the external excitations needs to be accounted for in such cases. The effect of the specific earthquakes has been accounted for in a few studies (Wu et al, 1994; Wu and Nagarajaiash, 1996).

For example Panarillo et al. (1997), introduced a method based on updating weighting matrices from a database of earthquakes. Nonetheless, in these studies, offline databases were still required. Biswajit Basu et al. (2008), proposed a wavelet-based adaptive LQR control to design the controller by updating the weighting matrices. This method determines the time-varying gain matrices by updating the weighting matrices online, through the Ricatti equation. Therefore, this method does not need prior information about external excitation, hence eliminating the need for an offline database.

In this study, a wavelet based adaptive linear quadratic regulator (WAVELET-LQR) formulation is used to determine the control force. The first objective of this study is to show applying the WAVELET- LQR control is effectiveness in reducing the response of structures. The second objective of this study is to show that by using updating LQR the magnitude of control force increases just on the resonant band of frequency so the response of structures reduce without higher penalty.





## **2. LITERATURE REVIEW**

### **2.1 Introduction**

Mitigating the seismic responses of major structures such as tall buildings, wind sensitive bridges, and potentially susceptible structures has been studied comprehensively over the years (Adeli and Saleh, 1997, 1998, 1999; Adeli and Kim, 2004; Jiang and Adeli, 2008a, 2008b; Kim and Adeli, 2004, 2005a, 2005b, 2005c, 2005d; Saleh and Adeli, 1994, 1997, 1998; Soong and Constantinou, 2002; Amini and Vahdani, 2008; Amini, 1995; Kim et al., 2010). The passive tuned mass damper (PTMD) is effective in reducing the vibration of structures caused by earthquakes with limited band frequency (Warburton and Ayorinde, 1980; Den Hartog, 1956).

TMD system relies on the damping forces introduced through the inertia force of a secondary system attached to the main structure by spring and dashpot to reduce the response of the main structure. The TMD concept was first applied by Frahm in 1909 to reduce the rolling motion of ships as well as ship hull vibrations. A theory for the TMD was presented later in the paper by Ormondroyd and Den Hartog (1928), followed by a detailed discussion of optimal tuning and damping parameters in Den Hartog's book on mechanical vibrations (1940). Hartog's book on mechanical vibrations (1940). The initial theory was applicable for an un-damped SDOF system subjected to a sinusoidal force excitation.

Active control devices operate by using an external power supply. Therefore, they are more efficient than passive control devices. However, the problems such as insufficient control force capacity and excessive power demands encountered by current technology in the context of structural control against earthquakes are unavoidable and need to be overcome. Recently a new control approach—semi-active control devices, which combine the best features of both passive and active control devices, is very attractive due to their low power demand and inherent stability. The earlier papers involving SATMDs may be traced to 1983. Hrovat et al. (1983) presented SATMD, a TMD with time-varying controllable damping. Under identical conditions, the behaviour of a structure equipped with SATMD instead of TMD is significantly improved. The control design of SATMD is less dependent on related parameters (e.g., mass ratios, frequency ratios and so on), so that there are greater choices in selecting them.

The first mode response of a structure with TMD tuned to the fundamental frequency of the structure can be substantially reduced but, in general, the higher modal responses may only be marginally suppressed or even amplified. To overcome the frequency-related limitations of TMDs, more than one TMD in a given structure, each tuned to a different dominant frequency, can be used. The concept of multiple tuned mass dampers (MTMDs) together with an optimization procedure was proposed by Clark (1988). Since, then, a number of studies have been conducted on the behaviour of MTMDs a doubly tuned mass damper (DTMD), consisting of two masses connected in series to the structure was proposed (Setareh 1994). In this case, two different loading conditions were considered: harmonic excitation and zero-mean white-noise random excitation, and the efficiency of DTMDs on response reduction was evaluated. Analytical results show that DTMDs are more efficient than the conventional single mass TMDs over the whole range of total mass ratios, but are only slightly more efficient than TMDs over the practical range of mass ratios (0.01-0.05).

Recently, numerical and experimental studies have been carried out on the effectiveness of TMDs in reducing seismic response of structures. In Villaverde(1994), three different structures were studied, in which the first one is a 2D two story shear building the second is a three-dimensional (3D) one-story frame building, and the third is a 3D cable-stayed bridge, using nine different kinds of earthquake records. Numerical and experimental results show that the effectiveness of TMDs on reducing the response of the same structure during different earthquakes, or of different structures during the same earthquake is significantly different; some cases give good performance and some have little or even no effect. This implies that there is a dependency of the attained reduction in response on the characteristics of the ground motion that excites the structure. This response reduction is large for resonant ground motions and diminishes as the dominant frequency of the ground motion gets further away from the structure's natural frequency to which the TMD is tuned. Also, TMDs are of limited effectiveness under pulse-like seismic loading.

Multiple passive TMDs for reducing earthquake induced building motion. Allen J. Clark (1988). In this paper a methodology for designing multiple tuned mass damper for reducing building response motion has been discussed. The technique is based on extending Den Hartog work from a single degree of freedom to multiple degrees of

freedom. Simplified linear mathematical models were excited by 1940 El Centro earthquake and significant motion reduction was achieved using the design technique.

Performance of tuned mass dampers under wind loads K. C. S. Kwok et al. (1995). The performance of both passive and active tuned mass damper (TMD) systems can be readily assessed by parametric studies which have been the subject of numerous research. Few experimental verifications of TMD theory have been carried out, particularly those involving active control, but the results of those experiments generally compared well with those obtained by parametric studies. Despite some serious design constraints, a number of passive and active tuned mass damper systems have been successfully installed in tall buildings and other structures to reduce the dynamic response due to wind and earthquakes.

Mitigation of response of high-rise structural systems by means of optimal tuned mass damper. A.N Blekherman(1996). In this paper a passive vibration absorber has been proposed to protect high-rise structural systems from earthquake damages. A structure is modelled by one-mass and n-mass systems (a cantilever scheme). Damping of the structure and absorber installed on top of it is represented by frequency independent one on the base of equivalent visco-elastic model that allows the structure with absorber to be described as a system with non-proportional internal friction. A ground movement is modelled by an actuator that produces vibration with changeable amplitude and frequency. To determine the optimum absorber parameters, an optimization problem, that is a minmax one, was solved by using nonlinear programming technique( the Hooke-Jeves method).

Survey of actual effectiveness of mass damper systems installed in buildings. T.Shimazu and H.Araki(1996). In this paper the real state of the implementation of mass damper systems, the effects of these systems were clarified based on various recorded values in actual buildings against both wind and earthquake. The effects are discussed in relation with the natural period of buildings equipped with mass damper systems, the mass weight ratios to building weight, wind force levels and earthquake ground motion levels.

A method of estimating the parameters of tuned mass dampers for seismic applications. Fahim Sadek et al. (1997). In this paper the optimum parameters of

TMD that result in considerable reduction in the response of structures to seismic loading has been presented. The criterion that has been used to obtain the optimum parameters is to select for a given mass ratio, the frequency and damping ratios that would result in equal and large modal damping in the first two modes of vibration. The parameters are used to compute the response of several single and multi-degree of freedom structures with TMDs to different earthquake excitations. The results show that the use of the proposed parameters reduces the displacement and acceleration responses significantly. The method can also be used for vibration control of tall buildings using the so-called 'mega-substructure configuration', where substructures serve as vibration absorbers for the main structure.

Structural control: past, present, and future G. W. Housner et al. (1996). This paper basically provides a concise point of departure for those researchers and practitioners who wishing to assess the current state of the art in the control and monitoring of civil engineering structures; and provides a link between structural control and other fields of control theory, pointing out both differences and similarities, and points out where future research and application efforts are likely to prove fruitful.

Structural vibration of tuned mass installed three span steel box bridge. Byung-Wan Jo et al. (2001). To reduce the structural vibration of a three span steel box bridge a three axis two degree of freedom system is adopted to model the mass effect of the vehicle; and the kinetic equation considering the surface roughness of the bridge is derived based on Bernoulli-Euler beam ignoring the torsional DOF. The effects of TMD on steel box bridge shows that it is not effective in reducing the maximum deflection, but it efficiently reduces the free vibration of the bridge. It proves that the TMD is effective in controlling the dynamic amplitude rather than the maximum static deflection.

Optimal placement of multiple tuned mass dampers for seismic structures. Genda Chen et al. (2001). In this paper effects of a tuned mass damper on the modal responses of a six-story building structure are studied. Multistage and multimode tuned mass dampers are then introduced. Several optimal location indices are defined based on intuitive reasoning, and a sequential procedure is proposed for practical design and placement of the dampers in seismically excited building structures. The proposed procedure is applied to place the dampers on the floors of the six-story building for maximum reduction of the accelerations under a stochastic seismic load

and 13 earthquake records. Numerical results show that the multiple dampers can effectively reduce the acceleration of the uncontrolled structure by 10- 25% more than a single damper. Time-history analyses indicate that the multiple dampers weighing 3% of total structural weight can reduce the floor acceleration up to 40%.

Seismic effectiveness of tuned mass dampers for damage reduction of structures. T. Pinkaew et al (2002). The effectiveness of TMD using displacement reduction of the structure is found to be insufficient after yielding of the structure, damage reduction of the structure is proposed instead. Numerical simulations of a 20-storey reinforced concrete building modelled as an equivalent inelastic single-degree-of-freedom (SDOF) system subjected to both harmonic and the 1985 Mexico City ground motions are considered. It is demonstrated that although TMD cannot reduce the peak displacement of the controlled structure after yielding, it can significantly reduce damage to the structure. In addition, certain degrees of damage protection and collapse prevention can also be gained from the application of TMD.

Tuned Mass Damper Design for Optimally Minimizing Fatigue Damage. Hua-Jun Li et al (2002). This paper considers the environmental loading to be a long-term non-stationary stochastic process characterized by a probabilistic power spectral density function. One engineering technique to design a TMD under a long-term random loading condition is for prolonging the fatigue life of the primary structure.

Seismic structural control using semi-active tuned mass dampers. Yang Runlin et al (2002). This paper focuses on how to determine the instantaneous damping of the semi-active tuned mass damper with continuously variable damping. This algorithm is employed to examine the control performance of the structure, SATMD system by considering damping as an assumptive control action. Two numerical simulations of a five-storey and a ten-storey shear structures with a SATMD on the roof are conducted. The effectiveness on vibration reduction of MDOF systems subjected to seismic excitations is discussed.

Structural vibration suppression via active/passive techniques. Devendra P. Garg et al (2003). The advances made in the area of vibration suppression via recently developed innovative techniques (for example, constrained layer damping (CLD) treatments) applied to civilian and military structures are investigated. Developing theoretical equations that govern the vibration of smart structural systems treated

with piezo-magnetic constrained layer damping (PMCLD) treatments; and developing innovative surface damping treatments using micro-cellular foams and active standoff constrained layer (ASCL) treatments.

Performance of a five-storey benchmark model using an active tuned mass damper and a fuzzy controller. Bijan Samali, Mohammed Al-Dawod(2003). This paper describes the performance of a five-storey benchmark model using an active tuned mass damper (ATMD), where the control action is achieved by a Fuzzy logic controller (FLC) under earthquake excitations. The advantage of the Fuzzy controller is its inherent robustness and ability to handle any non-linear behaviour of the structure. The simulation analysis of the five-storey benchmark building for the uncontrolled building, the building with tuned mass damper (TMD), and the building with ATMD with Fuzzy and linear quadratic regulator (LQR) controllers has been reported, and comparison between Fuzzy and LQR controllers is made. In addition, the simulation analysis of the benchmark building with different values of frequency ratio, using a Fuzzy controller is conducted and the effect of mass ratio, on the five-storey benchmark model using the Fuzzy controller has been studied.

Behaviour of soil-structure system with tuned mass dampers during near-source earthquakes. Nawawi Chouw(2004). In this paper the influence of a tuned mass damper on the behaviour of a frame structure during near-source ground excitations has been presented. In the investigation the effect of soil-structure interaction is considered, and the natural frequency of the tuned mass damper is varied. The ground excitations used are the ground motion at the station SCG and NRG of the 1994 Northridge earthquake. The investigation shows that the soil-structure interaction and the characteristic of the ground motions may have a strong influence on the effectiveness of the tuned mass damper. But in order to obtain a general conclusion further investigations are necessary.

Wind Response Control of Building with Variable Stiffness Tuned Mass Damper Using Empirical Mode Decomposition Hilbert Transform Nadathur Varadarajan et al (2004). The effectiveness of a novel semi-active variable stiffness-tuned mass damper SAVS-TMD for the response control of a wind-excited tall benchmark building is investigated in this study. The benchmark building considered is a proposed 76-story concrete office tower in Melbourne, Australia. Across wind load data from wind tunnel tests are used in the present study. The objective of this study

is to evaluate the new SAVS-TMD system, that has the distinct advantage of continuously retuning its frequency due to real time control and is robust to changes in building stiffness and damping. The frequency tuning of the SAVS-TMD is achieved based on empirical mode decomposition and Hilbert transform instantaneous frequency algorithm developed by the writers. It is shown that the SAVS-TMD can reduce the structural response substantially, when compared to the uncontrolled case, and it can reduce the response further when compared to the case with TMD. Additionally, it is shown the SAVS-TMD reduces response even when the building stiffness changes by  $\pm 15\%$ .

Effect of soil interaction on the performance of tuned mass dampers for seismic applications. A Ghosha, B. Basu(2004).The properties of the structure used in the design of the TMD are those evaluated considering the structure to be of a fixed-base type. These properties of the structure may be significantly altered when the structure has a flexible base, i.e. when the foundation of the structure is supported on compliant soil and undergoes motion relative to the surrounding soil. In such cases, it is necessary to study the effects of soil-structure interaction (SSI) while designing the TMD for the desired vibration control of the structure. In this paper, the behaviour of flexible-base structures with attached TMD, subjected to earthquake excitations has been investigated. Modified structural properties due to SSI has been covered in this paper.

Optimal design theories and applications of tuned mass dampers. Chien-Liang Lee et al (2006).An optimal design theory for structures implemented with tuned mass dampers (TMDs) is proposed in this paper. Full states of the dynamic system of multiple-degree-of-freedom (MDOF) structures, multiple TMDs (MTMDs) installed at different stories of the building, and the power spectral density (PSD) function of environmental disturbances are taken into account. The optimal design parameters of TMDs in terms of the damping coefficients and spring constants corresponding to each TMD are determined through minimizing a performance index of structural responses defined in the frequency domain. Moreover, a numerical method is also proposed for searching for the optimal design parameters of MTMDs in a systematic fashion such that the numerical solutions converge monotonically and effectively toward the exact solutions as the number of iterations increases. The feasibility of the proposed optimal design theory is verified by using a SDOF structure with a single

TMD (STMD), a five-DOF structure with two TMDs, and a ten-DOF structure with a STMD.

Optimum design for passive tuned mass dampers using viscoelastic materials. I Saidi, A D Mohammed et al (2007). This paper forms part of a research project which aims to develop an innovative cost effective Tune Mass Damper (TMD) using viscoelastic materials. Generally, a TMD consists of a mass, spring, and dashpot which is attached to a floor to form a two-degree of freedom system. TMDs are typically effective over a narrow frequency band and must be tuned to a particular natural frequency. The paper provides a detailed methodology for estimating the required parameters for an optimum TMD for a given floor system. The paper also describes the process for estimating the equivalent viscous damping of a damper made of viscoelastic material. Finally, a new innovative prototype viscoelastic damper is presented along with associated preliminary results.

Semi-active Tuned Mass Damper for Floor Vibration Control .Mehdi Setareh et al (2007). A semi-active magneto-rheological device is used in a pendulum tuned mass damper PTMD system to control the excessive vibrations of building floors. This device is called semi-active pendulum tuned mass damper SAPTMD. Analytical and experimental studies are conducted to compare the performance of the SAPTMD with its equivalent passive counterpart. An equivalent single degree of freedom model for the SAPTMD is developed to derive the equations of motion of the coupled SAPTMD-floor system. A numerical integration technique is used to compute the floor dynamic response, and the optimal design parameters of the SAPTMD are found using an optimization algorithm. Effects of off-tuning due to the variations of the floor mass on the performance of the PTMD and SAPTMD are studied both analytically and experimentally. From this study it can be concluded that for the control laws considered here an optimum SAPTMD performs similarly to its equivalent PTMD, however, it is superior to the PTMD when the floor is subjected to off-tuning due to floor mass variations from sources other than human presence.

Seismic Energy Dissipation of Inelastic Structures with Tuned Mass Dampers. K. K. F. Wong(2008).The energy transfer process of using a tuned mass damper TMD in improving the ability of inelastic structures to dissipate earthquake input energy is investigated. Inelastic structural behaviour is modelled by using the force analogy



method, which is the backbone of analytically characterizing the plastic energy dissipation in the structure. The effectiveness of TMD in reducing energy responses is also studied by using plastic energy spectra for various structural yielding levels. Results show that the use of TMD enhances the ability of the structures to store larger amounts of energy inside the TMD that will be released at a later time in the form of damping energy when the response is not at a critical state, thereby increasing the damping energy dissipation while reducing the plastic energy dissipation. This reduction of plastic energy dissipation relates directly to the reduction of damage in the structure.

Dynamic analysis of space structures with multiple tuned mass dampers. Y.Q. Guo, W.Q.Chen(2008). Formulations of the reverberation matrix method (RMM) are presented for the dynamic analysis of space structures with multiple tuned mass dampers (MTMD). The theory of generalized inverse matrices is then employed to obtain the frequency response of structures with and without damping, enabling a uniform treatment at any frequency, including the resonant frequency. For transient responses, the Neumann series expansion technique as suggested in RMM is found to be confined to the prediction of accurate response at an early time. The artificial damping technique is employed here to evaluate the medium and long time response of structures. The free vibration, frequency response, and transient response of structures with MTMD are investigated by the proposed method through several examples. Numerical results indicate that the use of MTMD can effectively alter the distribution of natural frequencies as well as reduce the frequency/transient responses of the structure. The high accuracy, lower computational cost, and uniformity of formulation of RMM are also highlighted in this paper.

Exploring the performance of a nonlinear tuned mass damper. Nicholas A. Alexander, Frank Schilder (2009).In this the performance of a nonlinear tuned mass damper (NTMD), which is modelled as a two degree of freedom system with a cubic nonlinearity has been covered. This nonlinearity is physically derived from a geometric configuration of two pairs of springs. The springs in one pair rotate as they extend, which results in a hardening spring stiffness. The other pair provides a linear stiffness term. In this paper an extensive numerical study of periodic responses of the NTMD using the numerical continuation software AUTO has been done. Two techniques have been employed for searching the optimal design parameters;

optimization of periodic solutions and parameter sweeps. In this paper the writers have discovered a family of resonance curves for vanishing linear spring stiffness.

Application of semi-active control strategies for seismic protection of buildings with MR dampers. Maryam Bitaraf et al (2010). Magneto-rheological (MR) dampers are semi-active devices that can be used to control the response of civil structures during seismic loads. They are capable of offering the adaptability of active devices and stability and reliability of passive devices. One of the challenges in the application of the MR dampers is to develop an effective control strategy that can fully exploit the capabilities of the MR dampers. This study proposes two semi-active control methods for seismic protection of structures using MR dampers. The first method is the Simple Adaptive Control method which is classified as a direct adaptive control method. The controller developed using this method can deal with the changes that occur in the characteristics of the structure because it can modify its parameters during the control procedure. The second controller is developed using a genetic-based fuzzy control method. In particular, a fuzzy logic controller whose rule base determined by a multi-objective genetic algorithm is designed to determine the command voltage of MR dampers.

Vibration control of seismic structures using semi-active friction multiple tuned mass dampers. Chi-Chang Lin et al.(2010) There is no difference between a friction-type tuned mass damper and a dead mass added to the primary structure if static friction force inactivates the mass damper. To overcome this disadvantage, this paper proposes a novel semi-active friction-type multiple tuned mass damper (SAF-MTMD) for vibration control of seismic structures. Using variable friction mechanisms, the proposed SAF-MTMD system is able to keep all of its mass units activated in an earthquake with arbitrary intensity. A comparison with a system using passive friction-type multiple tuned mass dampers (PF-MTMDs) demonstrates that the SAF-MTMD effectively suppresses the seismic motion of a structural system, while substantially reducing the strokes of each mass unit, especially for a larger intensity earthquake.

Extension of the theory to damped SDOF systems has been investigated by numerous researchers. (Kim and Adeli, 2005a). Lin et al. (2010) used initially accelerated passive TMD to suppress structural peak responses under near-fault ground motions. This study showed that the PTMD initial velocity is effective in

vibration control of structures under pulse-like ground motion. However, due to the limitation of PTMD stroke as well as the applied force, the initial velocity cannot be too large in practical applications. To overcome these shortcomings, the active control can be applied to TMD. Extensive reviews on using the active tuned mass damper (ATMD) can be found in civil engineering literature (Chang and Soong, 1980; Udwadia and Tabaie, 1981a, 1981b; Amini and Tavassoli, 2005; Ankireddi and Yang, 1996). Chey et al. (2010) proposed a semi-ATMD to mitigate the response of structures. In this study, the stiffness of the resettable device design was combined with rubber bearing stiffness. Moreover, Chase et al. (2011) developed an advanced control law for Semi-Active resettable devices. Also, Corman et al. (2012a, 2012b) proposed a new resettable device control to reduce the response of structures.

Comprehensive studies have been done to determine the optimal actuator force for the active Vibration control systems. The most widespread methods are linear quadratic regulator (LQR), LQG, H<sub>2</sub>, H<sub>∞</sub>, sliding mode control, pole assignment, Clippes Optimal Control and Bang-Bang control. Most control methods are based on the optimization technique of maximizing the performance using less control energy under certain constraint and most optimization algorithms used in control design are traditional methods.

In this approach, there are difficulties associated in selecting the suitable continuous differentiable cost function (Gray et al., 1995). Unlike traditional optimization methods, evolutionary algorithms such as genetic algorithm (GA) find an optimal solution from the complex and possibly discontinuous solution space. In the field of structural control, GAs have been applied to obtain gains for the optimal controller (Kundu and Kawata, 1996; Jiang and Adeli, 2008b), reduced order feedback control (Kim and Ghaboussi, 1999), optimal damper distribution (Wongprasert and Symans, 2004), and design and optimize the different parameters of the ATMD control scheme (Pourzeynali et al., 2007). Aldemir (2010), introduced a simple integral type quadratic functional as the performance index to suppress the seismic vibrations of buildings. He used the method of calculus of variations to minimize the proposed performance index and obtain the optimal control force. Also, Aldemir et al. (2012), proposed simple methods to obtain the suboptimal passive damping and stiffness parameters from the optimal control gain matrix to control structural response under earthquake excitation. Bitaraf et al. (2012), proposed a direct adaptive-control

method to control the behavior of an undamaged and a damaged structure using semi-active and active devices. Their method is defined in a way to optimize the response of the controlled structure. Puscasu and Codres (2011), proposed a new approach for nonlinear system identification and control based on modular neural networks. Their proposed method reduced the computational complexity of neural identification by decomposing the whole system into several subsystems.

## **2.2 Classification Of Control Method**

### **2.2.1 Passive control**

A passive control system does not require an external power source. Passive control devices impart forces that are developed in response to the motion of the structure. Total energy (structure plus passive device) cannot increase, hence inherently stable. Base isolation is one of the passive vibration control system that does not require any external power source for its operation and utilizes the motion of the structure to develop the control forces. Performance of base isolated buildings in different parts of the world during earthquakes in the recent past established that the base isolation technology is a viable alternative to conventional earthquake-resistant design of medium-rise buildings. The application of this technology may keep the building to remain essentially elastic and thus ensure safety during large earthquakes. Since a base-isolated structure has fundamental frequency lower than both its fixed base frequency and the dominant frequencies of ground motion, the first mode of vibration of isolated structure involves deformation only in the isolation system whereas superstructure remains almost rigid. In this way, the isolation becomes an attractive approach where protection of expensive sensitive equipments and internal non-structural components is needed. It was of interest to check the difference between the responses of a fixed-base building frame and the isolated-base building frame under seismic loading. This was the primary motivation of the present study.

### **2.2.2 Active control**

An active control system is one in which an external power source the control actuators are used that apply forces to the structure in a prescribed manner. These forces can be used to both add and dissipate energy from the structure. In an active feedback control system, the signals sent to the control actuators are a function of the

response of the system measured with physical sensors (optical, mechanical, electrical, chemical, and so on).

The early notion of actively controlled structures was presented by Zuk (1968). He distinguished between the active control, which is designed to reduce structural motion and that which generates structural motion. Kinetic structures which control enclosed space through structural manipulation belong to the second category. Earliest works on active structural control include prestressed tendon to stabilize tall structures, control of tall buildings by cables attached to jacks (Soong, 1988), and use of active systems which can provide increased strength to the structure to counter exceptional over-loading (Nordel, 1969). According to Soong (1988), Yao put forward the theory of formal active structural control which became the subject of intensive research subsequently.

Most of the control concepts have feed-back structure as shown in Figure 2.1. Actuators in the figure are powered by external energy sources to produce the required control force. Based on the control strategy, active control can be classified as: open loop control system (when the left side loop of Figure 2.1 is operative); close loop control (when the right side loop of Figure 2.1 is operative); and open–close loop control (when the both loops of Figure 2.1 are operative). An adaptive control system is a variation of open-close loop control with a controller which can adjust parameters of the system. The adaptive systems are generally used to control structures whose parameters are unknown and are based on tracking error between the measured response and the observed response. A learning control system is one which has an ability to learn and can switch over from open loop control system to close loop control system depending upon the requirements.

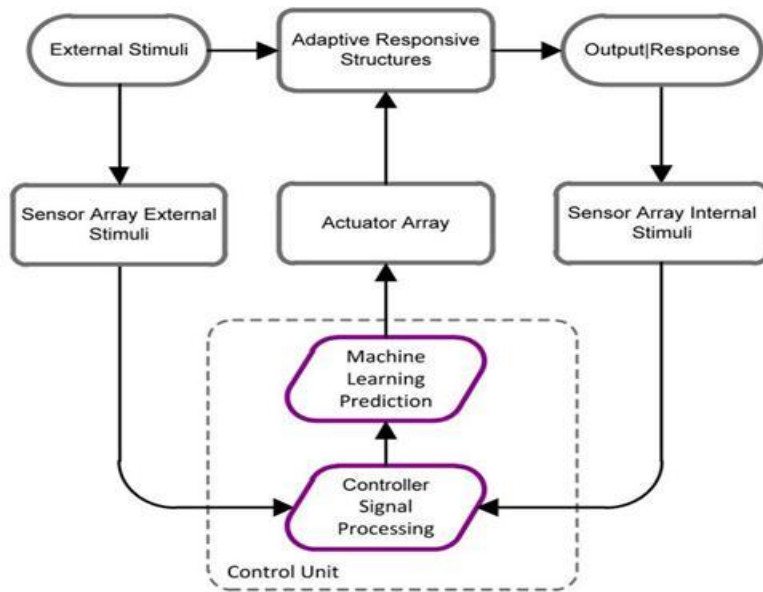


**Figure 2.1** : Active control feed-back structure

### 2.2.3 Hybrid control

The term "hybrid control" implies the combined use of active and passive control systems. Various combinations of passive and active systems have been attempted. Hybrid control is preferred when more stringent control of one or more response quantities is desired. It is governed by a control algorithm in which the dynamic characteristics of structural system include those of passive control devices. Formulation of active control problem remains the same, except that the structural system becomes non-classically damped. For example, a structure equipped with distributed viscoelastic damping supplemented with an active mass damper near the top of the structure, or a base isolated structure with actuators actively controlled to enhance performance.

### 2.2.4 Semi-active control

Semi-active control systems are a class of active control systems for which the external energy requirements are less than typical active control systems. Typically, semi-active control devices do not add mechanical energy to the structural system (including the structure and the control actuators), therefore bounded-input bounded-output stability is guaranteed. It originates from the passive control system, modified to allow the adjustment of mechanical properties based on feed-back from the

excitation or the measured response. As an active control system, it monitors the feed-back measurement, and generates appropriate command signal. As a passive control system, control forces are developed as a result of the motion of the structure. Control forces primarily act to oppose the motion, and are developed through appropriate control algorithms.

Different types of semi-active control devices include:

**(i) Stiffness control devices** - These devices are utilized to modify the stiffness, and hence, the natural frequency of the system. This establishes a new resonant condition during earthquakes. The devices used are stiffness bracings, which are engaged or released so as to include or not to include the additional stiffness in the system, and operate generally through fluid control within tubes by valves (Yang et al., 1996; Nagarajaiah, 1997; He et al., 2001).

**(ii) Electro-rheological dampers/magneto-rheological dampers** - They consist of a hydraulic cylinder containing micron-size dielectric particles suspended within a fluid. In the presence of current, particles polarize and offer an increased resistance to flow (a change from viscous fluid to yielding solid within milli-seconds). The magneto-rheological dampers are magnetic analogues of electrorheological dampers, and have electro-magnets located within the piston head which generate the magnetic field (Ehrgott and Masri, 1992, 1993; Spencer et al., 1996; Dyke et al., 1996b, 1997).

**(iii) Friction control devices** - They are energy dissipators within the lateral bracing of a structure, or are as components within the sliding isolation system. The coefficient of friction of sliding is controlled by the modulation of fluid pressure in a pneumatic pressure (Akbay and Aktan, 1991; Feng, 1993).

**(iv) Fluid viscous devices** - They consist of a hydraulic cylinder, with a piston dividing it into two sides. The cycling piston forces oil through an orifice, creating the output force. The output force is modulated by an external control valve which connects two sides of the cylinder (Sack et al., 1994; Symans and Constantinou, 1997).

**(v) TMDs and TLDs** - The dynamic characteristics of the TMDs are controlled by the external current. In the TLDs, the length of the hydraulic tanks is modified by adjusting the rotation of the rotatable baffles in the tank, and thus, the sloshing frequencies of the fluid are changed.

## 2.3 Type Of Control Devices

### 2.3.1 Metallic yeild dampers

One of the effective mechanisms available for the dissipation of energy, input to a structure from an earthquake is through inelastic deformation of metals. The idea of using metallic energy dissipators within a structure to absorb a large portion of the seismic energy began with the conceptual and experimental work of Kelly et al. (1972) and Skinner et al. (1975). Several of the devices considered include torsional beams, flexural beams, and V-strip energy dissipators. Many of these devices use mild steel plates with triangular or hourglass shapes so that yielding is spread almost uniformly throughout the material. A typical X-shaped plate damper or added damping and stiffness (ADAS) device is shown in Fig.2.2.

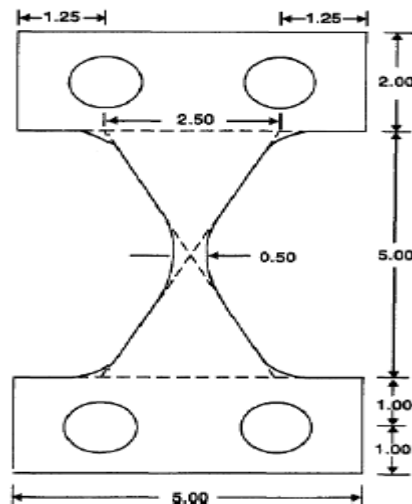


**Figure 2.2 :** X-shaped ADAS device.

### 2.3.2 Friction dampers

Friction provides another excellent mechanism for energy dissipation, and has been used for many years in automotive brakes to dissipate kinetic energy of motion. In the development of friction dampers, it is important to minimize stick-slip phenomena to avoid introducing high frequency excitation. Furthermore, compatible materials must be employed to maintain a consistent coefficient of friction over the intended life of the device. The Pall device is one of the damper elements utilizing the friction principle, which can be installed in a structure in an X-braced frame as illustrated in the figure:2.3 (Palland Marsh 1982).



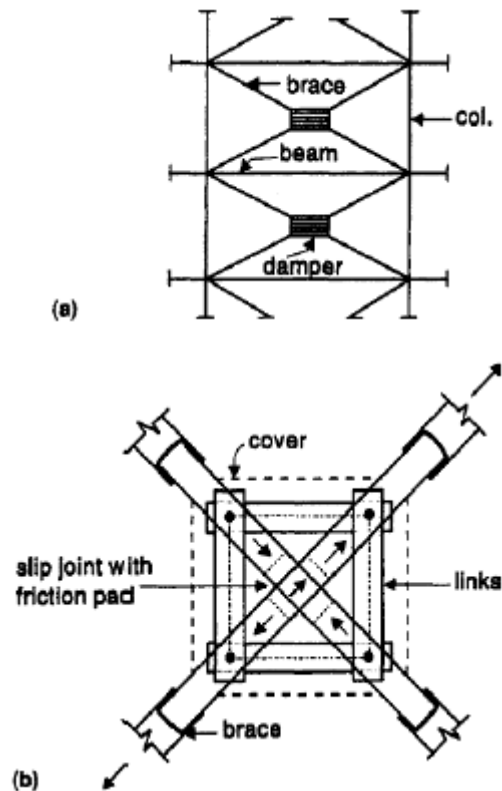
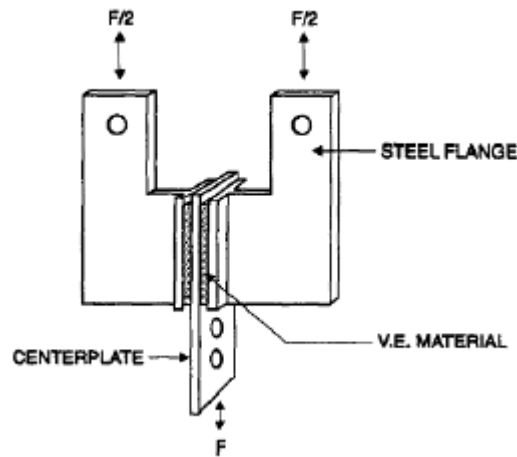


Figure 2.3 : Pall friction damper.

### 2.3.3 Viscoelastic dampers

The metallic and frictional devices described are primarily intended for seismic application. But, viscoelastic dampers find application in both wind and seismic application. Their application in civil engineering structures began in 1969 when approximately 10,000 visco-elastic dampers were installed in each of the twin towers of the World Trade Center in New York to reduce wind-induced vibrations. Further studies on the dynamic response of viscoelastic dampers have been carried out, and the results show that they can also be effectively used in reducing structural response due to large range of intensity levels of earthquake. Viscoelastic materials used in civil engineering structure are typical copolymers or glassy substances. A typical viscoelastic damper, developed by the 3M Company Inc., is shown in Fig.2.4 It consists of viscoelastic layers bonded with steel plates.



**Figure 2.4 :** Viscoelastic damper.

### 2.3.4 Viscous fluid dampers

Fluids can also be used to dissipate energy and numerous device configurations and materials have been proposed. Viscous fluid dampers, are widely used in aerospace and military applications, and have recently been adapted for structural applications (Constantinou et al. 1993). Characteristics of these devices which are of primary interest in structural applications, are the linear viscous response achieved over a broad frequency range, insensitivity to temperature, and compactness in comparison to stroke and output force. The viscous nature of the device is obtained through the use of specially configured orifices, and is responsible for generating damper forces that are out of phase with displacement. A viscous fluid damper generally consists of a piston in the damper housing filled with a compound of silicone or oil (Makris and Constantinou 1990; Constantinou and Symans 1992). A typical damper of this type is shown in Fig.2.5.

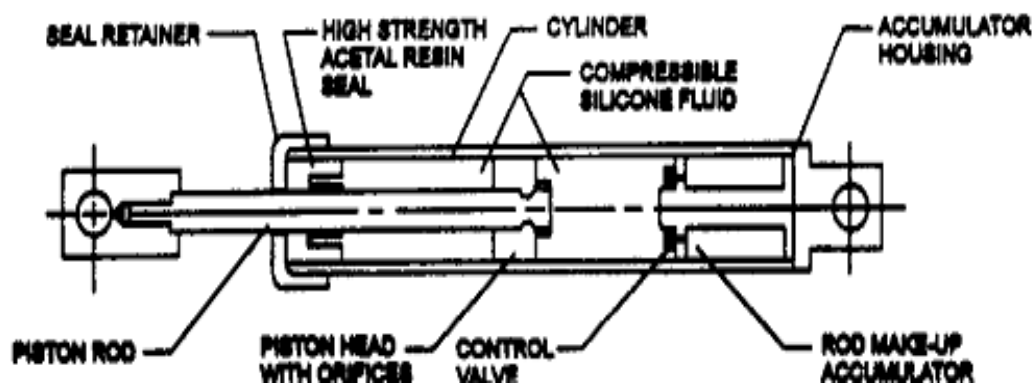


**Figure 2.5 :** Taylor device fluid damper.

### 2.3.5 Tuned liquid damper

A properly designed partially filled water tank can be utilized as a vibration absorber to reduce the dynamic motion of a structure and is referred to as a tuned liquid damper (TLD). Tuned liquid damper (TLD) and tuned liquid column damper (TLCD) impart indirect damping to the system and thus improve structural performance (Kareem, 1994). A TLD absorbs structural energy by means of viscous actions of the fluid and wave breaking. Tuned liquid column dampers (TLCDs) are a special type of tuned liquid damper (TLD) that rely on the motion of the liquid column in a U-shaped tube to counter act the action of external forces acting on the structure. The inherent damping is introduced in the oscillating liquid column through an orifice. The performance of a single-degree-of-freedom structure with a TLD subjected to sinusoidal excitations was investigated by Sun (1991), along with its application to the suppression of wind induced vibration by Wakahara et al. (1989). Welt and Modi (1989), were one of the first to suggest the usage of a TLD in buildings to reduce overall response during strong wind or earthquakes.

### 2.3.6 Tuned mass damper

The concept of the tuned mass damper (TMD) dates back to the 1940s (Den Hartog, 1947). It consists of a secondary mass with properly tuned spring and damping elements, providing a frequency-dependent hysteresis that increases damping in the primary structure. The success of such a system in reducing wind-excited structural vibrations is now well established. Recently, numerical and experimental studies have been carried out on the effectiveness of TMDs in reducing seismic response of structures (for instance, Villaverde, (1994))

## 2.4 The Equation Of Motion Of TMD

### 2.4.1 Concept of tuned mass damper using two mass system

The equation of motion for primary mass as shown in figure 2.6 is:

$$(1 + \bar{m}) \ddot{u} + 2\varepsilon\omega m \dot{u} + \omega^2 u = \frac{p}{m} - \bar{m} \ddot{u}_d \quad (2.1)$$

$\bar{m}$  is defined as the mass ratio,

$$\bar{m} = m_d/m \quad (2.2)$$

$$\omega^2 = k/m \quad (2.3)$$

$$C = 2\varepsilon m\omega \quad (2.4)$$

$$C_d = 2\varepsilon\omega_d m_d \quad (2.5)$$

where,  $\dot{u}$  is the velocity,  $\ddot{u}$  is the acceleration,  $\varepsilon$  is the damping factor of the primary mass.

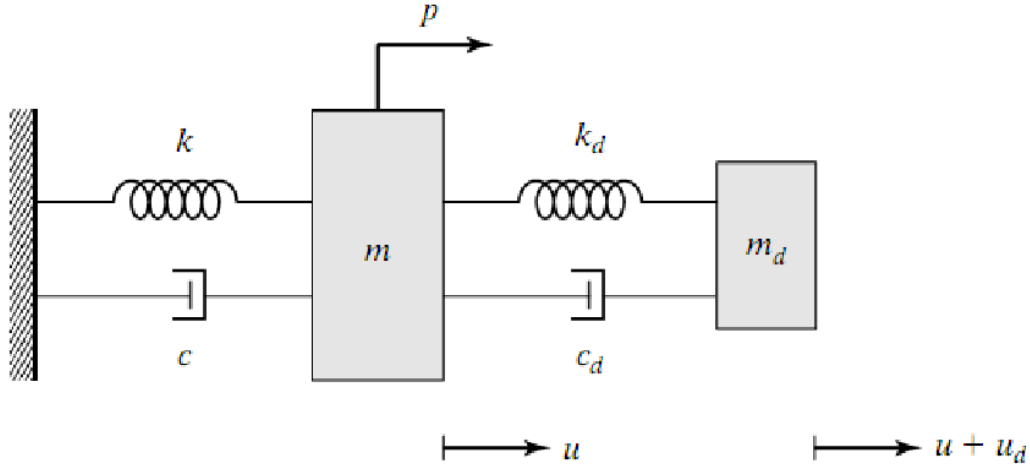


**Figure 2.6** : SDOD-TMD system.

The equation of motion for tuned mass is given by:

$$\ddot{u}_d + 2\varepsilon_d\omega_d\dot{u}_d + \omega_d^2 u_d = -\ddot{u} \quad (2.6)$$

The purpose of adding the mass damper is to control the vibration of the structure when it is subjected to a particular excitation. The mass damper is having the parameters; the mass  $m_d$ , stiffness  $k_d$ , and damping coefficient  $c_d$ . The damper is tuned to the fundamental frequency of the structure such that:

$$\omega_d = \omega \quad (2.7)$$

$$k_d = \bar{m}k \quad (2.8)$$

The primary mass is subjected to the following periodic sinusoidal excitation:

$$p = \hat{p} \sin \Omega t \quad (2.9)$$

then the response is given by:

$$u = \hat{u}_d \sin(\Omega t + \delta_1) \quad (2.10)$$

$$u_d = \hat{u}_d \sin(\Omega t + \delta_1 + \delta_2) \quad (2.11)$$

where  $\hat{u}$  and  $\delta$  denote the displacement amplitude and phase shift, respectively.

The critical loading scenario is the resonant condition, the solution for this case has the following form:

$$\hat{u} = \frac{\hat{p}}{m\kappa} \sqrt{1/(1 + (\frac{2\xi}{\bar{m}} + \frac{1}{2\xi_d})^2)} \quad (2.12)$$

$$\hat{u}_d = (\frac{1}{2\xi_d})\hat{u} \quad (2.13)$$

$$\tan \delta_1 = -(\frac{2\xi}{\bar{m}} + \frac{1}{2\xi_d}) \quad (2.14)$$

$$\tan \delta_2 = -\frac{\pi}{2} \quad (2.15)$$

The above expression shows that the response of the tuned mass is  $90^\circ$  out of phase with the response of the primary mass. This difference in phase produces the energy dissipation contributed by the damper inertia:

$$\hat{u} = \frac{\hat{p}}{k} (\frac{1}{2\xi_e}) \quad (2.16)$$

$$\delta_1 = -\frac{\pi}{2} \quad (2.17)$$

To compare these two cases, we can express Eq.2.12 in terms of an equivalent damping ratio:

$$\hat{u} = \frac{\hat{p}}{k} (\frac{1}{2\xi_e}) \quad (2.18)$$

Where

$$\xi_e = \frac{\bar{m}}{2} \sqrt{1/(1 + (\frac{2\xi}{\bar{m}} + \frac{1}{2\xi_d})^2)} \quad (2.19)$$

Equation 2.19 shows the relative contribution of the damper parameters to the total damping. Increasing the mass ratio magnifies the damping. However, since the added mass also increases, so there is a practical limit on it.

## 2.4.2 Tuned mass damper theory for SDOF systems.

Various cases ranging from fully undamped to fully damped conditions are considered and are presented as follows:

### 2.4.2.1 Undamped structure ,undamped TMD

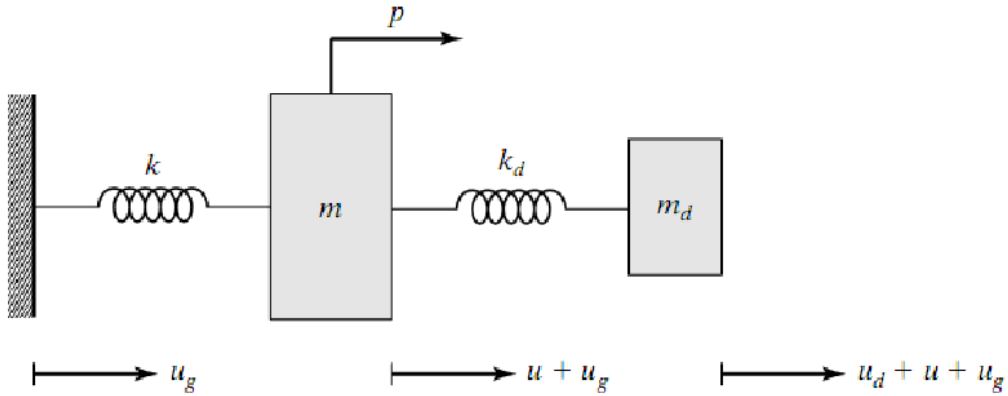


**Figure 2.7** : Undamped SDOF system coupled undamped TMD system.

Figure shows a SDOF system having mass  $m$  and stiffness  $k$ , subjected to both external forcing and ground motion. A tuned mass damper with mass  $m_d$ , and stiffness  $k_d$  is attached to the primary mass. The various displacement measures are  $u_g$  the absolute ground motion;  $u$ , the relative motion between the primary mass and the ground; and  $u_d$ , the relative displacement between the damper and the primary mass.

The equations for secondary mass and primary mass are as follows:

$$m_d(\ddot{u}_d + \ddot{u}) + k_d u_d = -m_d a_g \quad (2.20)$$

$$m\ddot{u} + ku - k_d u_d = -m a_g + p \quad (2.21)$$

where  $a_g$  is the absolute ground acceleration and  $p$  the loading applied to the primary mass. The excitation applied on the primary mass is considered to be periodic of frequency,  $\Omega$

$$a_g = \hat{a}_g \sin \Omega t \quad (2.22)$$

$$p = \hat{p} \sin \Omega t \quad (2.23)$$

Then the response is given by:

$$u = \hat{u} \sin \Omega t \quad (2.24)$$

$$u_d = \hat{u}_d \sin \Omega t \quad (2.25)$$

and substituting the values of  $u$  and  $u_d$ , the equations 2.20 and 2.21 can be written as follows:

$$(-m_d \Omega^2 + k_d) \hat{u}_d - m_d \Omega^2 \hat{u} = -m_d \hat{a}_g \quad (2.26)$$

$$k_d \hat{u}_g + (-m \Omega^2 + k) \hat{u} = -m \hat{a}_g + p \quad (2.27)$$

The solutions for  $\hat{u}$  and  $\hat{u}_d$  are given by:

$$\hat{u} = \frac{\hat{p}}{k \left( \frac{1 - \rho_d^2}{D_1} \right)} - m \hat{a}_g / k \left( (1 + \bar{m} - \rho_d^2) / D_1 \right) \quad (2.28)$$

$$\hat{u}_d = - \left( \frac{\hat{p}}{k_d} \right) \rho^2 + \left( \frac{m \hat{a}_g}{k_d} \right) \quad (2.29)$$

Where

$$D_1 = [1 - \rho^2][1 - \rho_d^2] - \bar{m} \rho^2 \quad (2.39)$$

and the  $p$  term is a dimensionless quantity i.e a frequency ratio given by:

$$\rho = \frac{\Omega}{\omega} = \Omega / \sqrt{k/m} \quad (2.40)$$

$$\rho_d = \Omega / \omega_d = \Omega / \sqrt{k_d/m_d} \quad (2.41)$$

Selecting appropriate combination of the mass ratio and damper frequency ratio such that:

$$\rho_d^2 + \bar{m} = 0 \quad (2.42)$$

reduces the solution to

$$\hat{u} = \left( \frac{\hat{p}}{k} \right) \quad (2.43)$$

$$\hat{u}_d = - \left( \frac{\hat{p}}{k_d} \right) \rho^2 + \left( \frac{m \hat{a}_g}{k_d} \right) \quad (2.44)$$

A typical range for  $\bar{m}$  is 0.01 to 0.1. Then the optimal damper frequency is very close to the forcing frequency. The exact relationship follows from Eq. 2.42

$$\omega_d |opt| = \Omega / \sqrt{1 + \bar{m}} \quad (2.43)$$

the corresponding damper stiffness is determined as

$$k_d|opt| = [\omega_{dopt}]^2 m_d = (\Omega^2 m \bar{m}) / (1 + \bar{m}) \quad (2.44)$$

### 2.4.2.2 Undamped structure ,damped TMD

The equations of motion for this case are:

$$m_d \ddot{u}_d + c_d \dot{u}_d + k_d u_d + m_d \ddot{u} = -m_d a_g \quad (2.45)$$

$$m \ddot{u} + k u - c_d \dot{u}_d - k_d u_d = -m a_g + p \quad (2.46)$$

The inclusion of the damping terms in Eqn 2.45 and 2.46 produces a phase shift between the periodic excitation and the response. So, it is convenient to consider the solution expressed in terms of complex quantities. Then the excitation is expressed as

$$a_g = \hat{a}_g e^{i\Omega t} \quad (2.47)$$

$$p = \hat{p} e^{i\Omega t} \quad (2.48)$$

Where  $u_g$  and  $p$  are real quantities.

Then the response is given by:

$$u = \bar{u} e^{i\Omega t} \quad (2.49)$$

$$u_d = \bar{u}_d e^{i\Omega t} \quad (2.50)$$

where the response amplitudes,  $u$  and  $u_d$ , are considered as complex quantities.

Substituting Eqn 2.49 and 2.50 in the equations 2.45 and 2.46 and cancelling  $e^{i\Omega t}$  from both sides results in the following equations

$$[-m_d \Omega^2 + i c_d \Omega + k_d] \bar{u}_d - m_d \Omega^2 \bar{u} = -m_d \hat{a}_g \quad (2.51)$$

$$-[i c_d \Omega + k_d] \bar{u}_d + [-m \Omega^2 + k] \bar{u} = -m \hat{a}_g + \hat{p} \quad (2.52)$$

The solution of the governing equations is:

$$\bar{u} = \frac{\hat{p}}{k D_2 [f^2 - \rho^2 + i 2 \varepsilon_d \rho f]} - \hat{a}_g m / k D_2 [(1 + \bar{m}) f^2 - \rho^2 + i 2 \varepsilon_d \rho f (1 + \bar{m})] \quad (2.53)$$



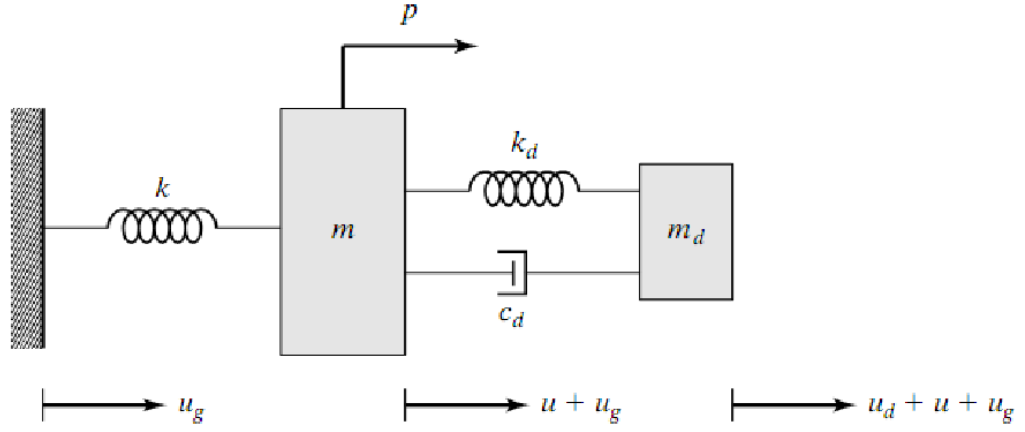


**Figure 2.8** : Undamped SDOF system coupled damped TMD system.

$$\bar{u}_d = \left( \frac{\hat{p}\rho^2}{kD_2} \right) - \left( \frac{\hat{a}_g m}{kD_2} \right) \quad (2.54)$$

Where

$$D_2 = [1 - \rho^2][f^2 - \rho^2] - \bar{m}\rho^2 f^2 + i2\varepsilon_d \rho f [1 - \rho^2(1 + \bar{m})] \quad (2.55)$$

$$f = \omega_d / \omega \quad (2.56)$$

Converting the complex solutions to polar form leads to the following expressions:

$$\bar{u} = \frac{\hat{p}}{k} H_1 e^{i\delta_1} - \left( \frac{\hat{a}_g m}{k} \right) H_2 e^{i\delta_2} \quad (2.57)$$

$$\hat{u}_d = \frac{\hat{p}}{k} H_3 e^{-i\delta_3} - \left( \frac{\hat{a}_g m}{k} \right) H_4 e^{-i\delta_3} \quad (2.58)$$

where the  $H$  factors define the amplification of the pseudo-static responses, and the  $\delta$ 's are the phase angles between the response and the excitation. The various  $H$  terms are as follows

$$H_1 = (\sqrt{[f^2 - \rho^2]^2 + [2\varepsilon_d \rho f]^2}) / |D_2| \quad (2.59)$$

$$H_2 = \sqrt{[(1 + \bar{m})f^2 - \rho^2]^2 + [2\varepsilon_d \rho f(1 + \bar{m})]^2} \quad (2.60)$$

$$H_3 = \rho^2 / |D_2| \quad (2.61)$$

$$|D_2| = \sqrt{([1 - \rho^2][f^2 - \rho^2] - \bar{m}\rho^2 f^2)^2 + (2\varepsilon_d \rho f [1 - \rho^2(1 + \bar{m})])^2} \quad (2.62)$$

## 2.5 The Equation Of Motion Of ATMD

When n-degree-of-freedom (N-DOF) systems with “m” ATMDs are subjected to external excitation and control forces, they govern equations of motion and can be written as

$$M\ddot{q}(t) + C\dot{q}(t) + Kq(t) = L.u(t) + H.fe(t) \quad (2.63)$$

where M, C, and K are the mass, damping, and stiffness matrices of the structure, respectively, of the order (n+m)×(n+m). If “q” in Equation 2.63 is taken as the relative displacement with respect to the ground, then mass matrix M is considered to be diagonal. Damping matrix C takes a form similar to K.

$$M = \begin{bmatrix} m_1 & 0 & 0 & \cdot & \cdot & 0 \\ 0 & m_2 & 0 & \cdot & \cdot & 0 \\ 0 & 0 & \cdot & \cdot & \cdot & 0 \\ \cdot & \cdot & \cdot & m_{i=j} & \cdot & \cdot \\ \cdot & \cdot & \cdot & \cdot & \cdot & \cdot \\ 0 & 0 & 0 & \cdot & \cdot & m_n \end{bmatrix} \quad (2.64)$$

$$C = \begin{bmatrix} c_1 + c_2 & -c_2 & 0 & \cdot & \cdot & 0 \\ -c_2 & c_2 + c_3 & -c_3 & \cdot & \cdot & 0 \\ 0 & -c_3 & \cdot & \cdot & \cdot & 0 \\ \cdot & \cdot & \cdot & c_i + c_{i+1} & -c_{i+1} & \cdot \\ \cdot & \cdot & \cdot & -c_{i+1} & \cdot & -c_n \\ 0 & 0 & 0 & \cdot & -c_n & c_n \end{bmatrix} \quad (2.65)$$

$$K = \begin{bmatrix} k_1 + k_2 & -k_2 & 0 & \cdot & \cdot & 0 \\ -k_2 & k_2 + k_3 & -k_3 & \cdot & \cdot & 0 \\ 0 & -k_3 & \cdot & \cdot & \cdot & 0 \\ \cdot & \cdot & \cdot & k_i + k_{i+1} & -k_{i+1} & \cdot \\ \cdot & \cdot & \cdot & -k_{i+1} & \cdot & -k_n \\ 0 & 0 & 0 & \cdot & -k_n & k_n \end{bmatrix} \quad (2.66)$$

$$q = [q_1 q_2 q_3 \dots q_n q_d] \quad (2.67)$$

Displacement vector is defined as  $q(t) = (m + n) \times 1$  and  $q_i$  is the displacement of ith floor relative to ground ( $i = 1, 2, \dots, N$ ),  $q_d$  is the displacement of damper relative to ground, control force vector,  $u(t)$ , is of the order  $l \times 1$ , and  $fe(t)$  is the external dynamic force vector of dimension  $r \times 1$ ,  $L$  and  $H$  are  $(n + m) \times l$  and  $(n + m) \times r$  location matrices, which define locations of the control forces and the external excitations, respectively. A state-space representation of Equation 2.63 can be written as:

$$\{\dot{x}\} = [A]\{x\} + [B]\{u\} + [E]fe \quad (2.68)$$

Where

$$\{x\} = \begin{bmatrix} q(t) \\ \dot{q}(t) \end{bmatrix} \quad (2.69)$$

$\{x\}$  is the state vector of dimension  $2(m + n) \times 1$ , and

$$\{u\} = -\{G\}\{x\} \quad (2.70)$$

$\{G\}$  is the gain matrix;

$$A = \begin{bmatrix} 0 & I \\ -M^{-1}K & -M^{-1}C \end{bmatrix} \quad (2.71)$$

$$B = \begin{bmatrix} 0 \\ M^{-1}L \end{bmatrix} \quad (2.72)$$

$$E = \begin{bmatrix} 0 \\ M^{-1}H \end{bmatrix} \quad (2.73)$$

$2(m + n) \times 2(m + n)$ ,  $2(m + n) \times l$ , and  $2(m + n) \times r$  are the system matrix, control location, and external excitation location matrices, respectively. The matrices “0” and “I” in Equations 2.68 to 2.70 denote the zero and identity matrices of size  $(m + n) \times (m + n)$ , respectively.

## 2.6 Optimal Linear Control (LQR)

The LQR control method is a widely used technique for controlling active devices. The control force in this method is calculated based on the velocity and displacement of structures. In this algorithm, minimization of a quadratic performance index  $J$  of the following form is carried out:

$$J = \int_0^{t_f} (x^T(t)Qx(t) + u^T Ru(t))dt \quad (2.74)$$

Matrices  $Q$  and  $R$  are weight matrices for the optimization of  $J$  and it is assumed that  $Q$  and  $R$  are semi-positive definite and positive definite, respectively. The control

forces are calculated based on solving the algebraic Riccati equation. The control forces  $u(t)$  and gain matrix  $G$  is obtained from the minimization of the performance index  $J$ , as follows:

$$u(t) = -\frac{1}{2} R^{-1} B^T P(t) x(t) = Gx(t) \quad (2.75)$$

where  $G$  is called the gain matrix and matrix  $P$  is the solution of the classical Riccati equation that is obtained from:

$$A^T P + PA - (PB + N)R^{-1}(B^T P + N^T) + Q = 0 \quad (2.76)$$

The weighting matrices  $[Q]$  and  $[R]$  in the classical LQR formulation represent the relative importance to be assigned to the structural response or the control effort respectively. A relative larger weight would impose a higher penalty on the corresponding term for optimization of the total cost functional. Hence, if the reduction of the structural response is of prime concern irrespective of the cost of control or even at the expense of higher cost of control, a lower weighting force is to assigned to term associated with the calculation of the control effort and vice versa. This concept of using the weighting matrices works well in the classical LQR case when there is no necessity of updating the weighting matrices or changing the assignment of relative importance of the structural response and the control effort. However, there may be cases for systems subjected to external excitations such that the response has time-varying frequency content due to the variation in the excitation frequency over time. The closeness of the frequency of excitation to the natural frequencies of the system and its amplitude may require a revised weighting function on the term associated with the control to have a better effectiveness. Earthquake excitations are known to be highly non-stationary in both amplitude and frequency content. The excitation causes the structural response to be non-stationary with the possibility of short duration impulsive nature to sudden change in the frequency to long periods. To account for this, the classical LQR formulation has to be modified to accommodate the importance of the local time-varying frequency content, which if close to the natural frequencies of vibration of the system results in a large response locally. These transient phenomena could be captured by the use of time-frequency analysis.

## **2.7 Wavelet Method**

### **2.7.1 History of wavelets**

From an historical point of view, wavelet analysis is a new method, though its mathematical underpinnings date back to the work of Joseph Fourier in the nineteenth century. Fourier laid the foundations with his theories of frequency analysis, which proved to be enormously important and influential. The attention of researchers gradually turned from frequency-based analysis to scale-based analysis when it started to become clear that an approach measuring average fluctuations at different scales might prove less sensitive to noise. The first recorded mention of what we now call a "wavelet" seems to be in 1909, in a thesis by Alfred Haar. The concept of wavelets in its present theoretical form was first proposed by Jean Morlet and the team at the Marseille Theoretical Physics Center working under Alex Grossmann in France. The methods of wavelet analysis have been developed mainly by Y. Meyer and his colleagues, who have ensured the methods' dissemination. The main algorithm dates back to the work of Stephane Mallat in 1988. Since then, research on wavelets has become international. Such research is particularly active in the United States, where it is spearheaded by the work of scientists such as Ingrid Daubechies, Ronald Coifman, and Victor Wickerhauser. Barbara Burke Hubbard describes the birth, the history, and the seminal concepts in a very clear text. See *The World According to Wavelets*, A.K. Peters, Wellesley, 1996. The wavelet domain is growing up very quickly. A lot of mathematical papers and practical trials are published every month.

### **2.7.2 Advantages of wavelet transform to fourier transform**

Fourier analysis is used as a starting point to introduce the wavelet transforms, and as a benchmark to demonstrate cases where wavelet analysis provides a more useful characterization of signals than Fourier analysis. Fourier analysis was occasionally compared to wavelets. The basic Fourier transform gives a global picture of a data set's spectrum, whereas wavelet transforms are more better way to examine a signal, a function or an image. In addition, wavelet transforms also provide information on where or when each frequency component is occurring. These advantages are

especially embraced in studying non-stationary or inhomogeneous objects. Mathematically, the process of Fourier analysis is represented by the Fourier transform:

$$F(\omega) = \int_{-\infty}^{\infty} f(t)e^{-j\omega t} dt \tag{2.77}$$

which is the integral (sum) over all time of the signal  $f(t)$  multiplied by a complex exponential. Recall that a complex exponential can be broken down into real and imaginary sinusoidal components. Note that the Fourier transform maps a function of a single variable into another function of a single variable. The integral defining the Fourier transform is an inner product. For each value of  $\omega$ , the integral (or sum) over all values of time produces a scalar,  $F(\omega)$ , that summarizes how similar the two signals are. These complex-valued scalars are the Fourier coefficients. Conceptually, multiplying each Fourier coefficient,  $F(\omega)$ , by a complex exponential (sinusoid) of frequency  $\omega$  yields the constituent sinusoidal components of the original signal. Graphically, the process looks like:

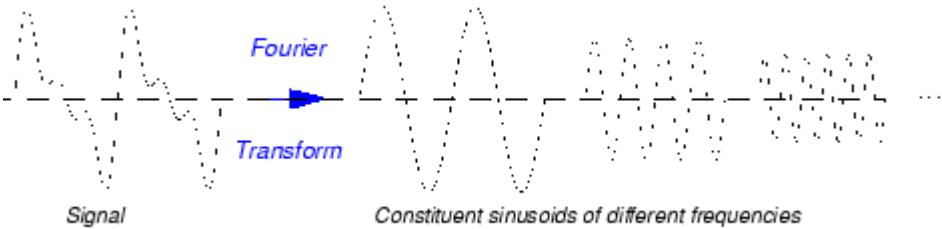


**Figure 2.9:** Fourier transform

Because  $e^{j\omega t}$  is complex-valued,  $F(\omega)$  is, in general, complex-valued. If the signal contains significant oscillations at an angular frequency of  $\omega_0$ , the absolute value of  $F(\omega_0)$  will be large. By examining a plot of  $|F(\omega_0)|$  as a function of angular frequency, it is possible to determine what frequencies contribute most to the variability of  $f(t)$ .

**2.7.3 Continues wavelet transform**

Like the Fourier transform, the continuous wavelet transform (CWT) uses inner products to measure the similarity between a signal and an analyzing function. In the

Fourier transform, the analyzing functions are complex exponentials,  $e^{j\omega t}$ . The resulting transform is a function of a single variable,  $\omega$ . In the short-time Fourier transform, the analyzing functions are windowed complex exponentials,  $(t)e^{j\omega t}$ , and the result is a function of two variables. The STFT coefficients,  $F(\omega, \tau)$  represent the match between the signal and a sinusoid with angular frequency  $\omega$  in an interval of a specified length centered at  $\tau$ .

In the CWT, the analyzing function is a wavelet,  $\psi$ . The CWT compares the signal to shifted and compressed or stretched versions of a wavelet. Stretching or compressing a function is collectively referred to as dilation or scaling and corresponds to the physical notion of scale. By comparing the signal to the wavelet at various scales and positions, you obtain a function of two variables. The two-dimensional representation of a one-dimensional signal is redundant. If the wavelet is complex-valued, the CWT is a complex-valued function of scale and position. If the signal is real-valued, the CWT is a real-valued function of scale and position.

For a scale parameter,  $a > 0$ , and position,  $b$ , the CWT is:

$$C(a, b; f(t), \Psi(t)) = \int_{-\infty}^{\infty} f(t) \frac{1}{\sqrt{a}} \Psi^* \left( \frac{t-b}{a} \right) dt \quad (2.78)$$

Where  $*$  denotes the complex conjugate. Not only do the values of scale and position affect the CWT coefficients, the choice of wavelet also affects the values of the coefficients. By continuously varying the values of the scale parameter,  $a$ , and the position parameter,  $b$ , you obtain the cwt coefficients  $C(a, b)$ . Note that for convenience, the dependence of the CWT coefficients on the function and analyzing wavelet has been suppressed. Multiplying each coefficient by the appropriately scaled and shifted wavelet yields the constituent wavelets of the original signal.

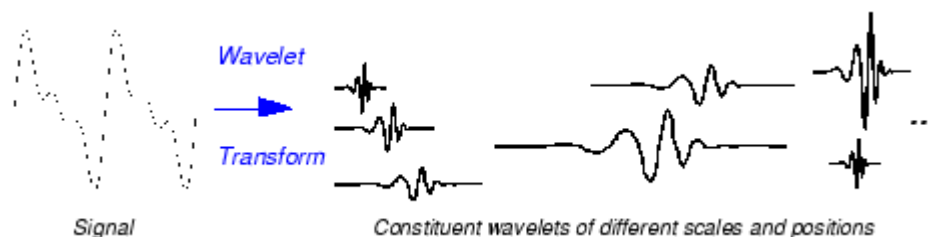


**Figure 2.10 :** Continues wavelet transform

There are many different admissible wavelets that can be used in the CWT. While it may seem confusing that there are so many choices for the analyzing wavelet, it is actually a strength of wavelet analysis. Depending on what signal features you are trying to detect, you are free to select a wavelet that facilitates your detection of that feature. For example, if you are trying to detect abrupt discontinuities in your signal, you may choose one wavelet. On the other hand, if you are interesting in finding oscillations with smooth onsets and offsets, you are free to choose a wavelet that more closely matches that behavior.

#### **2.7.4 Discrete wavelet transform**

Calculating wavelet coefficients at every possible scale is a fair amount of work, and it generates an awful lot of data. What if we choose only a subset of scales and positions at which to make our calculations? It turns out, rather remarkably, that if we choose scales and positions based on powers of two — so-called dyadic scales and positions — then our analysis will be much more efficient and just as accurate. We obtain such an analysis from the discrete wavelet transform (DWT). An efficient way to implement this scheme using filters was developed in 1988 by Mallat . The Mallat algorithm is in fact a classical scheme known in the signal processing community as a two-channel subband coder (see page 1 of the book *Wavelets and Filter Banks*, by Strang and Nguyen [StrN96]). This very practical filtering algorithm yields a fast wavelet transform — a box into which a signal passes, and out of which wavelet coefficients quickly emerge. Let's examine this in more depth.

##### **2.7.4.1 One-Stage filtering**

For many signals, the low-frequency content is the most important part. It is what gives the signal its identity. The high-frequency content, on the other hand, imparts flavor or nuance. Consider the human voice. If you remove the high-frequency components, the voice sounds different, but you can still tell what's being said. However, if you remove enough of the low-frequency components, you hear gibberish. In wavelet analysis, we often speak of approximations and details. The approximations are the high-scale, low-frequency components of the signal. The details are the low-scale, high-frequency components.

The filtering process, at its most basic level, looks like this.



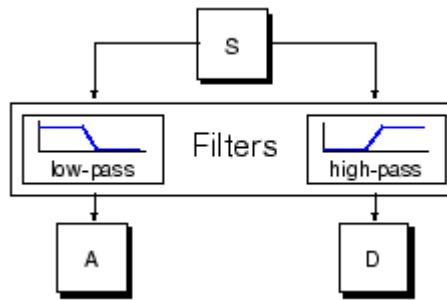


**Figure 2.11 :** Wavelet filtering process

The original signal,  $S$ , passes through two complementary filters and emerges as two signals. Unfortunately, if we actually perform this operation on a real digital signal, we wind up with twice as much data as we started with. Suppose, for instance, that the original signal  $S$  consists of 1000 samples of data. Then the resulting signals will each have 1000 samples, for a total of 2000. These signals  $A$  and  $D$  are interesting, but we get 2000 values instead of the 1000 we had. There exists a more subtle way to perform the decomposition using wavelets. By looking carefully at the computation, we may keep only one point out of two in each of the two 2000-length samples to get the complete information. This is the notion of down sampling. We produce two sequences called  $cA$  and  $cD$ .



**Figure 2.12 :** Wavelet down sampling process.

The process on the right, which includes down sampling, produces DWT coefficients. To gain a better appreciation of this process, let's perform a one-stage discrete wavelet transform of a signal. Our signal will be a pure sinusoid with high-frequency noise added to it. Here is our schematic diagram with real signals inserted into it.

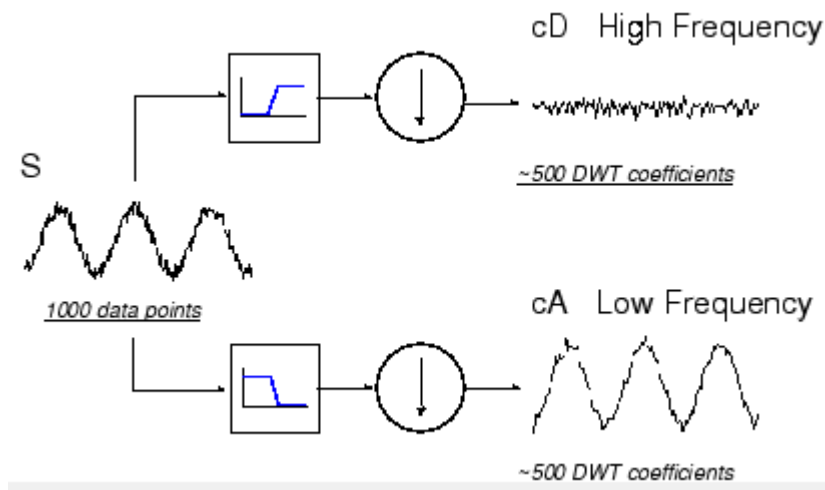


**Figure 2.13 :** Wavelet schematic diagram with real signals inserted into it.

You may observe that the actual lengths of the detail and approximation coefficient vectors are slightly more than half the length of the original signal. This has to do with the filtering process, which is implemented by convolving the signal with a filter. The convolution "smears" the signal, introducing several extra samples into the result.

#### 2.7.4.2 Multiple-level decomposition

The decomposition process can be iterated, with successive approximations being decomposed in turn, so that one signal is broken down into many lower resolution components. This is called the wavelet decomposition tree.

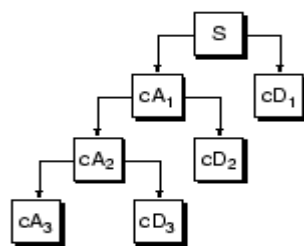


**Figure 2.14 :** Wavelet decomposition tree.

Looking at a signal's wavelet decomposition tree can yield valuable information.

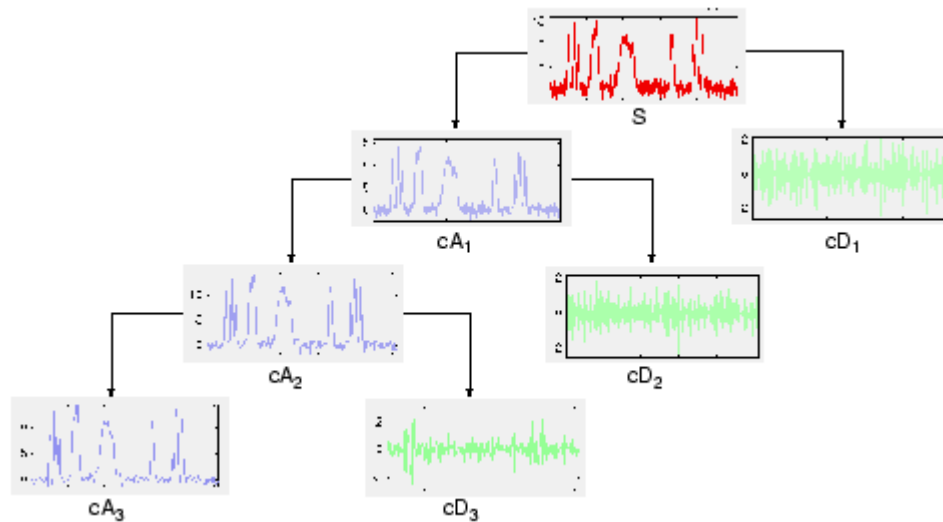


**Figure 2.15 : Wavelet decomposition can be continued indefinitely.**

Since the analysis process is iterative, in theory it can be continued indefinitely. In reality, the decomposition can proceed only until the individual details consist of a single sample or pixel. In practice, you'll select a suitable number of levels based on the nature of the signal, or on a suitable criterion such as entropy.



### 3. PROPOSED METHOD

#### 3.1 Introduction

Excitations, such as earthquakes, are extremely non-stationary in amplitude and frequency. Therefore, the probability of existence of the natural frequency of the system, in the frequency domain of ground motion, is high, which causes resonance in the system. In LQR classic method the weighting matrices are determined offline and are not updated when the structure is subjected to external excitations. Therefore, to account for the effect of resonance, the classical LQR has to be modified by adapting weighting matrices. The control effort will be more costly if the components of R are large relative to those of Q, for the whole period of external force. Therefore, the response in these undesirable frequency bands must be mitigated without increasing the gain over all the frequency bands, by changing the control energy weighting matrices in these bands. In other words, the weighting matrices should change if the local frequency content of earthquake is close to the natural frequency of the system. These transient phenomena could be captured by the use of time-frequency analysis. Wavelet analysis has been recognized as one of the most powerful and versatile time-frequency tools, which has the ability to resolve frequency locally in time. Apart from being able to provide the most optimized time-frequency resolution it has the advantage of providing a variety of different basis functions for analysis and fast exact reconstruction techniques using multi-resolution analysis. The results from the wavelet analysis of the response in real time have been used to modify the classical LQR problem. The use of wavelet analysis enables the capturing of the local variation in the frequency content with an adaptive updating of the weighting in the WAVELET- LQR formulation.

#### 3.2 Decomposition Of Signal

In this study, the real time DWT controller is updated at regular time steps from the initial time ( $t_0$ ) until the current time ( $t_c$ ) to achieve the local energy distribution of the motivation over frequency bands. The time interval under consideration  $[t_0, t_c]$  is sub-divided into time window bands. The time of  $i_{th}$  window is  $[t_{i-1}, t_i]$  of which the signal can be decomposed into time frequency bands by wavelet. Through discrete wavelet transform (DWT) with multi resolution analysis (MRA) algorithm

the exact decomposition of signals over a time window bands are obtained in real time. The local energy content at different frequency bands over the considered time window are given by the MRA. It is obvious, the frequency contains maximum energy is domain frequency of that window. When the domain frequency of each window closes to the natural frequency of the system, the resonances occurred in the structure. This causes high displacement response in system.

The capability of the wavelet for carrying out time frequency analysis has been exploited in this study to resolve frequency locally in time.  $W_f(a, b)$ , CWT of a signal  $f(t)$ , is defined as

$$W_f = \frac{1}{\sqrt{|a|}} \int_{-\infty}^{\infty} f(t) \Psi^* \left( \frac{t-b}{a} \right) dt \quad (3.1)$$

Where (“ $\Psi$ ”) is a continuous function in both the time domain and the frequency domain called the mother wavelet and  $\Psi^*$  represents the complex conjugate of a base function. “ $a$ ” and “ $b$ ” are scale and translation parameters, respectively. The scaling parameter, “ $a$ ,” represents the frequency content of the wavelet. The translation parameter, “ $b$ ,” represents the location of wavelet in time. Thus, in comparison to the Fourier transform, the basic function of the wavelet transform retains the time zone, as well as the frequency zone. The main idea of DWT is the same as that of CWT. In DWT, the scale parameter “ $a$ ” and the translation parameter “ $b$ ” are discretized by using the dyadic scale, that is:

$$a = 2^j \quad (3.2)$$

$$b = k.2^j \quad (3.3)$$

$$j, k \in \mathbb{Z} \quad (3.4)$$

where  $z$  is a set of positive integers. In this study, the following relationship is used to compute the pseudo-frequencies corresponding to that scale (MATLAB, 2010):

$$F_a = \frac{F_c}{\alpha \cdot \Delta} \quad (3.5)$$

where “ $\alpha$ ” is a scale, “ $\Delta$ ” is the sampling period,  $F_c$  is the frequency maximizing the Fourier amplitude of the wavelet modulus (center frequency in Hz), and  $F_a$  is the pseudo-frequency corresponding to the scale “ $a$ ,” in Hz. In the case of DWT, the wavelet plays the role of dyadic filter. The DWT analyzes the signal by implementing a wavelet filter of a particular frequency band to propagate along a time axis. The signal can be decomposed to wavelet details and wavelet approximations at various levels, as follows:

$$f(t) = A_j + \sum_{j \leq J} D_j \quad (3.6)$$

where  $D_j$  denotes the wavelet detail and  $A_j$  stands for the wavelet approximation, respectively. DWT can be very useful for real-time control of structures, because it can detect the time of earthquake frequency change efficiently. The exclusive range of frequency of  $D_j$  is denoted as follows:

frequency range of level

$$j = [f_{1j}, f_{2j}] \quad (3.7)$$

where  $f_{1j}$  and  $f_{2j}$  are expressed as follows:

$$f_{1j} = \frac{2^{-j-1}}{\Delta_t} \quad (3.8)$$

$$f_{2j} = \frac{2^{-j}}{\Delta_t} \quad (3.9)$$

where  $\Delta_t$  is the time step of  $f(t)$ .

To mitigate the displacement responses of structure, the high control force is needed. In order to mitigate the responses of structure, it is suitable to decrease the value of the control energy weighting matrix  $[R]$ . The advantage of this local optimal solution is that it has the ability to change the value of the matrix  $R$  on special frequency in contrast to the classical LQR which is a global optimal solution. To achieve this, the cost function integral is developed with weighing matrices of each of the windows,  $[Q]_i$  and  $[R]_i$ . The cost function is given by

$$J_i = \int_{t_{i-1}}^{t_i} (x^T(t)Q_i x(t) + u^T R_i u(t)) dt \quad (3.10)$$

$$\{u\} = -[G]_i \{x\} \quad (3.11)$$

Where  $[G]_i$ , the gain matrix of the  $i_{th}$  window, is employed to achieve the desired control of the response. The gain matrix  $[G]_i$ , in the steady-state case is obtained by solution of Riccati algebraic equation similar to the traditional LQR problem but using the updated weighting matrices  $[Q]_i$  and  $[R]_i$ . The  $2(n + m) \times 2(n + m)$  state weight matrix  $Q$  is considered to be diagonal with the following structure:

$$[Q] = \begin{bmatrix} Q_{11} & 0 \\ 0 & Q_{22} \end{bmatrix} \quad (3.12)$$

The diagonal matrix component  $Q_{11}$  and  $Q_{22}$  contain the weights associated with the relative displacements and velocities, respectively. The weighting matrices for the



response states are assumed to have a constant value for total time duration. The control energy weighting matrices are updated for every time window by a scalar multiplier and can be defined as:

$$[R]_i = [\delta]_i[I] \quad (3.13)$$

where  $\delta_i$ , is a scalar parameter used to scale the weighting matrix and is obtained based on the time-frequency analysis of a response state. Hence, the scalar parameter of gain matrix can be written as:

$$\begin{aligned} \delta_i &\neq 1 && \text{if frequency of excitation is closed to natural frequency of system} \\ \delta_i &= 1 && \text{Otherwise} \end{aligned}$$

The value of  $\delta_i$  has been proposed less than one when the resonance happens. This makes it possible to change the weighting matrices for different frequency bands. Updating weighting matrix for the control effort  $[R]$  leading to the algebraic Riccati equation in a steady state case for each of the windows. The updated weighting matrix and optimal control gains are obtained for each of windows independent of the neighboring windows. In other words, in solution of modified optimal control problem does not need to consider the transition conditions between two windows. In the WAVELET-LQR problem, the total duration of the external excitation is subdivided into a number of time windows. For each of these windows, the cost functional is to be minimized subject to the constraint given by Eq.2.65 by updating the weight matrices online.

The control energy weighting matrices are reduced when the structure has significant high value of displacement response. This reduction of weighting matrices sets off the lesser displacement without penalty. Therefore, the positive aspect of WAVELET-LQR is that, the gain matrices are adaptively calculated by using the time varying weighting matrices depending on online response characteristics instead of considering the fixed matrix which chooses offline.

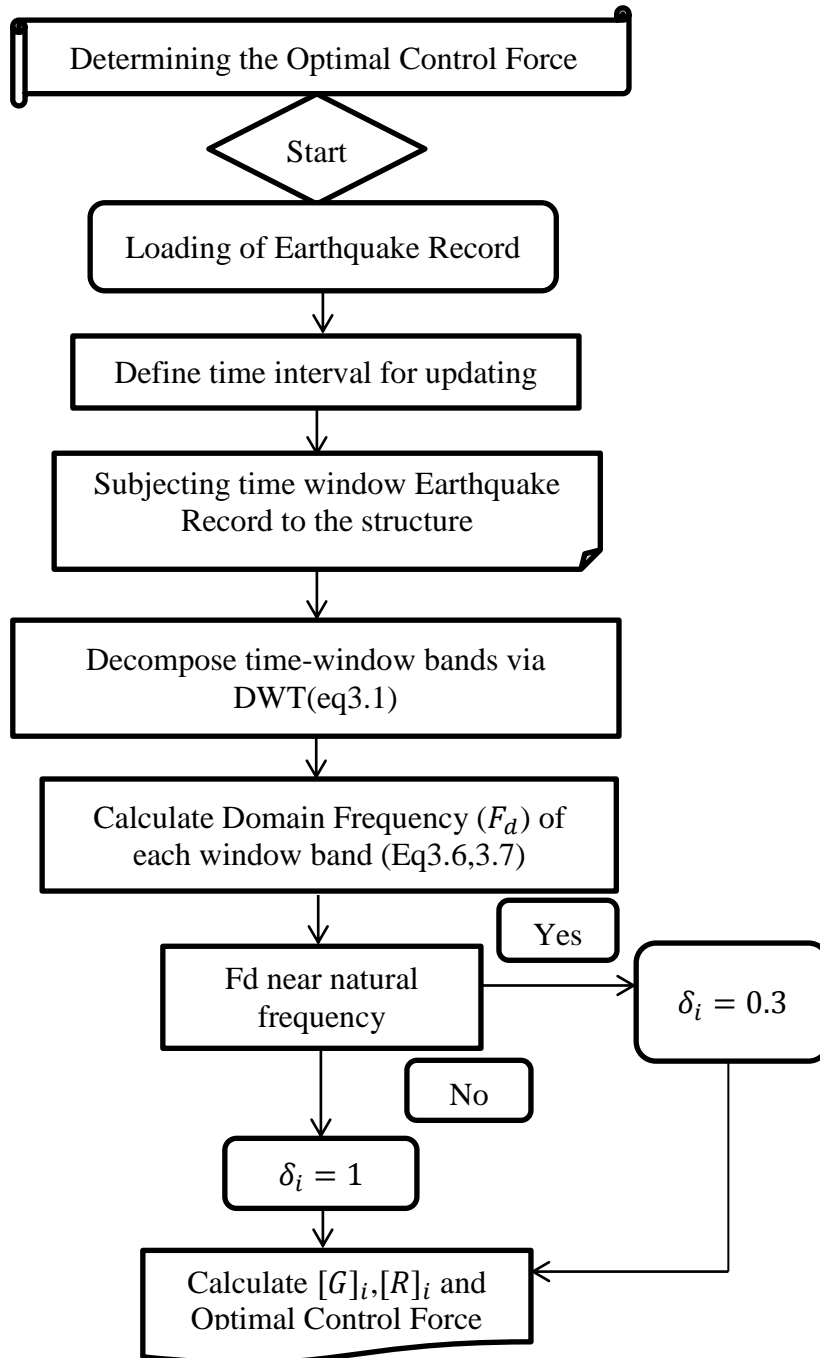


**Figure 3.1:** Flowchart of proposed method.

## 4. NUMERICAL EXAMPLES

### 4.1 Introduction

In this section, the results of dynamic analysis of the typical MDOF structure with only one ATMD on the top floor are discussed. To illustrate the potential application of the proposed method an example of a 10-storey shear-frame building structure which has been excited by a number of near fault pulse-like earthquake ground motions has been considered.

### 4.2 Results

The structure represents a typical shear building with 10 stories, which has the lumped mass at top storey. The masses and the stiffness at each storey are supposed to be 10 ton and  $2 \times 10^6 N/m$ , respectively. The modal damping ratio is uniformly assumed to be 2% for each mode. The TMD frequency is assumed to be close to the building's first modal frequency; that is, 2.11 rad/s. The mass and damping ratio of TMD is supposed to be 3% of the total mass of the system and 7%, respectively. The ATMD switches on when the displacement of the top floor is more than the allowable displacement of structure, which is assumed to be one thousandth of the height of the structure. The parameter  $\delta$  used for scaling the weighting matrices is assumed 0.3 when the central frequency of each window band is close to the natural frequency of the MDOF system, and for others frequencies is assumed to be 1. Hence, the weighting matrix component  $[R]$ , equals to  $\delta[I]$  for resonance frequency bands and for the rest of the frequency bands it is kept as  $[I]$ .

In as much as the diagonal matrices  $Q_{11}$  and  $Q_{22}$  contain the weights associated with the relative displacements and the relative velocities, respectively, these matrices are chosen as

$$Q_{11} = \text{diag}(1, 1, 1, 1, 1, 1, 1, 1, 1, 1, 0.001)$$

$$Q_{22} = \text{diag}(1, 1, 1, 1, 1, 1, 1, 1, 1, 1, 0.001)$$

The state-weighting matrix  $Q$  is chosen and is similar to classic LQR for all frequency bands. Daubechies wavelet of order 4 (db4), is used as a mother wavelet to

decompose the time history of acceleration for different window bands, to determine the frequency distribution of each band. The Daubechies wavelets have reasonably good localization in time and frequency to capture the effects of local frequency content in a time signal, and allow for fast decomposition by using MRA. The signals recorded in real time are decomposed for each interval window, which is considered as 0.5 second for updating. The updating interval has been decided upon based on the practical consideration in implementation of the updating as well as (i) expected range of local frequency content which is dependent on the excitations (in this case earthquakes) and (ii) the possible range of the structural natural period (Basu and Nagarajaiah, 2008). The gain matrices are updated for each window by solving the Riccati equation. Therefore, the control forces and controlled responses are calculated. The MATLAB software is utilized to calculate all computation.

For numerical example, the response of structure of the typical MDOF structure with only one ATMD on the top floor is compared with the corresponding Wavelet-LQR ones under Whittier Narrows-01 (LB – Orange Ave. 1987), Chi-Chi, Taiwan-03 (CHY080.1999) , and Yountville (Napa Fire Station #3,2000) ground motions.

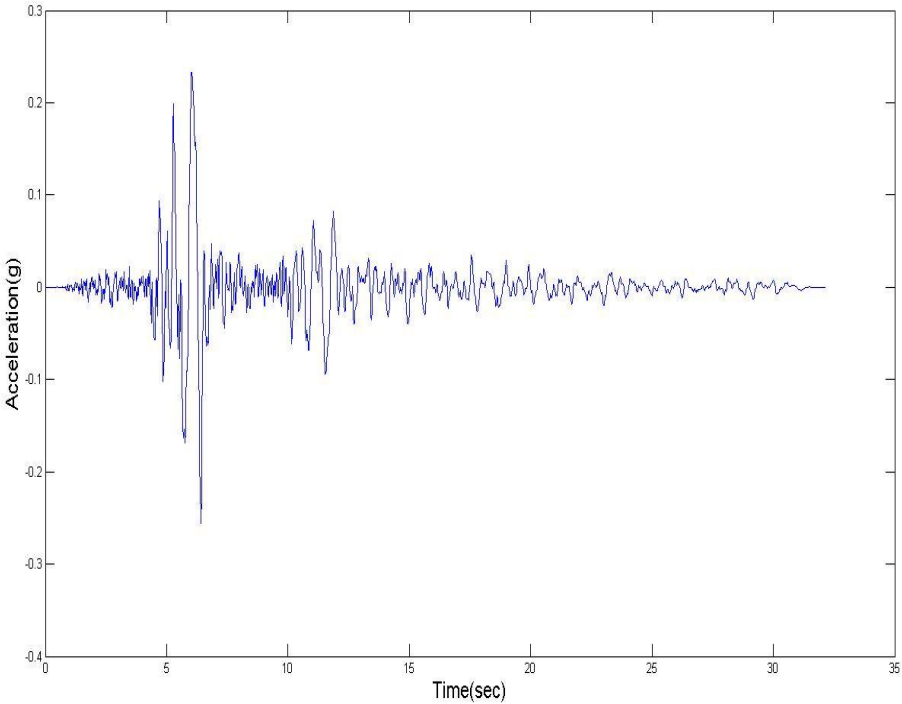


**Figure 4.1 :** Whittier Narrows earthquake acceleration time history.

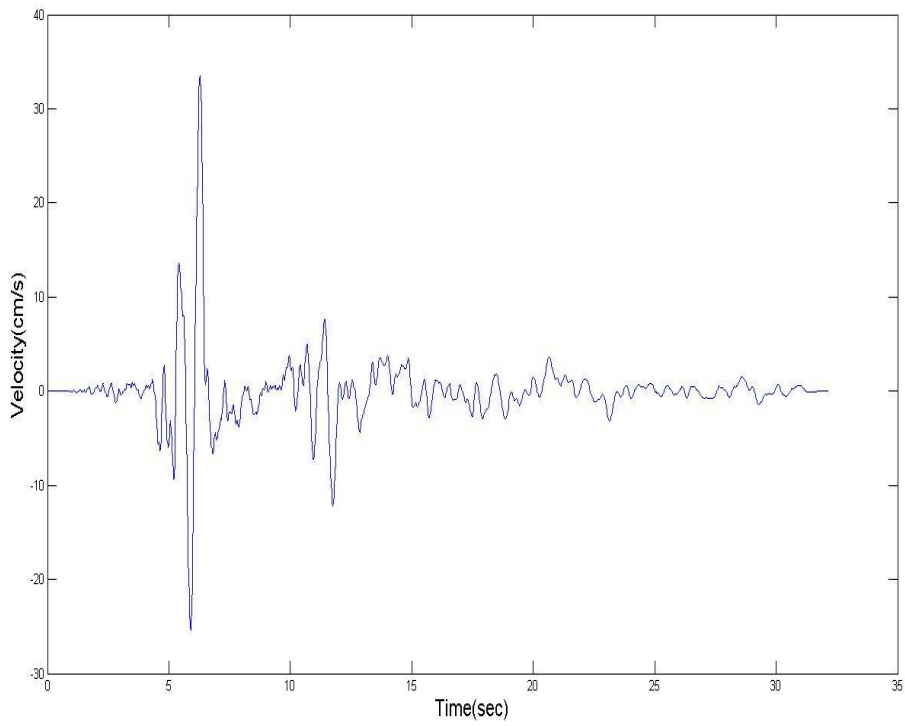


**Figure 4.2 :** Whittier Narrows earthquake velocity time history.

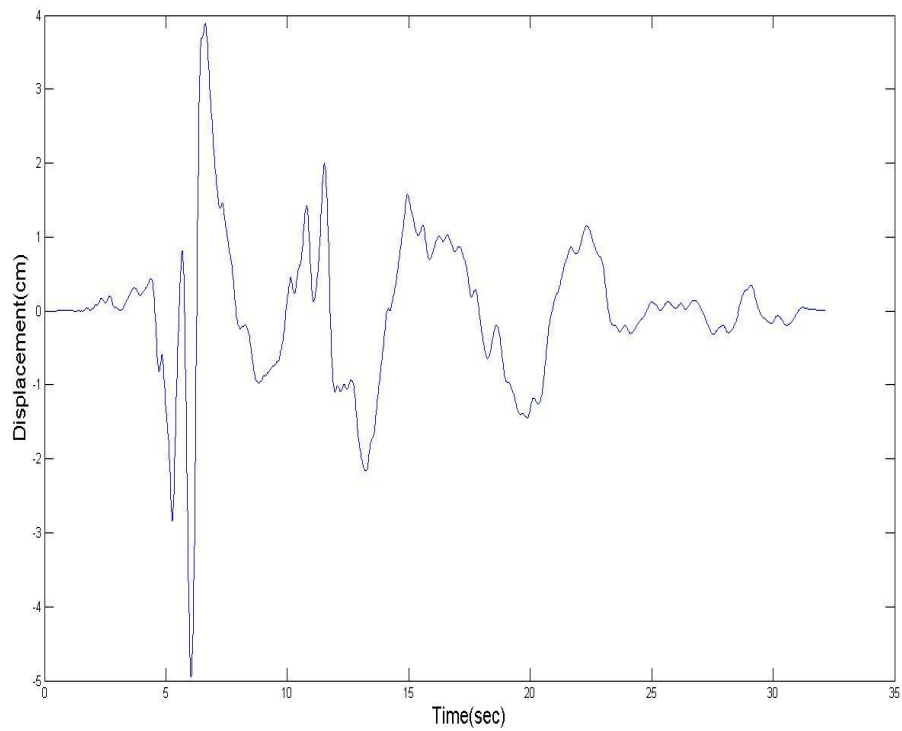


**Figure 4.3 :** Whittier Narrows earthquake displacement time history.

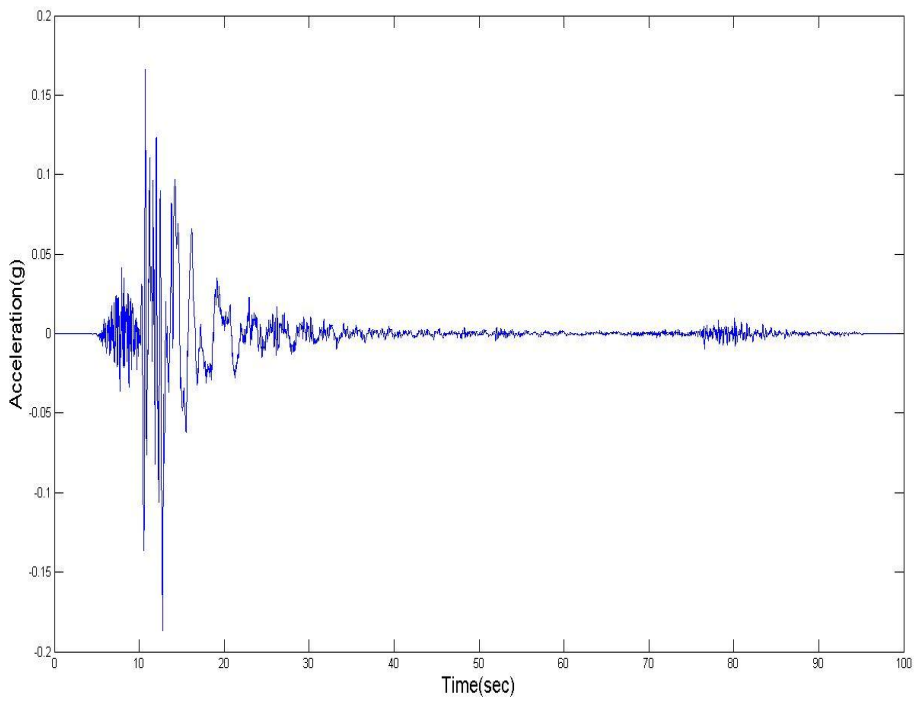


**Figure 4.4 :** Chi-Chi, Taiwan earthquake acceleration time history.

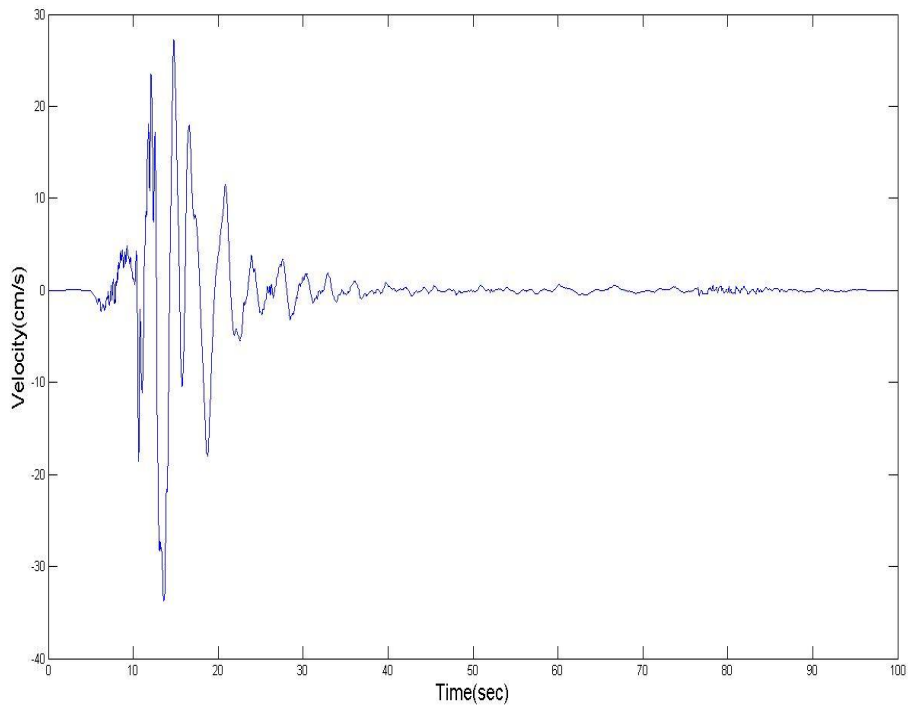


**Figure 4.5 :** Chi-Chi, Taiwan earthquake velocity time history.

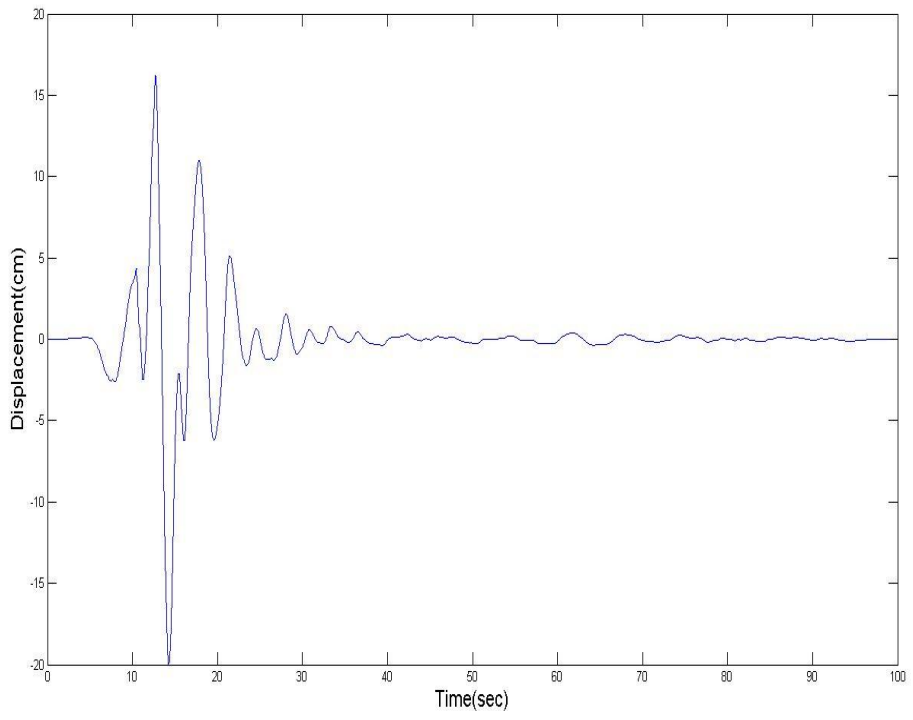


**Figure 4.6 :** Chi-Chi, Taiwan earthquake displacement time history.

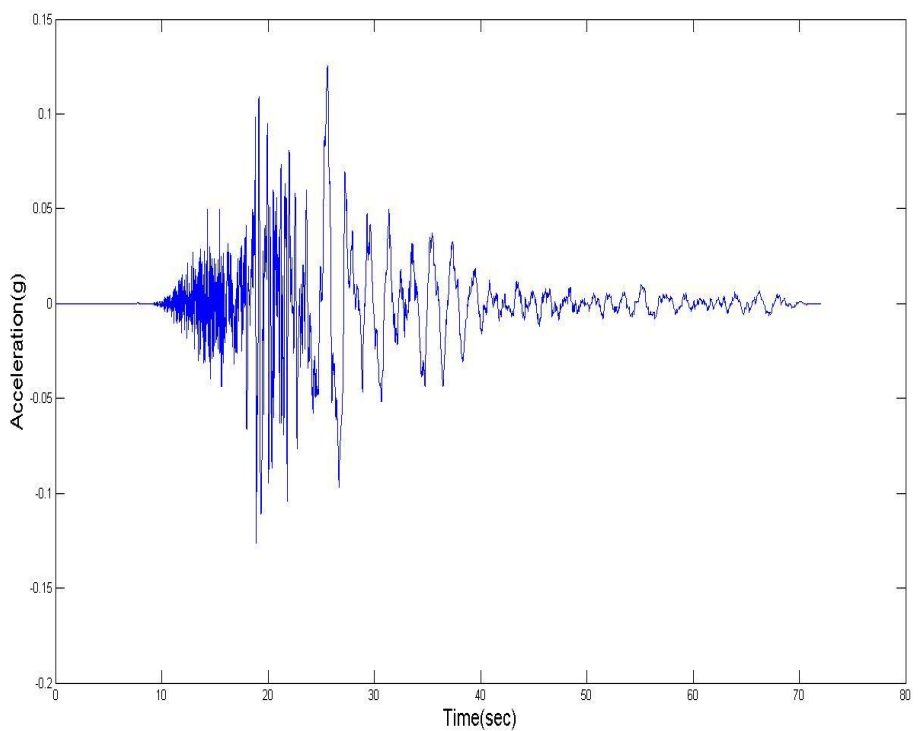


**Figure 4.7 :** Yountville earthquake acceleration time history.

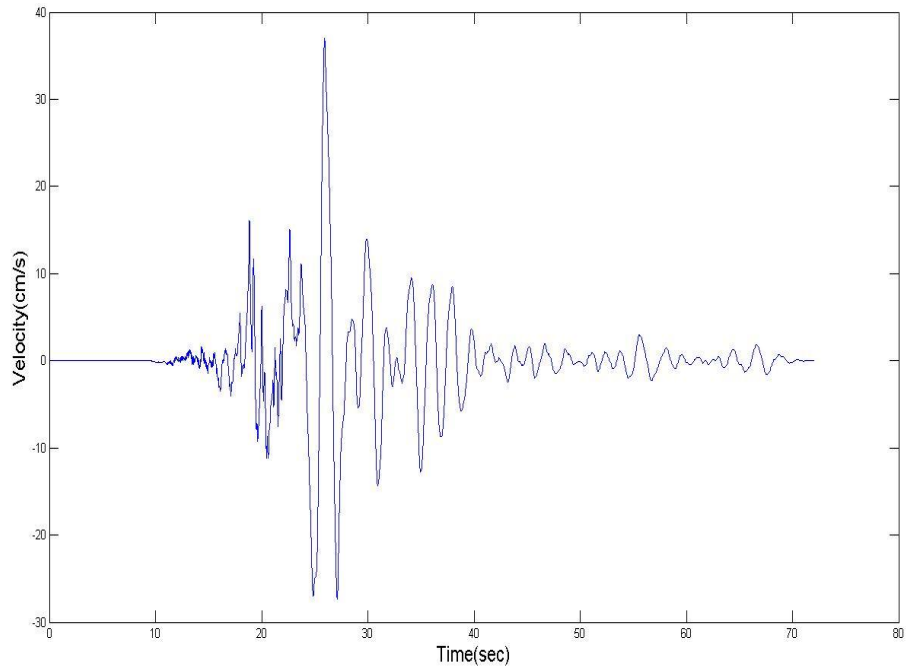


**Figure 4.8 :** Yountville earthquake velocity time history.

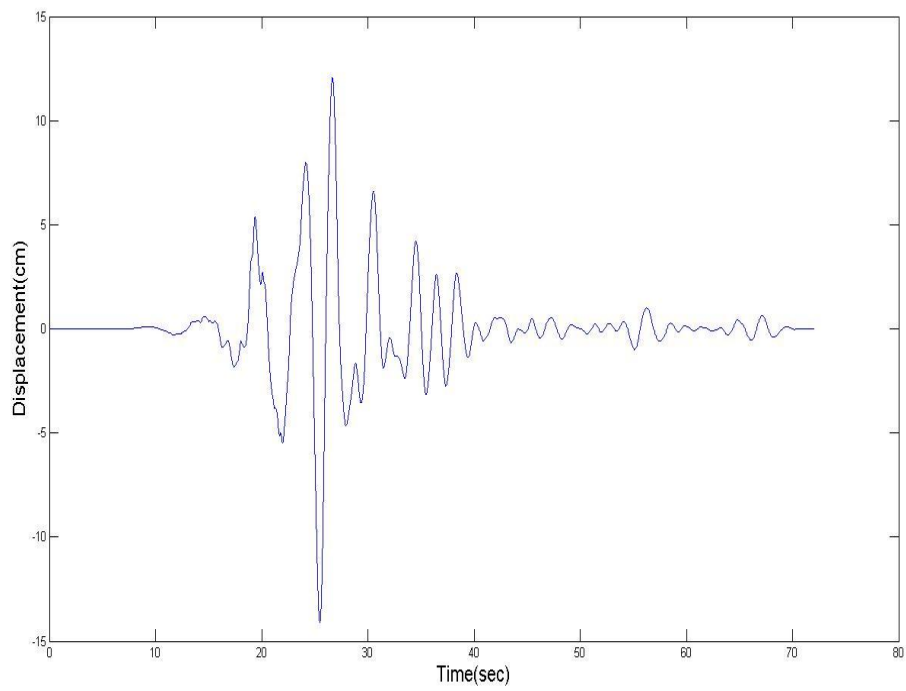


**Figure 4.9 :** Yountville earthquake displacement time history.



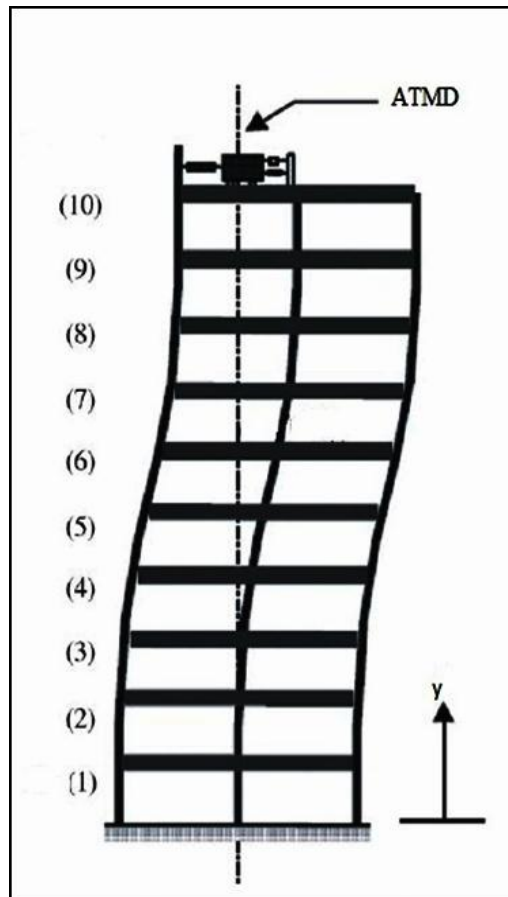


**Figure 4.10** :10 stories building which has the lumped masse at top storey.

Figures 4.11 to 4.18 shows the related results for the case of Whittier Narrows-01 (LB – Orange Ave. 1987) earthquake. Fig.4.11 shows us comparison of uncontrolled response of 10<sup>th</sup> floor with displacement that achieved by suggested WAVELET-LQR method and Fig.4.12 shows the consequential of controlled displacement of 10th floor achieved by the classical LQR and suggestion WAVELET\_LQR method. As can be seen from the fig.4.11 and fig.4.12 the maximum displacement of the top floor has reduced to 101mm and 88mm from the maximum uncontrolled displacement of about 114mm, for the classic LQR and suggested WAVELET-LQR systems respectively. Therefore, it shows that the proposed adaptive LQR is more efficient than the classical LQR.

On the other hand, as can be seen from fig.4.13 the control forces for the two systems are not very different for most of the times over the duration except from the peak control. The peak control force increases slightly (about 34%) on the resonant band of frequency compared to the classic LQR, therefore, the response of structures decreases without higher penalty.

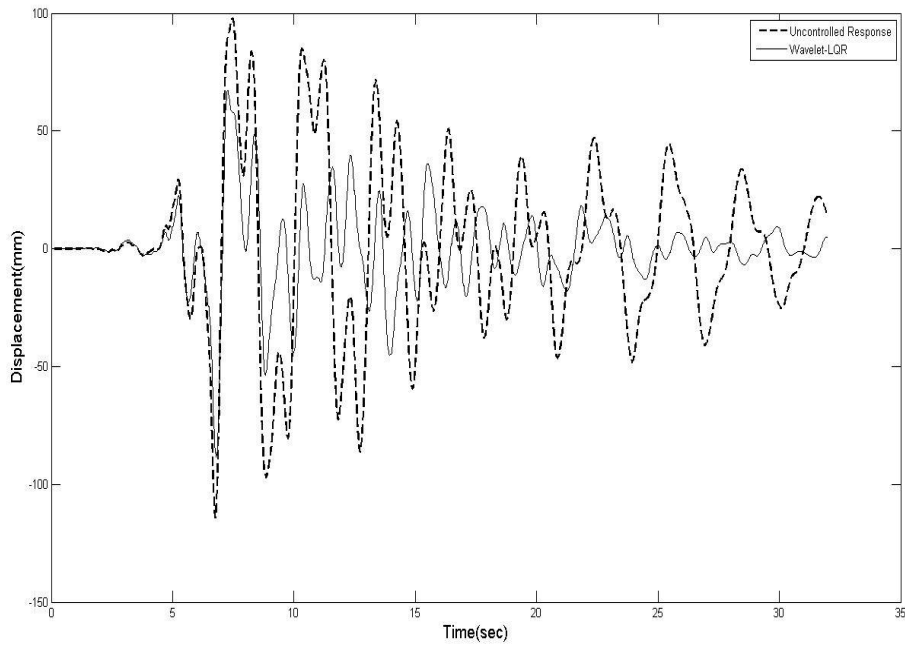


**Figure 4.11:** Results for Whittier Narrows earthquake, compared uncontrolled response with proposed (WAVELET-LQR) controlled response for 10<sup>th</sup> floor.

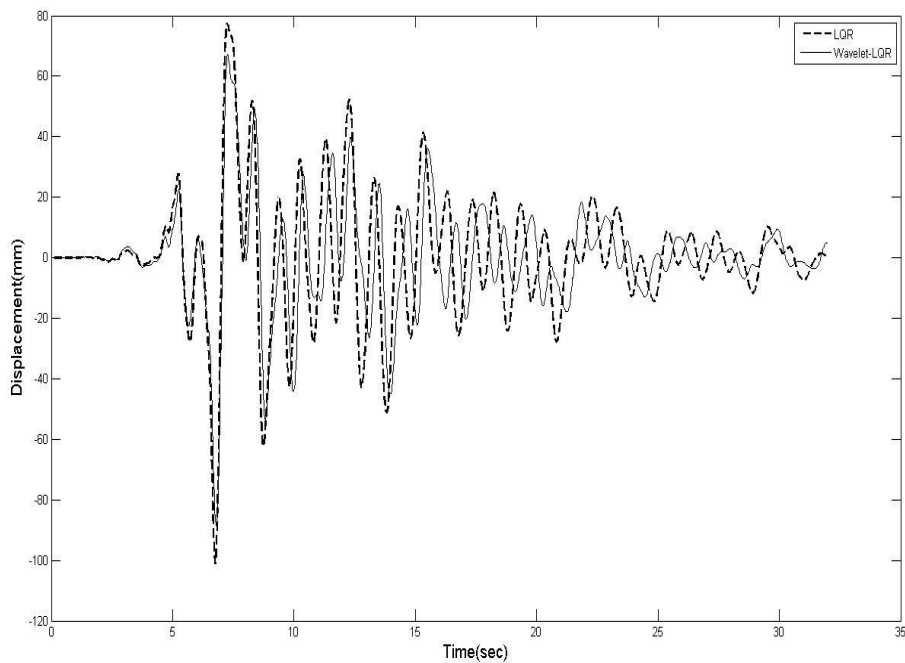


**Figure 4.12 :** Results for Whittier Narrows earthquake, controlled displacement response using LQR and proposed WAVELET-LQR algorithms for 10<sup>th</sup> floor.

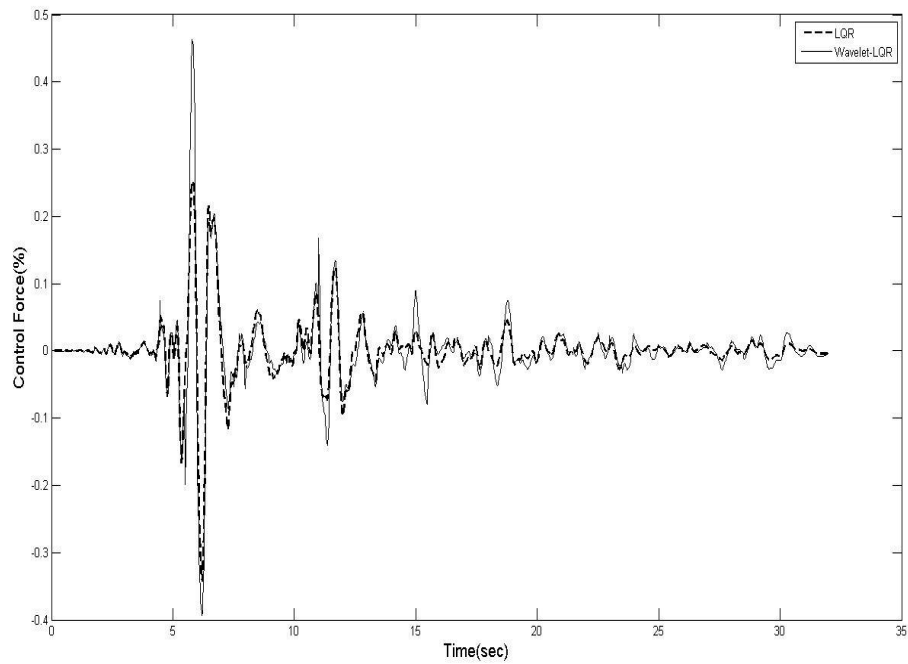


**Figure 4.13** :Results for Whittier Narrows earthquake, control force compared in two method (LQR , WAVELET-LQR).

Also, to illustrate the potential application of the proposed method, the energy corresponding to the controller for the proposed method are compared with conventional LQR.

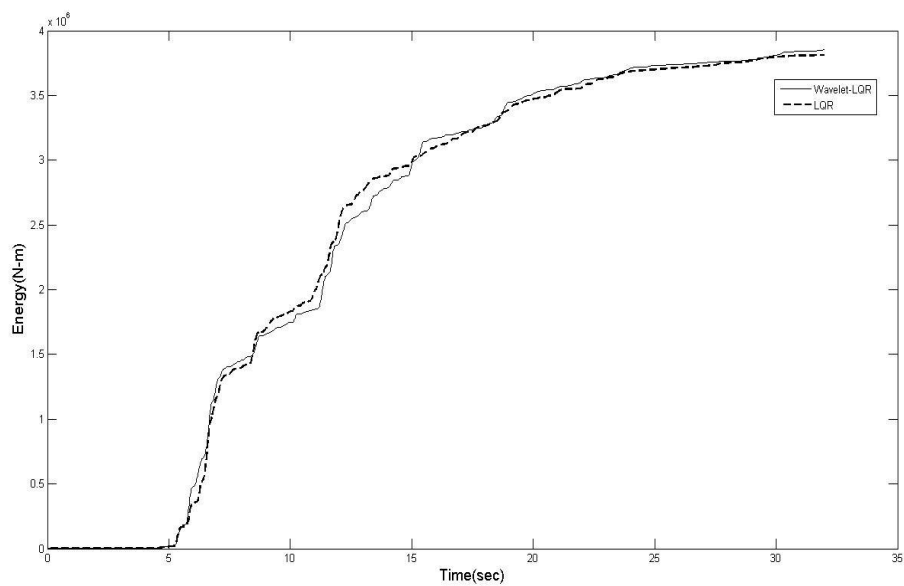


**Figure 4.14** :Results for Whittier Narrows earthquake, energy demand compared in two method (LQR , WAVELET-LQR).

Figures 4.14 show that the control energy demand, for the two systems are not different for most of time over duration.

For more research and comparing result, same figures are drawn for 1<sup>th</sup> and 5<sup>th</sup> floors. Figure 4.15 to 4.18 show that the same results in this floors like 10<sup>th</sup> floor.

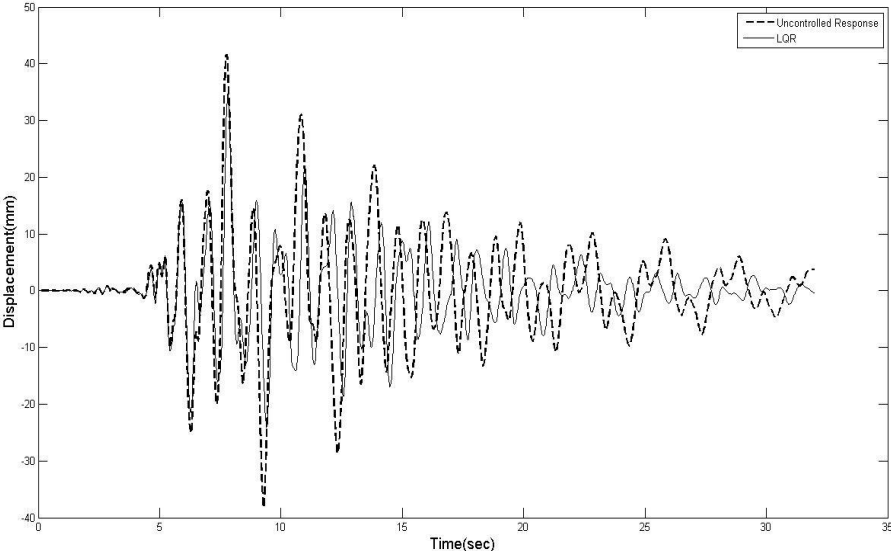


**Figure 4.15 :** Results for Whittier Narrows earthquake, compared uncontrolled response with proposed (WAVELET-LQR) controlled response for 1<sup>th</sup> floor.

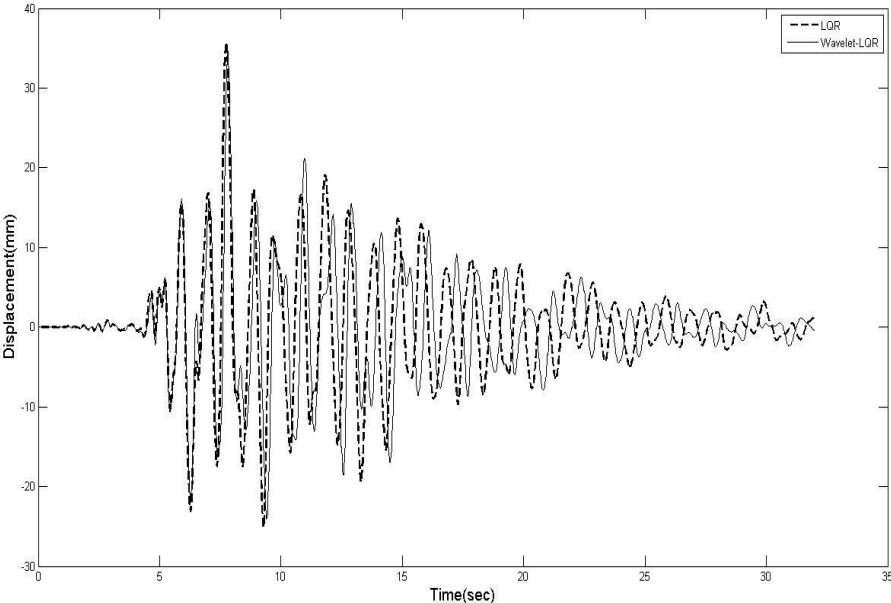


**Figure 4.16 :** Results for Whittier Narrows earthquake, controlled displacement response using LQR and proposed WAVELET-LQR algorithms for 1<sup>th</sup> floor.

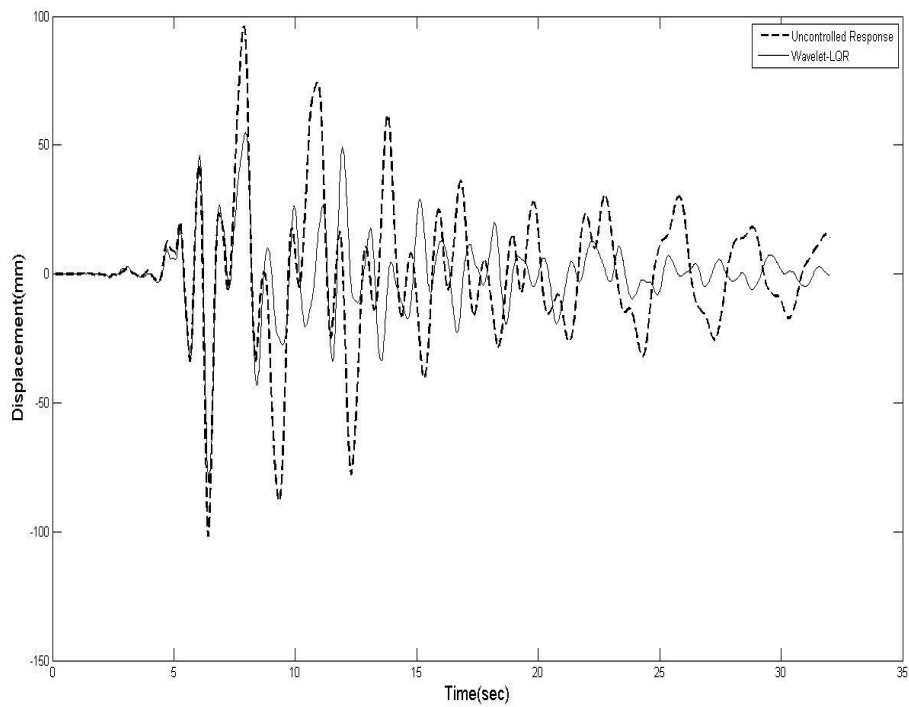


**Figure 4.17:** Results for Whittier Narrows earthquake, compared uncontrolled response with proposed (WAVELET-LQR) controlled response for 5<sup>th</sup> floor.

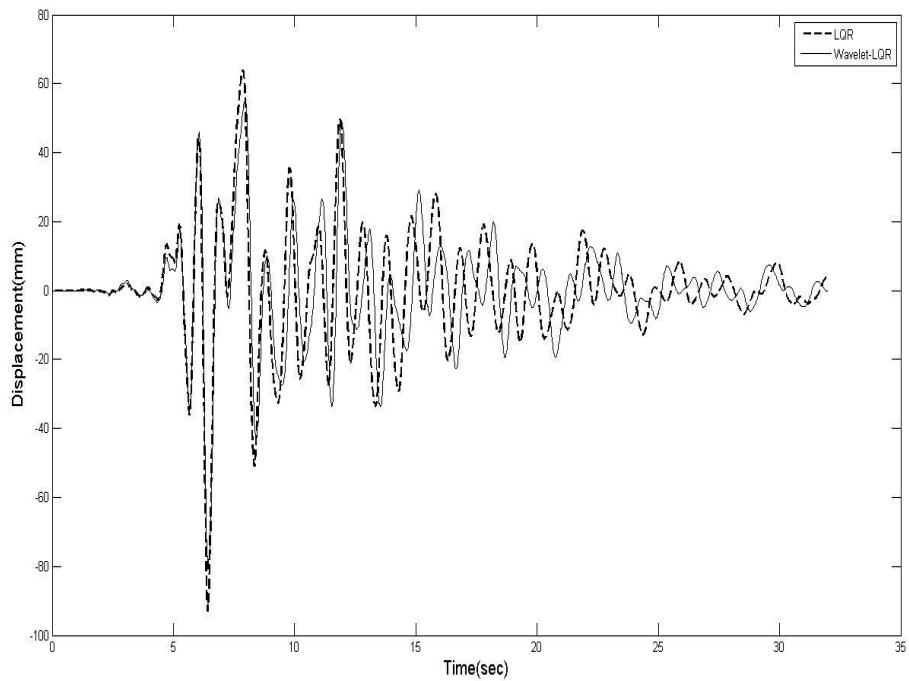


**Figure 4.18 :** Results for Whittier Narrows earthquake, controlled displacement response using LQR and proposed WAVELET-LQR algorithms for 5<sup>th</sup> floor.

Moreover, all maximum displacements of each stories that obtained with both algorithms and uncontrolled displacements of stories are given in Table:4.1. Also accelerations and velocities of each stories that obtained with both control system are given in Table:4.2. The obtained results indicated that the proposed method is a strong and viable method to the problem of active control in the structures.

**Table 4.1 :** Comparison of effectiveness of two controller systems used in this study for Whittier Narrows earthquake ground motion.

Building Floor	Maximum uncontrolled response(mm)	Controlled response		Percent of decrease [3]-[4]/[4]
		ATMD (LQR) [3]	ATMD (WB-LQR) [4]	
[1]	[2]	[3]	[4]	
1	41.568	35.734	34.658	3.01
2	73.899	61.748	58.137	5.84
3	90.419	72.001	65.231	9.40
4	94.475	83.799	71.024	15.24
5	101.569	92.960	80.718	13.17
6	99.887	92.232	81.547	11.58
7	86.081	79.598	71.498	10.17
8	86.274	74.231	64.381	13.27
9	94.744	83.282	70.798	14.99
10	114.169	101.100	88.448	12.51

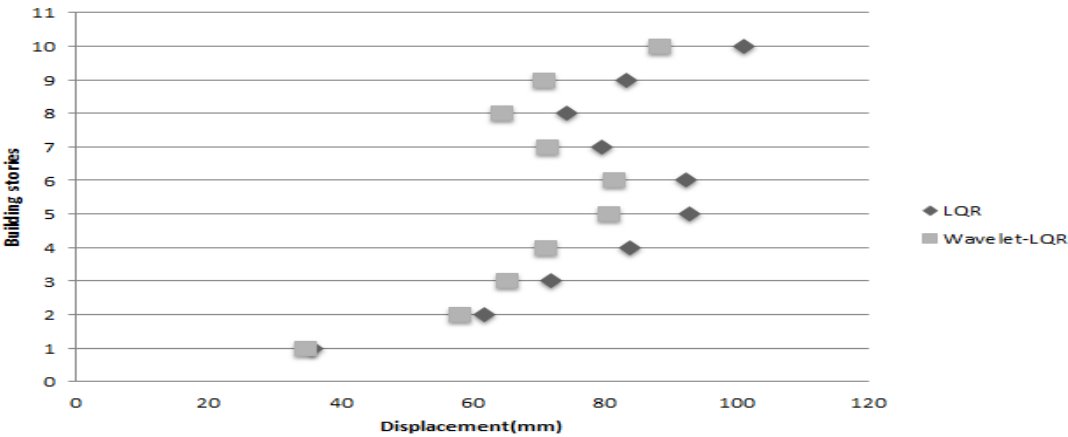


**Figure 4.19 :**Results for Whittier Narrows earthquake, displacement in each story compared in two method (LQR , WAVELET-LQR).

**Table 4.2 :** Comparison of acceleration and velocity effectiveness of two controller systems used in this study for Whittier Narrows earthquake ground motion.

Building Floor	Maximum velocity LQR ( $m/s$ )	Maximum velocity WB-LQR ( $m/s$ )	Maximum acceleration LQR ( $m/s^2$ )	Maximum acceleration WB-LQR ( $m/s^2$ )
1	0.256	0.246	1.971	2.887
2	0.362	0.336	3.293	3.174
3	0.383	0.368	3.685	3.594
4	0.517	0.474	4.843	4.645
5	0.583	0.564	5.025	4.852
6	0.555	0.549	4.895	4.552
7	0.471	0.441	4.017	3.752
8	0.324	0.325	2.755	2.581
9	0.464	0.421	2.511	2.421
10	0.608	0.569	4.176	3.784

To observe the efficiency of the suggested WAVELET-LQR control more critically, the other two earthquakes are considered next. For these ground motions almost the same behavior can be observed as for the Whittier Narrows-01 (LB – Orange Ave. 1987) earthquake. Figures 4.20 to 4.27 shows the related results for the case of Chi-Chi, Taiwan-03 (CHY080.1999) earthquake. Fig.4.20 shows us comparison of uncontrolled response of 10<sup>th</sup> floor with displacement that achieved by suggested WAVELET-LQR method and Fig.4.21 shows the consequential of controlled displacement of 10th floor achieved by the classical LQR and suggestion WAVELET\_LQR method. As can be seen from the fig.4.20 and fig.4.21 the maximum displacement of the top floor has reduced to 349mm and 278mm from the maximum uncontrolled displacement of about 682mm, for the classic LQR and suggested WAVELET-LQR systems respectively. The suggested WAVELET-LQR algorithm reduces the peak displacement of top floor to 278 mm, which reduces the response of structure more than 20 percent than conventional LQR. The maximum control forces for adaptive LQR controller in the Chi-Chi, Taiwan increases about

48% just on the resonant band of frequency compared to the classic LQR that is seen in Fig.4.22.

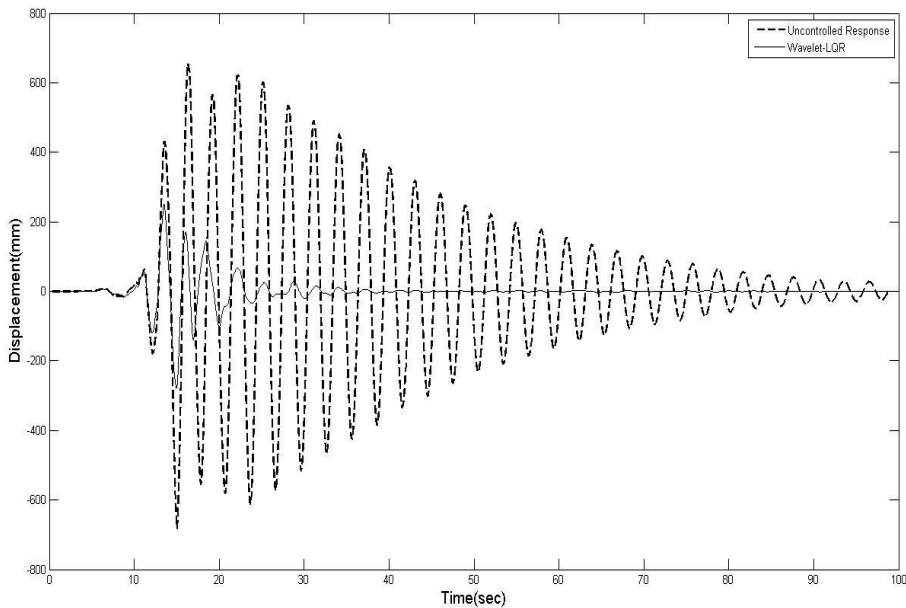


**Figure 4.20** :Results for Chi-Chi, Taiwan earthquake, compared uncontrolled response with proposed (WAVELET-LQR) controlled response for 10<sup>th</sup> floor.

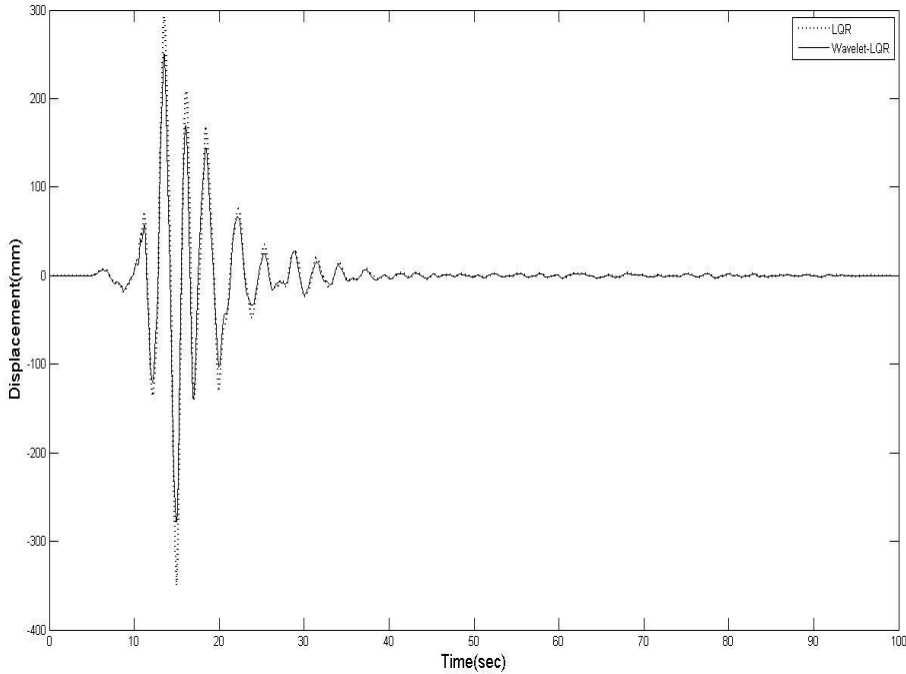


**Figure 4.21** : Results for Chi-Chi, Taiwan earthquake, controlled displacement response using LQR and proposed WAVELET-LQR algorithms for 10<sup>th</sup> floor.



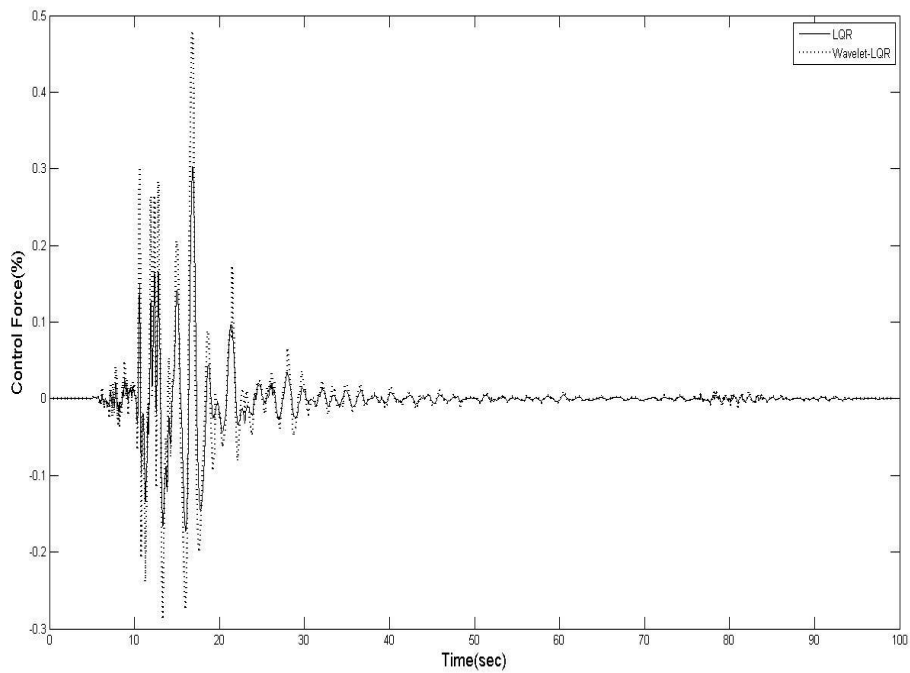


**Figure 4.22 :** Results for Chi-Chi, Taiwan earthquake, control force compared in two methods (LQR, WAVELET-LQR).

Figures 4.23 show the control energy demand, that for the proposed method slightly are more than classic LQR. It seem that more peak time cause this increasing.

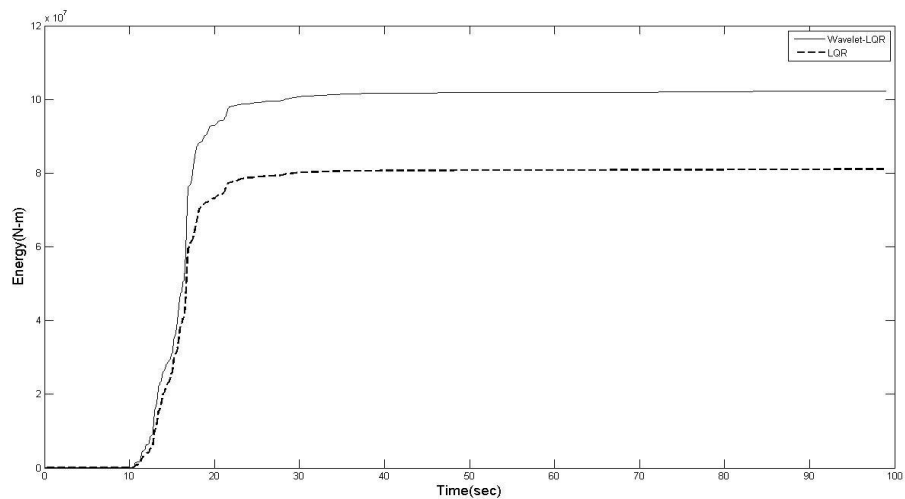


**Figure 4.23 :** Results for Chi-Chi, Taiwan-03 (CHY080.1999) earthquake, energy demand compared in two methods (LQR, WAVELET-LQR).

For more research and comparing result, same figures are drawn for 1<sup>th</sup> and 5<sup>th</sup> floors. Figure 4.24 to 4.27 show that the same results in this floors like 10<sup>th</sup> floor. This figures show that similar behavior like 10<sup>th</sup> floor.

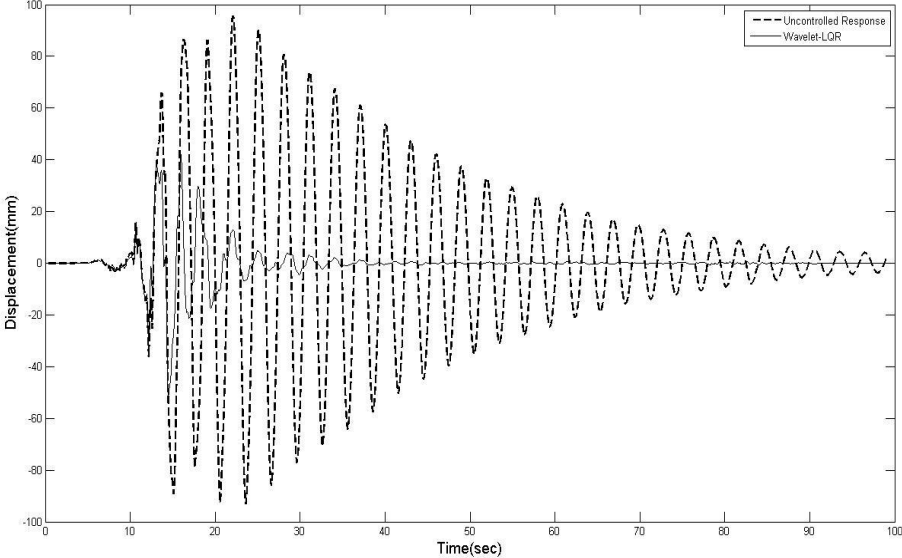


**Figure 4.24 :** Results for Chi-Chi, Taiwan earthquake compared uncontrolled response with proposed (WAVELET-LQR) controlled response for 1<sup>th</sup> floor.

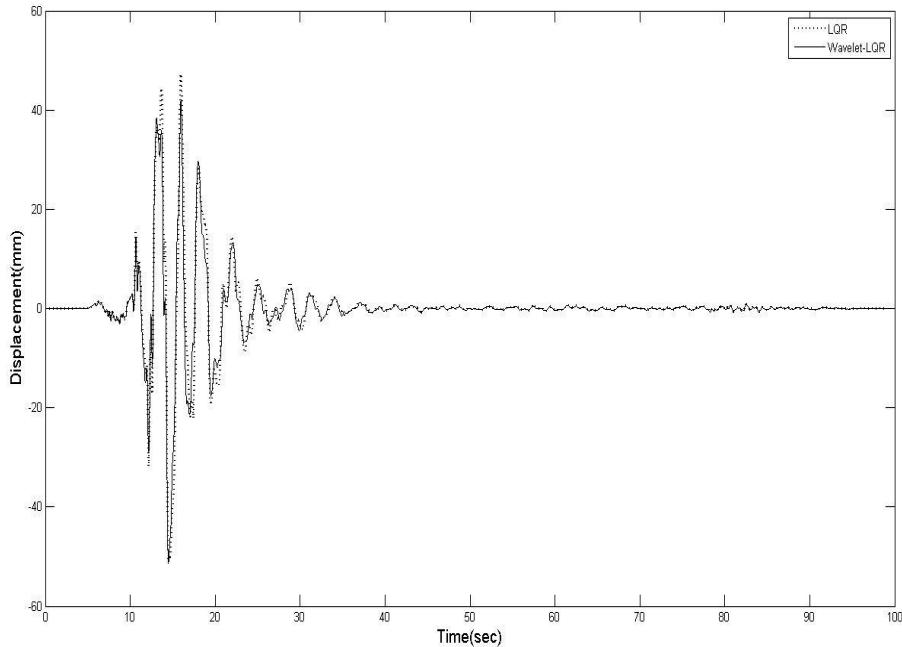


**Figure 4.25 :** Results for Chi-Chi, Taiwan earthquake controlled displacement response using LQR and proposed WAVELET-LQR algorithms for 1<sup>th</sup> floor.

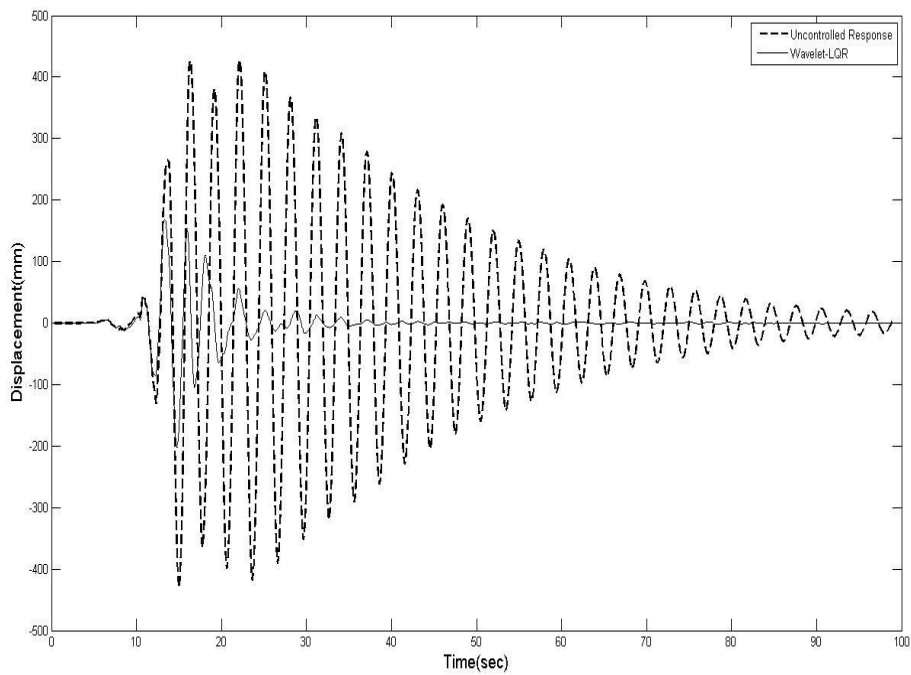


**Figure 4.26** : Results for Chi-Chi, Taiwan earthquake compared uncontrolled response with proposed (WAVELET-LQR) controlled response for 5<sup>th</sup> floor.

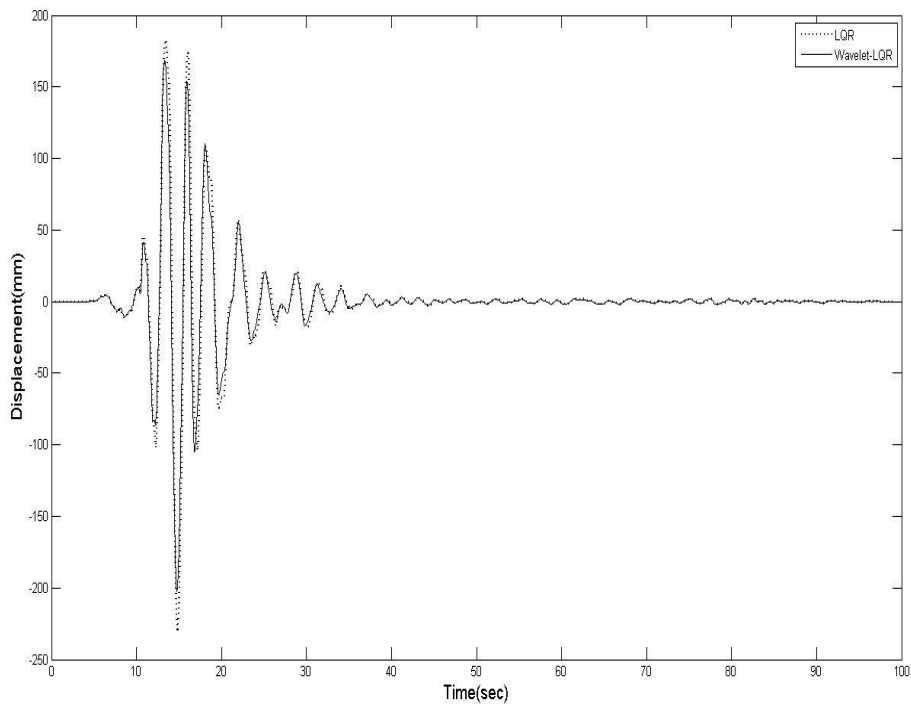


**Figure 4.27** : Results for Chi-Chi, Taiwan earthquake controlled displacement response using LQR and proposed WAVELET-LQR algorithms for 5<sup>th</sup> floor.

Also, the results of the case corresponding to the excitation of Yountville (Napa Fire Station #3, 2000) earthquake are seen in figures 4.28 to 4.35. Fig.4.28 shows us comparison of uncontrolled response of 10<sup>th</sup> floor with displacement that achieved by suggested WAVELET-LQR method and Fig.4.29 shows the consequential of controlled displacement of 10th floor achieved by the classical LQR and suggestion WAVELET\_LQR method. As can be seen from the fig.4.28 and fig.4.29 the maximum displacement of the top floor has reduced to 324mm and 272mm from the maximum uncontrolled displacement of about 511mm, for the classic LQR and suggested WAVELET-LQR systems respectively. The suggested WAVELET-LQR algorithm reduces the peak displacement of top floor to 272 mm, which reduces the response of structure more than 16 percent than conventional LQR and with same result for control force and energy (fig.4.30 and fig.4.31)

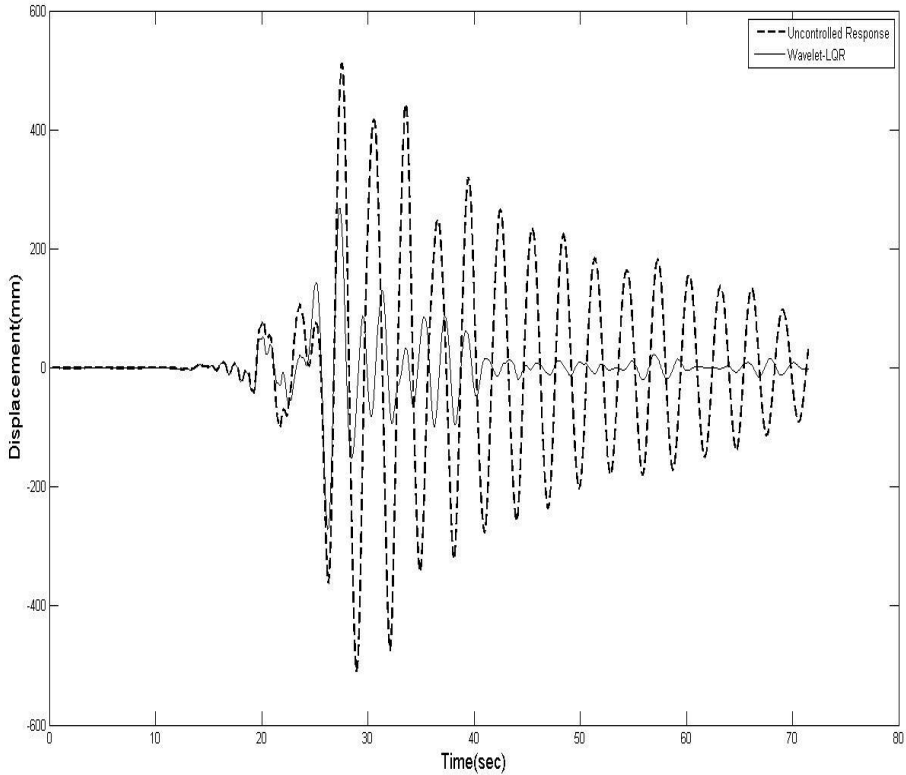


**Figure 4.28** :Results for Yountville earthquake, compared uncontrolled response with proposed (WAVELET-LQR) controlled response for 10<sup>th</sup> floor.

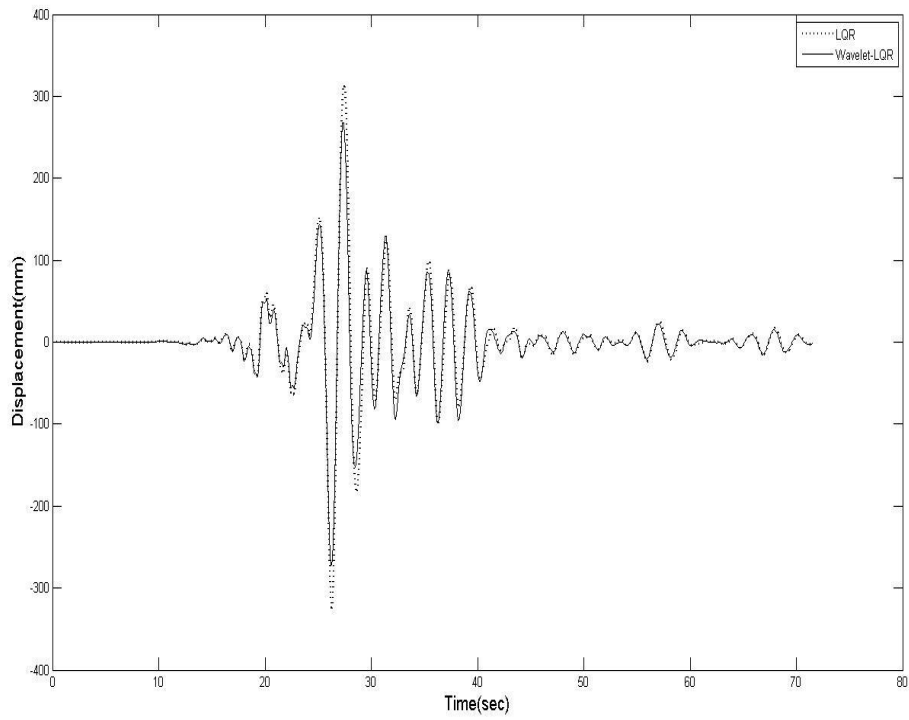


**Figure 4.29** :Results for Yountville earthquake, controlled displacement response using LQR and proposed WAVELET-LQR algorithms for 10<sup>th</sup> floor.

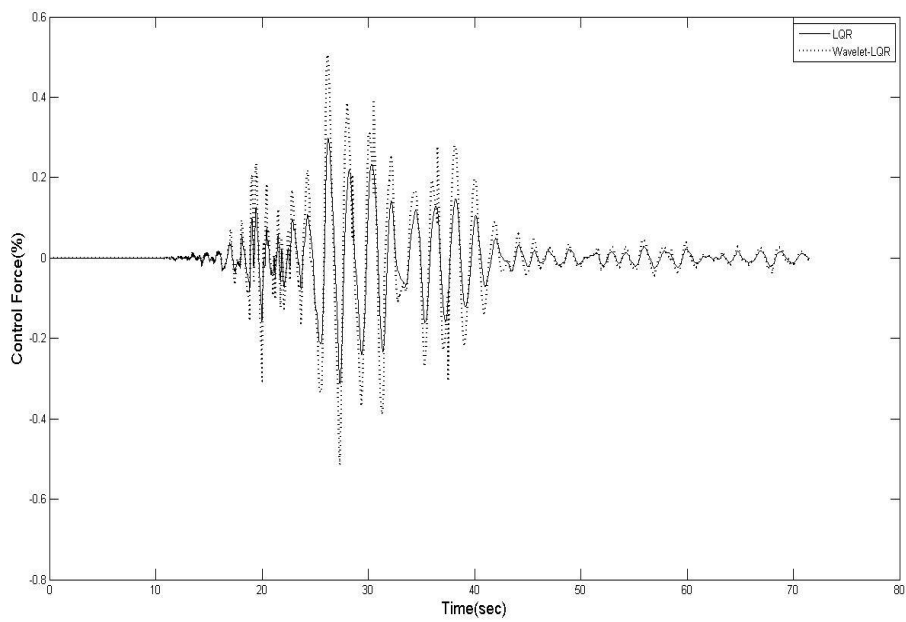


**Figure 4.30** :Results for Yountville earthquake, control force compared in two method (LQR , WAVELET-LQR).

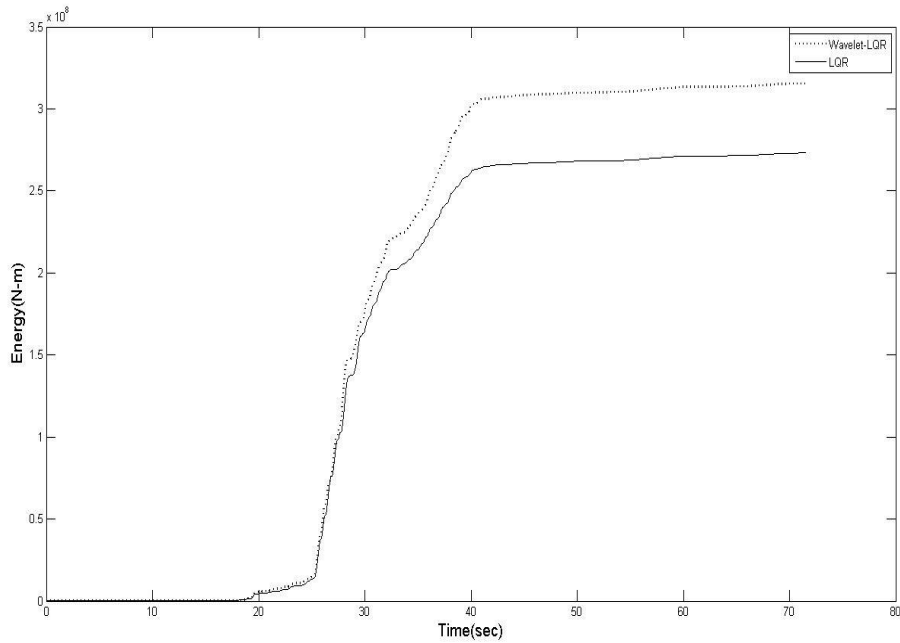


**Figure 4.31** :Results for Yountville earthquake, energy demand compared in two method (LQR , WAVELET-LQR).

For more research and comparing result, same figures are drawn for 1<sup>th</sup> and 5<sup>th</sup> floors. Figure 4.32 to 4.35 show that the same results in this floors like 10<sup>th</sup> floor. This figures show that similar behavior like 10<sup>th</sup> floor.

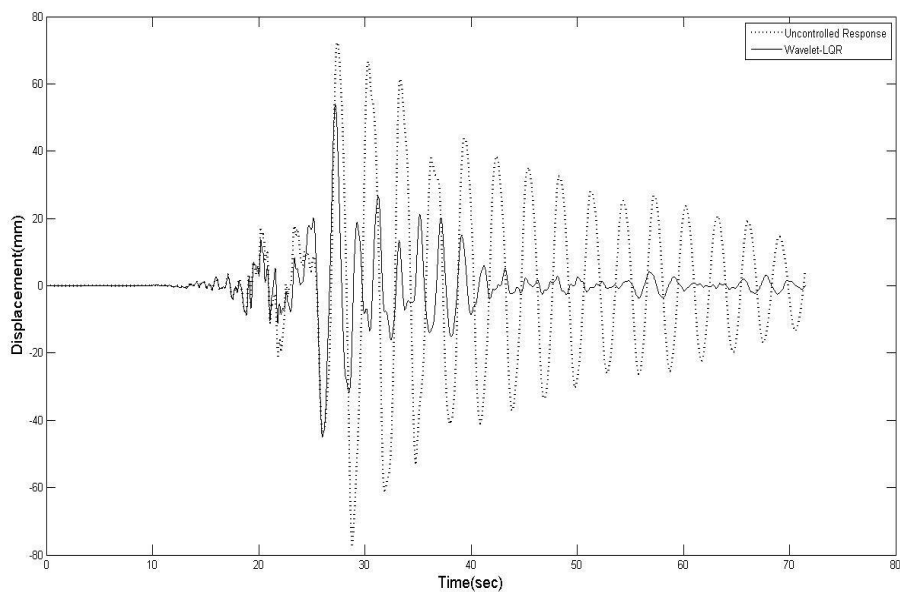


**Figure 4.32** :Results for Yountville earthquake, compared uncontrolled response with proposed (WAVELET-LQR) controlled response for 1<sup>th</sup> floor.

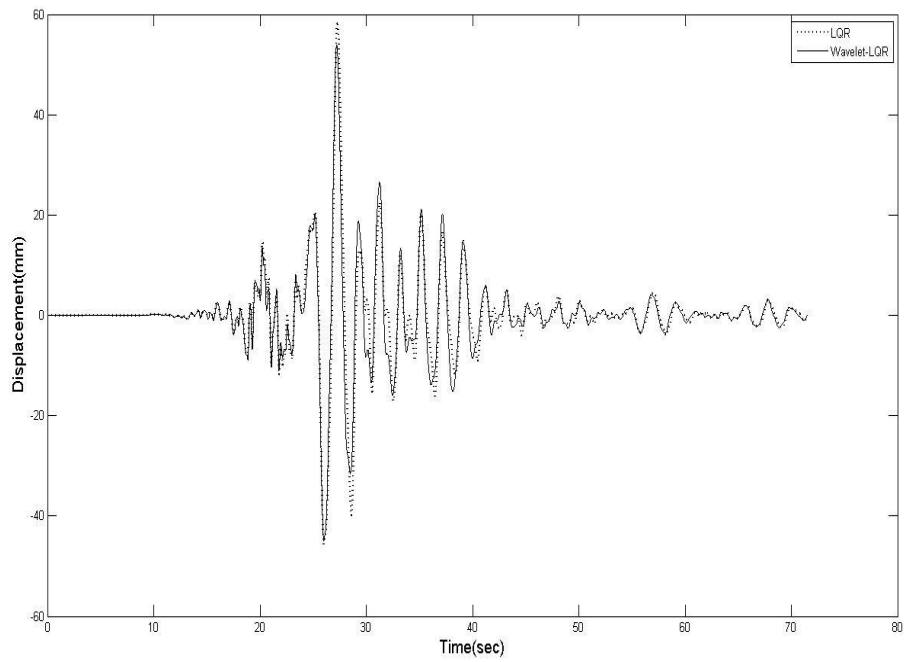


**Figure 4.33** :Results for Yountville earthquake, controlled displacement response using LQR and proposed WAVELET-LQR algorithms for 1<sup>th</sup> floor.

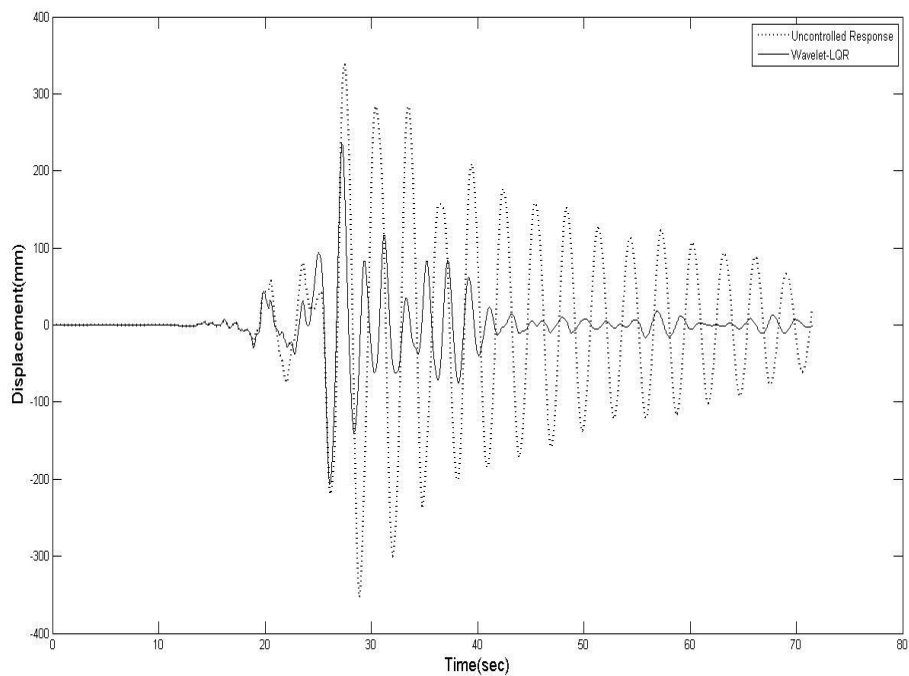


**Figure 4.34** :Results for Yountville earthquake, compared uncontrolled response with proposed (WAVELET-LQR) controlled response for 5<sup>th</sup> floor.

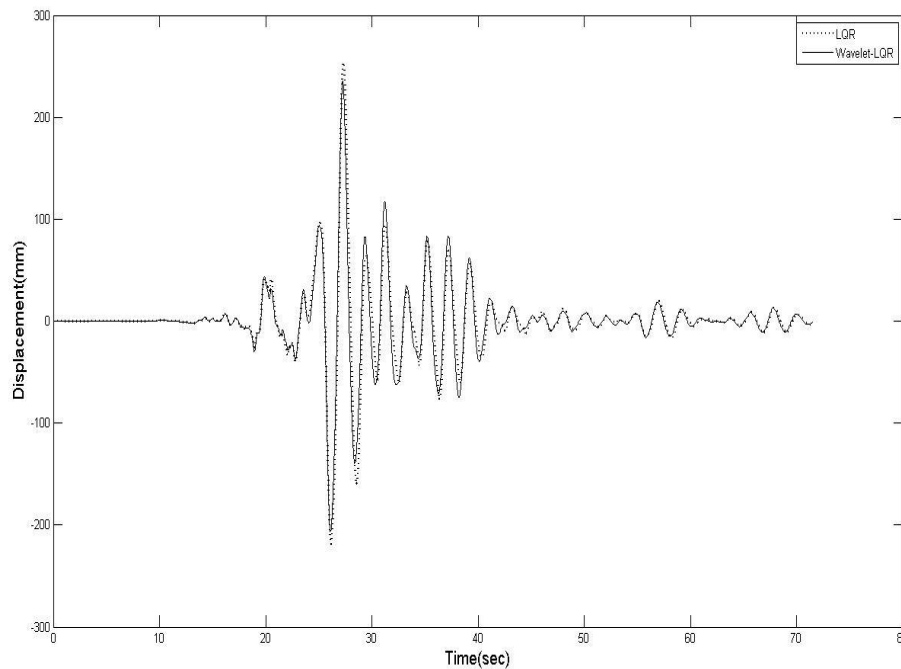


**Figure 4.35** :Results for Yountville earthquake, controlled displacement response using LQR and proposed WAVELET-LQR algorithms for 5<sup>th</sup> floor.

Like first example, all displacements of each stories that obtained with both algorithms and uncontrolled displacements of stories are given in Table:4.3 and Table:4.4 for Chi-Chi, Taiwan-03 and Yountville earthquakes. Also accelerations and velocities of each stories that obtained with both control system are given in Table:4.5 and Table:4.6. Also maximum displacement at each floors for LQR and WAVELET-LQR method are drawn in figures 4.36 and 4.37.

Accelerations and velocities results like displacement shows that the reduction when are used proposed WAVELET-LQR method.

The results show that the proposed modified LQR controller performs significantly better than the conventional LQR controller in reducing the displacement response of the structure.



**Table 4.3 :** Comparison of effectiveness of two controller systems used in this study for Chi-Chi, Taiwan earthquake ground motion.

Building Floor	Maximum uncontrolled response(mm)	Controlled response		Percent of decrease [3]-[4]/[4]
		ATMD (LQR) [3]	ATMD (WB-LQR) [4]	
[1]	[2]	[3]	[4]	
1	95.623	50.610	51.278	-1.319
2	188.378	98.016	95.724	2.338
3	275.697	141.863	135.663	4.370
4	355.674	184.723	168.693	8.677
5	431.759	229.398	202.049	11.922
6	503.597	271.359	234.423	13.611
7	566.795	304.148	260.123	14.474
8	613.394	323.452	272.904	15.627
9	655.788	336.373	274.701	18.334
10	682.070	349.194	278.767	20.168

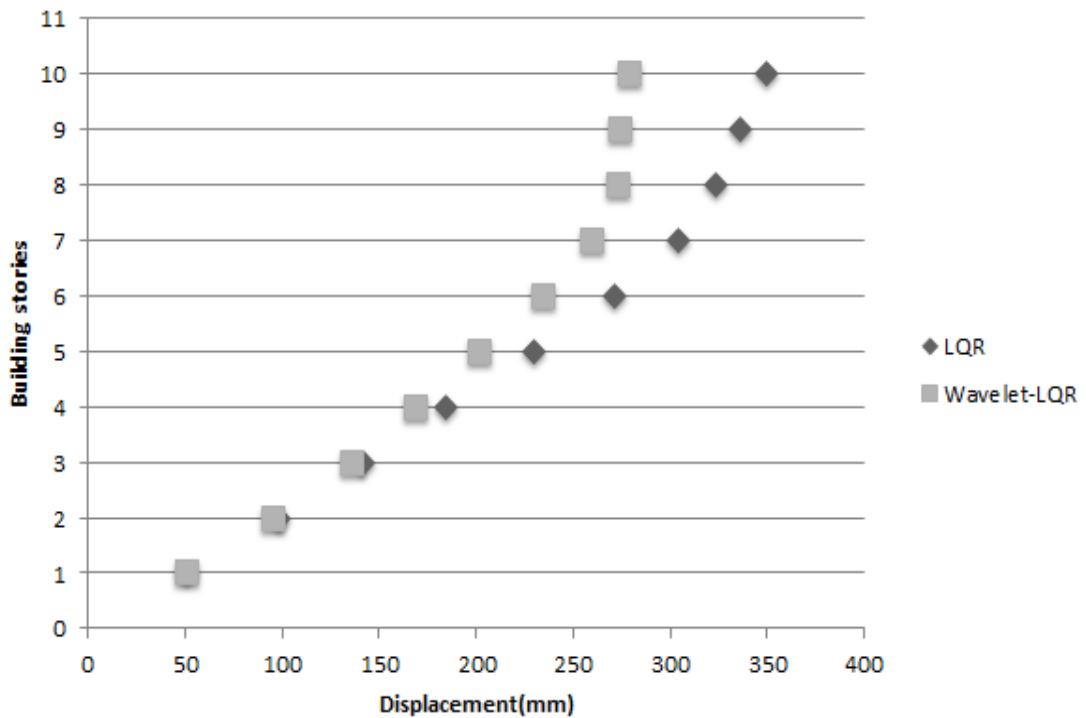


**Figure 4.36 :** Results for Chi-Chi, Taiwan-03 (CHY080.1999) earthquake, displacement for each story compared in two methods (LQR, WAVELET-LQR).

**Table 4.4 :** Comparison of effectiveness of two controller systems used in this study for Yountville earthquake ground motion.

Building Floor	Maximum uncontrolled response(mm)	Controlled response		Percent of decrease [3]-[4]/[4]
		ATMD (LQR)	ATMD (WB-LQR)	
[1]	[2]	[3]	[4]	
1	77.688	58.132	53.986	7.13
2	153.710	116.088	108.277	6.72
3	225.995	170.051	158.641	6.70
4	292.862	216.903	201.652	7.03
5	352.896	254.327	235.565	7.37
6	405.158	282.463	259.584	8.09
7	448.099	302.975	274.202	9.49
8	480.276	314.801	280.827	10.79
9	500.786	320.919	278.902	13.09
10	511.054	324.911	272.334	16.18

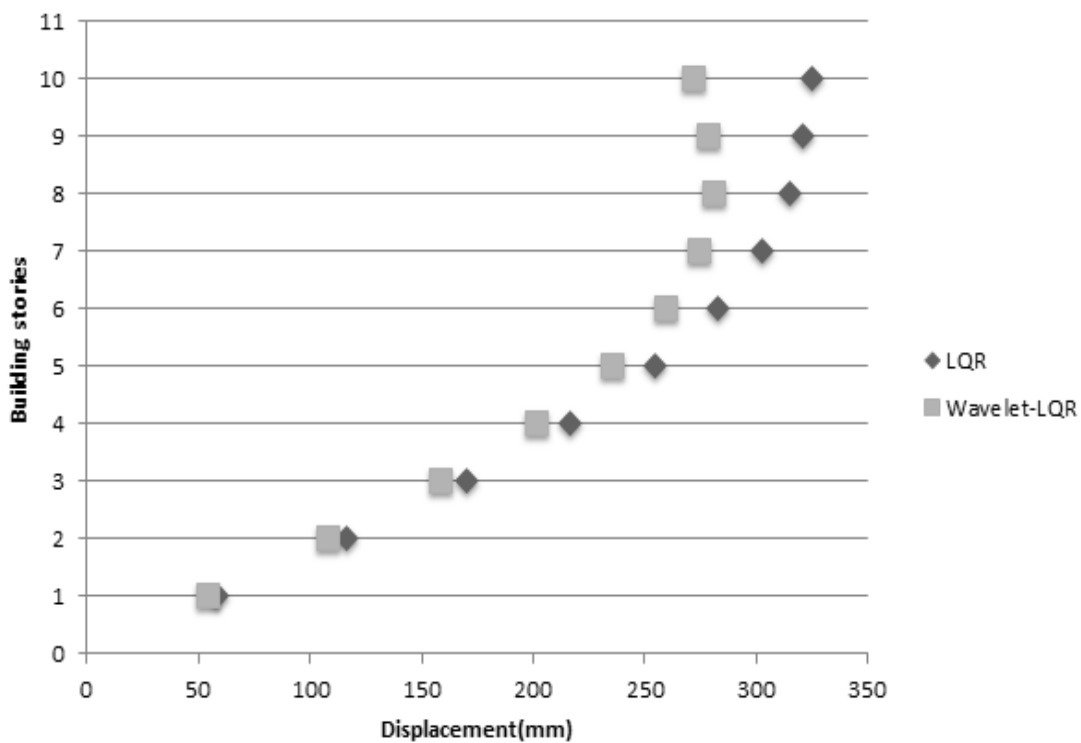


**Figure 4.37 :**Results for Yountville (Napa Fire Station #3, 2000) earthquake, displacement for each story compared in two method (LQR , WAVELET-LQR).

**Table 4.5 :** Comparison of acceleration and velocity effectiveness of two controller systems used in this study for Chi-Chi, Taiwan-1999 earthquake ground motion.

Building Floor	Maximum velocity LQR ( $m/s$ )	Maximum velocity WB-LQR ( $m/s$ )	Maximum acceleration LQR ( $m/s^2$ )	Maximum acceleration WB-LQR ( $m/s^2$ )
1	0.272	0.237	2.357	2.291
2	0.444	0.381	2.751	2.722
3	0.478	0.434	2.927	2.855
4	0.531	0.471	2.718	2.431
5	0.635	0.541	2.503	2.656
6	0.692	0.579	2.607	2.173
7	0.691	0.596	3.562	3.565
8	0.737	0.662	3.581	3.457
9	0.733	0.664	2.585	2.333
10	0.727	0.652	4.064	3.477

**Table 4.6 :** Comparison of acceleration and velocity effectiveness of two controller systems used in this study for Yountville. 2000 earthquake ground motion.

Building Floor	Maximum velocity LQR ( $m/s$ )	Maximum velocity WB-LQR ( $m/s$ )	Maximum acceleration LQR ( $m/s^2$ )	Maximum acceleration WB-LQR ( $m/s^2$ )
1	0.272	0.237	2.357	2.291
2	0.444	0.381	2.751	2.722
3	0.478	0.434	2.927	2.855
4	0.531	0.471	2.718	2.431
5	0.635	0.541	2.503	2.656
6	0.692	0.579	2.607	2.173
7	0.691	0.596	3.562	3.565
8	0.737	0.662	3.581	3.457
9	0.733	0.664	2.585	2.333
10	0.727	0.652	4.064	3.477



## 5. CONCLUSIONS AND RECOMMENDATIONS

A wavelet-based adaptive time-varying controller has been proposed and investigated in this study. In this research, to produce time-frequency signal representing the effect of the nonstationary ground excitations on the structural dynamic system, the MRA based the discrete wavelet transform (DWT) is used. DWT with MRA-based application are utilized to aid a fast numerical algorithm. Hence, it is effective process to modify the conventional LQR controller in real time. To update the weighting matrices for each window band the wavelet analysis is implemented which is lead to generate time-varying gain matrices. This eliminates the requirement of making a previous decision on the weighting matrices which typically did in the conventional LQR method. Via the Ricatti equation, the control forces based on time-varying gain matrices are obtain for each time interval. The proposed modified LQR controller with adaptive gains has been used to simulate the controlled responses of 10-floor shear building with single controller which subjected to several near fault earthquakes. From the numerical results of the study, it is found that the proposed WB-LQR can significantly reduce the responses of system when the resonance happens with slightly increase the peak control force. The results show that this method is practicable and worthwhile for vibration control of structures.



## **6. FUTURE STUDIES**

For future studies use MR dampers instead of TMD with proposed algorithm and study about behaviour of MR dampers in active control when used Wavelet-LQR method. Effectiveness of pulse period in near fault earthquake and study about behaviour of structure that used proposed algorithm. Search to finding method for determine the  $\delta$  for R matrix and improve optimal methods in Wavelet- LQR algorithm. Study about that how and when switch off ATMD when domain frequency dosen't near natural frequency of system in proposed method.





## REFERENCES

- Adeli H, Kim H.** (2004) Wavelet-hybrid feedback-least-mean-square algorithm for robust control of structures. *Journal of Structural Engineering, ASCE*; 130(1):128-37.
- Adeli, H. & Saleh, A.** (1997), Optimal control of adaptive smart bridge structures, *Journal of Structural Engineering*, **123**(2), 218–26.
- Adeli, H. & Saleh, A.** (1998), Integrated structural/control optimization of large adaptive/smart structures, *International Journal of Solids and Structures*, **35**(28–29), 3815–30.
- Adeli, H. & Saleh, A.** (1999), *Control, Optimization, and Smart Structures—High-Performance Bridges and Buildings of the Future*, John Wiley and Sons, New York.
- Aldemir, U.** (2010), A simple active control algorithm for earthquake excited structures, *Computer-Aided Civil and Infrastructure Engineering*, **25**(3), 218–25.
- Aldemir, U., Yanik, A. & Bakioglu, M.** (2012), Control of structural response under earthquake excitation, *Computer-Aided Civil and Infrastructure Engineering*, **27**(8), 620–38.
- Amini, F.** (1995). Response of tall structures subjected to earthquake using a new combined method of pole assignment and optimal control, in *Proceedings of the SEE-2, Tehran, Iran*.
- Amini, F. & Vahdani, R.** (2008). Fuzzy optimal control of uncertain dynamic characteristics in tall buildings subjected to seismic excitation. *Journal of Vibration and Control*. **14**(12),1843–67.
- Amini, F. & Tavassoli, M. R.** (2005). Optimal structural active control force, number and placement of controllers. *Engineering Structures* **27**(9), 1306–16.
- Ankireddi, S. & Yang, H. T. Y.** (1996). Simple ATMD control methodology for tall buildings subject to wind loads, *Journal of Structural Engineering*, **122**, 83–91
- Basu B, Nagarajaiah S.** (2008). A wavelet-based time-varying adaptive LQR algorithm for structural control, *Engineering structures*.p.2470-2477
- Bitaraf, M., Hurlebaus, S. & Barroso, L. R.** (2012), Active and semi-active adaptive control for undamaged and damaged building structures under seismic load, *Computer-Aided Civil and Infrastructure Engineering*, **27**(1), 48–64.
- Chang, J. C. H. & Soong, T. T.** (1980). Structural control using active tuned mass damper, *Journal of the Engineering Mechanics Division*, **106**, 1091–8.
- Chase, G. J., Rodgers, G. W., Corman, S. & MacRae, G. A.** (2011), Development and spectral analysis of an advanced control law for semi-active resettable devices, *Proceedings of the 9th Pacific Conference on Earthquake Engineering*, Auckland, New Zealand, April 14–16, 2011.

- Chey, M. H., Chase, J. G., Mander, J. B. & Carr, A. J.** (2010), Semi-active tuned mass damper building systems: design, *Earthquake Engineering and Structural Dynamics*, 39; 119–39.
- Corman, S., Chase, J. G., MacRae, G. A. & Rodgers, G. W.** (2012a), Development and spectral analysis of an advanced diamond shaped resettable device control law, *Engineering Structures*, 40(1), 1–8.
- Corman, S., MacRae, G. A., Rodgers, G. W. & Chase, J. G.** (2012b), Nonlinear design and sizing of semi-active resettable dampers for seismic performance, *Engineering Structures*, 39, 139–47.
- Datta TK.** (1996) Indo-US symposium on emerging trends in vibration and noise engg, Control of dynamic response of structures, p. 18-20.
- Den Hartog, J. P.** (1956), *Mechanical Vibrations*, 4th edn. McGraw-Hill, New York.
- Gray, G. J., Li, Y., Murray-Smith, D. J. & Sharman, K. C.** (1995), Specification of a control system fitness function using constraints of genetic algorithm based design methods, in *Proceedings of the 1st International Conference Genetic Algorithms in Engineering Systems: Innovations and Applications*, GALESIA, 12–14 September 1995, venue, Halifax Hall, University of Sheffield, UK, pp. 530–5.
- Jiang, X. & Adeli, H.** (2008a), Dynamic fuzzy wavelet neuroemulator for nonlinear control of irregular highrise building structures, *International Journal for Numerical Methods in Engineering*, 74(7), 1045–66.
- Jiang, X. & Adeli, H.** (2008b), Neuro-genetic algorithm for nonlinear active control of highrise buildings, *International Journal for Numerical Methods in Engineering*, 75(8), 770–86
- Kim, H. & Adeli, H.** (2004), Hybrid feedback-least mean square algorithm for structural control, *Journal of Structural Engineering*, 130(1), 120–27.
- Kim, H. & Adeli, H.** (2005a), Hybrid control of smart structures using a novel wavelet-based algorithm, *Computer-Aided Civil and Infrastructure Engineering*, 20(1), 7–22.
- Kim, H. & Adeli, H.** (2005b), Wavelet hybrid feedback-LMS algorithm for robust control of cable-stayed bridges, *Journal of Bridge Engineering*, 10(2), 116–23.
- Kim, H. & Adeli, H.** (2005c), Hybrid control of irregular steel highrise building structures under seismic excitations, *International Journal for Numerical Methods in Engineering*, 63(12), 1757–74.
- Kim, H. & Adeli, H.** (2005d), Wind-induced motion control of 76-story benchmark building using the hybrid damper tuned liquid column damper system, *Journal of Structural Engineering*, 131(12), 1794–802.
- Kim, Y.-J. & Ghaboussi, J.** (1999), A new method of reduced order feedback control using genetic algorithms, *Earthquake Engineering & Structural Dynamics*, 28, 235–54.

- Kim, Y., Langari, R. & Hurlebaus, S.** (2010), Model-based multi-input, multi-output supervisory semiactive nonlinear fuzzy controller, *Computer-Aided Civil and Infrastructure Engineering*, 25(5), 387–93.
- Kundu, S. & Kawata, S.** (1996), Genetic algorithms for optimal feedback control design, *Engineering Applications of Artificial Intelligence*, 9(4), 403–11.
- Lin, C. C., Chen, C. L. & Wang, J. F.** (2010), Vibration control of structures with initially accelerated passive tuned mass dampers under near-fault earthquake excitation, *Computer-Aided Civil and Infrastructure Engineering*, 25, 69–75.
- Pourzeynali, S., Lavasani, H. H. & Modarayi, A. H.** (2007), Active control of high rise building structures using fuzzy logic and genetic algorithms, *Engineering Structures*, 29, 346–57.
- Puscasu, G. & Codres, B.** (2011), Nonlinear system identification and control based on modular neural networks, *International Journal of Neural Systems*, 21(4), 319–34.
- Panariello GF, Betti R, Longman RW.** (1997) Optimal structural control via training on ensemble of earthquakes. *Journal of Engineering Mechanics*, ASCE;123(11):1170-9.
- Saleh, A. & Adeli, H.** (1994), Parallel algorithms for integrated structural and control optimization, *Journal of Aerospace Engineering*, 7(3), 297–314
- Saleh, A. & Adeli, H.** (1997), Robust parallel algorithms for solution of the Riccati equation, *Journal of Aerospace Engineering*, 10(3), 126–33.
- Saleh, A. & Adeli, H.** (1998), Optimal control of adaptive building structures under blast loading, *Mechatronics*, 8(8), 821–44.
- Soong, T. T. & Constantinou, M. C.** (2002), *Passive and Active Structural Vibration Control in Civil Engineering*, Springer Verlag, New York.
- Udwadia, F. E. & Tabaie, S.** (1981a). Pulse control of single degree-of-freedom. *ASCE Journal of the Engineering Mechanics Division*, 107, 997–1009.
- Udwadia, F. E. & Tabaie, S.** (1981b). Pulse control of structural and mechanical systems. *ASCE Journal of the Engineering Mechanics Division*, 107, 1011–28
- Warburton, G. B. & Ayorinde, E. O.** (1980). Optimum absorber parameters for simple systems, *Earthquake Engineering and Structural Dynamics*, 8, 197–217.
- Wongprasert, N. & Symans, M. D.** (2004), Application of a genetic algorithm for optimal damper distribution within the nonlinear seismic benchmark building, *Journal of Engineering Mechanics*, ASCE, 130(4), 401–06.
- Wu JC, Yang JN, Schmitendorf WE.** (1998) Reduced-order H1 and LQR control for wind-excited tall buildings. *Engineering Structures* , 20(3):222-36.

- Wu W-H, Chase JG, Smith HA.** (1994). Inclusion of forcing function effects in optimal structural control. In: Proc. first world conf. on struct. control. IASC, TP2-22-TP2-31.
- Wu W, Nagarajaiah S.** (1996). Application of partitioned predictor corrector approach in nonlinear dynamic structural analysis and optimal control. Report 974. Missouri (Columbia, MO): Dept of Civil Engineering.
- Yang JN.** (1988) Recent advances in active control of civil engineering structures. Probab Eng Mech; 3(4).

## **CURRICULUM VITAE**

**Name Surname: Mahdi Abdollahirad**

**Place and Date of Birth: Iran-Ardebil 22.05.1983**

**Address:**

**E-Mail:m.abdolahirad@yahoo.com**

**B.Sc.:Civil Engineering**

**Professional Experience and Rewards:**

**List of Publications and Patents:**

**PUBLICATIONS/PRESENTATIONS ON THE THESIS**